REPUBLIQUE ALGERIENNE DEMOCRATIQUE ET POPULAIRE

MINISTERE DE L'ENSEIGNEMENT SUPERIEUR ET DE LA RECHERCHE SCIENTIFIQUE

UNIVERSITE YAHIA FARES DE MEDEA

Laboratoire des Energies Renouvelables et Matériaux-LERM

جامعة يحيى فارس - المدية

جامعة المدية
نائب العميد
المكلف بما بعد
التدرج
كلية التكنولوجيا

Faculté de Technologie

Département du Génie Electrique

# Thèse de doctorat en sciences

Présenté par :

**Mr. Abdelkrim KHERKHAR**

Filière : Génie Electrique

Spécialité : Génie Electrique

# Commande d'un dispositif de réfrigération thermoélectrique fonctionnant à base des matériaux semi-conducteurs

La soutenance aura lieu, le **06/10/2022** à **09h30**, Bloc des laboratoires de recherche

Devant le jury composé de :

| | | | |
|---|---|---|---|
| Dr. Noureddine HENINI | Maitre de conférences | Université de Médéa | Président |
| Dr. Smaïl SEMAOUI | Maitre de recherche | CDER, Alger | Examinateur |
| Prof. Hamza HOUASSINE | Professeur | Université de Bouira | Examinateur |
| Dr. Mohamed REZKI | Maitre de conférences | Université de Bouira | Examinateur |
| Prof. Younes CHIBA | Professeur | Université de Médéa | Directeur de thèse |
| Prof. Abdelhalim TLEMÇANI | Professeur | Université de Médéa | Co-directeur de thèse |

Année universitaire : 2022/2023

Scanné avec CamScanner

REPUBLIQUE ALGERIENNE DEMOCRATIQUE ET POPULAIRE
MINISTERE DE L'ENSEIGNEMENT SUPERIEUR ET DE LA RECHERCHE SCIENTIFIQUE

UNIVERSITE YAHIA FARES DE MEDEA
Laboratoire des Energies Renouvelables et Matériaux-LERM




Faculté de Technologie
Département du Génie Electrique

# Thèse de doctorat en sciences

Présenté par :
**Mr. Abdelkrim KHERKHAR**
Filière : Génie Electrique
Spécialité : Génie Electrique

# Commande d'un dispositif de réfrigération thermoélectrique fonctionnant à base des matériaux semi-conducteurs

La soutenance aura lieu, le **06/10/2022** à **09h30**, Bloc des laboratoires de recherche
Devant le jury composé de :

| | | | |
|---|---|---|---|
| Dr. Noureddine HENINI | Maitre de conférences | Université de Médéa | Président |
| Dr. Smaïl SEMAOUI | Maitre de recherche | CDER, Alger | Examinateur |
| Prof. Hamza HOUASSINE | Professeur | Université de Bouira | Examinateur |
| Dr. Mohamed REZKI | Maitre de conférences | Université de Bouira | Examinateur |
| Prof. Younes CHIBA | Professeur | Université de Médéa | Directeur de thèse |
| Prof. Abdelhalim TLEMÇANI | Professeur | Université de Médéa | Co-directeur de thèse |

Année universitaire : 2022/2023

**ملخص:**

في السنوات الأخيرة، دفعت أزمة الطاقة مع التدهور البيئي جنبًا إلى جنب، المجتمع للبحث عن نهج جديد لأنظمة تبريد مقتصدة للطاقة وصديقة للبيئة. أصبح هذا مكننا من خلال تطور أجهزة التبريد الكهروحرارية التي لها مزايا مهمة على عكس أنظمة التبريد التقليدية بضغط البخار. في هذه الأطروحة، تم استخدام نهج تجريبي وعددي من أجل تقييم أداء وكفاءة التحكم في المبرد الكهروحراري (TEC). لهذا الغرض، تم تصميم نظام تبريد حراري جديد باستخدام مادة أشباه الموصلات التي تعمل تحت تأثير بلتيير وجهازArduino. يتم التحقق باستخدام النموذج المصمم من كفاءة النظام من خلال معامل الأداء وامتداد درجة الحرارة للسائل الحامل بين المبادل الساخن والبارد. بالإضافة إلى ذلك، تم استخدام نهج التحكم PID من أجل الحفاظ على درجة حرارة التبريد ونقل الحرارة لنظام TEC في حلقة مغلقة من خلال دائرة القيادة، والتي تم تصميمها خصيصًا لـ TEC والتي يمكنها ضبط تيار الإدخال بسهولة، والذي يمر عبر الثلاجة للاستفادة الكاملة من مزايا طاقة التبريد السريع. النتائج الرئيسية التي تم الحصول عليها بما في ذلك معامل الأداء الأقصى المسجل هي 0.73 إلى 0.1 مع مجال درجة حرارة مقدر بـ 51 درجة مئوية. تؤكد النتائج التجريبية كفاءة أداء الجهاز المقترح، بحيث أنه خلال الفترة الزمنية 0-20 دقيقة الأولى، انخفضت درجة الحرارة الداخلية للثلاجة الكهروحرارية بمعدل 1.5 درجة مئوية في الدقيقة. من خلال أخذ $k_p = 0.9$، $k_i = 0.15$، و $k_d = 0$ =وقيمة تيار التغذية 5 أمبير، تنخفض درجة التبريد إلى 5 درجات مئوية خلال 21 ثانية فقط، مما يعني أن هذه الأنظمة تستجيب لعامل مهم و هو الوقت. وحدة التحكم المقترحة قادرة على الوصول إلى خطأ 0.1 درجة مئوية مع الحد الأدنى من التجاوز يقل عن 20 ثانية.

**الكلمات المفتاحية:** تأثير بلتيير، تحكم PID، مبرد حراري، تحكم في درجة الحرارة، دراسة تجريبية، معامل أداء.

**Abstract:**

In recent years, energy crunch along with environmental degradation has driven the society in search of novel approach of eco-friendly cooling systems. This can be possible through the evolution of thermoelectric cooling devices which have important advantages Unlike the traditional vapor compression cooler systems. In this thesis, an experimental and numerical approach is used in order to evaluate the thermoelectric cooler (TEC) control performance and efficiency. For this purpose, a novel thermoelectric refrigeration system is designed by using the semiconductor material operating under Peltier effect, and Arduino device. The efficiency of the system is investigated through the performance coefficient and temperature span for carrier liquid between the hot and cold exchanger by using the prototype designed. In addition, PID control approach is used in order to maintain the cooling temperature and heat transfer of the system TEC in a closed-loop through the driving circuit, which is specially designed for the TEC can conveniently adjust the input current, which passes through the refrigerator so as to fully make use of quick cooling power advantages. The main results obtained including the maximum coefficient of performance registered is 0.73 to 0.1 with a temperature span about of 51 °C. The experimental results confirm that during the time interval 0–20 min, the inside temperature of thermoelectric refrigerator has been decreased rate of 1.5 °C/min. By taking $k_p = 0.9$, $k_i = 0.15$, and $k_d = 0$ and supply current value is 5A, the cooling temperature decreases to 5 °C over 21 sec only, which means that these systems work in time-dependent conditions. The proposed controller is able to reach an error of 0.1 °C with minimal overshoot under than 20 seconds.

**Keywords:** Peltier effect, PID controller, Thermoelectric cooler, Temperature control, Experimental study, Coefficient of Performance.

**Résumé :**

Ces dernières années, la pénurie d'énergie ainsi que la dégradation de l'environnement ont poussé la société à rechercher une nouvelle approche des systèmes de réfrigération respectueux de l'environnement. Cela peut être possible grâce à l'évolution des dispositifs de réfrigération thermoélectriques (TEC) qui présentent des avantages importants contrairement aux systèmes de réfrigération traditionnels à compression de vapeur. Dans cette thèse, une approche expérimentale et numérique est utilisée afin d'évaluer les performances et l'efficacité du contrôle du réfrigérateur thermoélectrique. À cet effet, un nouveau système de TEC est conçu en utilisant le matériau semi-conducteur fonctionnant sous effet Peltier et Arduino. L'efficacité du système est étudiée à travers le coefficient de performance (COP) et la plage de température pour le fluide caloporteur entre la source chaude et froide en utilisant le prototype conçu. De plus, l'approche de commande PID est utilisée afin de maintenir la température de réfrigération et le transfert de chaleur du système TEC en boucle fermée à travers le circuit d'entraînement, qui est spécialement conçu pour que le TEC puisse facilement ajuster le courant d'entrée, qui traverse le réfrigérateur et de tirer des avantages de la puissance de refroidissement rapide. Les principaux résultats obtenus dont le COP maximal enregistré est de 0,73 à 0,1 avec une plage de température d'environ 51°C. Les résultats expérimentaux confirment que pendant l'intervalle de temps de 0 à 20 min, la température intérieure du réfrigérateur thermoélectrique a été réduite de 1,5°C/min. En prenant $k_p = 0,9$, $k_i = 0,15$ et $k_d = 0$ et la valeur du courant d'alimentation est de 5 A, la température de la source froide diminue à 5 °C en 21 secondes seulement, ce qui signifie que ces systèmes fonctionnent dans des conditions dépendant du temps. Le contrôleur proposé est capable d'atteindre une erreur de 0,1°C avec un dépassement minimal inférieur à 20 secondes.

**Mots clés :** Effet Peltier, Commande PID, Réfrigérateur thermoélectrique, Contrôle de température, Etude expérimentale, Coefficient de Performance.

# *Dedicated*

*To the soul of my dear Father and Mother, which time will not return,*
*I dedicate this Thesis.*

*I would like to thank them for their unconditional love, understanding and encouragement. Their infinite faith in me always motivates me to push the limit of myself. This thesis, and all of my accomplishments in life are rewards to their love.*

*Karim*

# Acknowledgements

First and foremost, the great thanks are due to **ALLAH**, the Almighty the Creator, the Sustainer and the Magnificent for the good health and well-being that were necessary to compile this research at this material time.

I would like to express my deepest gratitude to my principle supervisor **Prof. Chiba Younes**, Professor at the University of Medea, for providing me the opportunity to pursue my PhD degree. I am very grateful to your invaluable inspiration, insightful discussions, great enthusiasm, passionate presentation skills, and worthwhile recommendations during my research career at Medea University. My deep and sincere gratitude goes to my co-supervisor **Prof. Tlemçani Abdelhalim**, Professor at the University of Medea, for his constructive criticism, creative vision, intuitive scientific discussions and immense knowledge on the research projects, which made me determined, active and motivated in my work through the right path.

I would also like to extend my thanks to my committee members, **Dr. Noureddine HENINI**, associate professor at the University of Medea and **Dr. Smail SEMAOUI**, senior researcher at the CDER Research Center, Algiers, **Prof. Hamza HOUASSINE**, Professor at the University of Bouira and **Dr. Mohamed REZKI**, associate professor at the University of Bouira, for their guidance and suggestions to improve the quality of this work.

Last but not least, I would like to express my greatest gratitude to all members of my family, please accept my warmest and deepest gratitude.

My lovely, sensitive and caring wife Samir Imane, and your sister Sarah. Thank you so much for standing beside me during my PhD thesis work, I was not able to finish it without your kind support and motivation.

My Princess Amira and Adem, this thesis for you all to make a high goals and excellent achievements for your future life, make us proud my lovely Kids.

This doctoral thesis might have been an unrealistic dream without the support and contributions from many inspiring individuals that formed a productive environment for me to work in. Therefore, I would like to express my sincere gratitude to all the people who contributed in forming such stimulating atmosphere that helped me over the years to complete my thesis successfully.

# TABLE OF CONTENTS

Abstract

Dedicated ..... i

Acknowledgements ..... ii

Table of Contents ..... iii

List of Figures..... vi

List of Tables..... viii

Nomenclature ..... ix

Chapter I: Introduction and Literature Review

I.1. Introduction..... 01

I.2. Motivation..... 03

I.2.1. Approach..... 04

I.3. Overview of Thermal Management Techniques..... 04

I.3.1. Passive Cooling..... 04

I.3.2. Active Cooling..... 04

I.3.3. Basic Thermoelectric Phenomena..... 05

I.3.3.1. Seebeck Effect..... 05

I.3.3.2. Peltier Effect..... 06

I.3.3.3. Thomson Effect..... 07

I.3.3.4. Thermodynamic Relations Between Coefficients (Kelvin Relations) ..... 08

I.4. Choosing Materials..... 08

I.5. TEC Advantages..... 09

I.6. Current Research Works on Thermoelectric Coolers..... 10

I.6.1. Thermoelectric cooler Temperature Control..... 10
I.6.2. Performance investigation..... 11
I.6.3. Optimization of TEC..... 12
I.6.4. TEC application areas..... 13
I.7. Overview of Thesis..... 13
I.8. Aims and results obtained in the Thesis..... 15

Chapter II: Modeling and Simulation of Thermoelectric Cooler System

II.1. Introduction..... 16
II.2. Description of the main TEC cooler model..... 17
II.2.1. TEC Baseline Model..... 17
II.2.2. Assumptions of thermoelectric ideal (standard) equations..... 20
II.3. Modelling and Design of TEC Overview..... 22
II.4. Results and Discussions..... 31
II.5. Conclusion..... 39

Chapter III: PID Control Design of Thermoelectric Cooler

III.1. Introduction..... 40
III.2. Temperature control approach of TEC..... 41
III.2.1. Structure Design of Control System..... 41
III.3. PID control algorithm design..... 43
III.4. Results and discussions..... 48
III.5. Conclusion..... 51

Chapter IV: Experimentation

IV.1. Introduction..... 52
IV.2. The experimental system set-up..... 52
IV.3. Experimental Method ..... 54
IV.4. Hardware construction..... 55
IV.5. Effective Material Properties ..... 56
IV.5.1. Heat Sink exchanger design..... 56
IV.5.2. DC Fan design..... 58
IV.5.3. Temperature Sensors..... 58
IV.5.4. TEC Device Selection..... 59
IV.6. Results and Discussion..... 60
IV.7. Conclusion..... 64

Chapter V: Conclusions and Suggestions for Future Work

V.1. Conclusions..... 65
V.1.1. Broad-Based Findings..... 65
V.1.2. Contributions..... 66
V.2. Suggestions for Future Work ..... 67
V.2.1. Thermoelectric Refrigerator Control..... 67
V.2.2. Thermoelectric Refrigerator Design..... 67
References ..... 68
Appendix – TEC1-12706 Datasheet ..... 77
Liste of publications..... 80

# LIST OF FIGURES

## Chapter I

Figure I.1. Conceptual schematic of (a) the Seebeck effect and (b) the Peltier effect..... 05
Figure I.2. Thomson heat addition to a thermocouple..... 07
Figure I.3. Functional diagram of (a) thermoelectric cooler (TEC) and (b) thermoelectric generator (TEG)..... 09

## Chapter II

Figure II.1 (a) Single-stage TEC (b) Exploded view of TEC [107] ..... 17
Figure II.2 (a) Thermoelectric couple (b) Thermal resistance model..... 18
Figure II.3 The baseline model diagram..... 19
Figure II.4 Baseline model thermal resistance network..... 19
Figure II.5 Thermal Resistance Network for TE Cooler..... 19
Figure II.6 Modeling schematic of thermoelectric cooling system (TEC)..... 23
Figure II.7 Cold-side temperature achievable based on number of TEMs and $\psi_h$..... 24
Figure II.8 Generalized charts for TEC where $Z\bar{T} = 1$ [34] ..... 30
Figure II.9 COP and Power consumption as a function of current..... 32
Figure II.10 Cooling/Heating power and COP versus input current for given model: (a) Cooling mode and (b) Heating mode..... 33
Figure II.11 TEC junctions Cooling/Heating power versus input current..... 33
Figure II.12 TEC Hot and cold junction temperatures versus current..... 34
Figure II.13 Refrigeration chamber temperature and cooling power as a function of current ..... 35
Figure II.14 Power consumption and temperature comparison of the model and the experiment ..... 35
Figure II. 15 Effect of heat sink thermal resistance $\psi_h$ and number of modules $N_{mod}$ on the internal space temperature $T_{int}$ profile ..... 36
Figure II. 16 Effect of heat sink thermal resistance $\psi_h$ and number of modules $N_{mod}$ on the maximum cooling power $Q_{c_max}$ profile..... 37
Figure II.17 Thermoelectric cooling system thermal resistance sensitivity..... 37

Chapter III

Figure III.1 Open-loop Control system block diagram..... 42
Figure III.2 Typical temperature feedback control system..... 42
Figure III.3 Functional block diagram of PID controller..... 43
Figure III.4 Incremental PID control algorithm program flow chart..... 46
Figure III.5 Open-loop Simulink block diagram..... 47
Figure III.6 Closed-loop Simulink block diagram..... 47
Figure III.7 Thermoelectric cold-side temperature with PID and Without PID controller... 49
Figure III.8 Time series error with PID and Without PID controller..... 50

Chapter IV

Figure IV.1 Schematic diagram of the experiment set-up..... 53
Figure IV.2 A complete assembled to the thermoelectric refrigerator..... 55
Figure IV.3 External configuration of the minichannel cooler Block..... 56
Figure IV.4 Conduction on a plane, thickness $\Delta x$ and area $A$ [5] ..... 57
Figure IV.5 (a) DC Fan used in the TEC System (b) The design with two Heat Sink (c) minichannel cooler block..... 58
Figure IV.6 Temperature sensors: (a) DHT22 sensor (b) LM35 sensor..... 58
Figure IV.7 Thermoelectric module TEC1-12706..... 60
Figure IV.8 Inner temperature, ambient temperature of TE refrigerator profiles versus time ..... 61
Figure IV.9 COP variations during test time..... 62
Figure IV.10 Experimental relationship of time and temperatures..... 62
Figure IV.11 Experimental relationship of time and temperatures of internal minichannel block $T_{int_water_block}$, external minichannel block temperature $T_{ext_water_block}$, and cooling storage tank temperature $T_{water_tank}$..... 63

# LIST OF TABLES

## Chapter II

Table II.1. Optimization potential for the various parameters ..... 21
Table II.2 The characteristic of available TEMs materials [102,103] ..... 29

## Chapter III

Table III.1 Tuning effects of PID controller terms ..... 44

## Chapter IV

Table IV.1 Specifications of the minichannel liquid-cooler block ..... 53
Table IV.2 Heatsink Dimensions ..... 57
Table IV.3 Performance specifications of Thermoelectric Module (TEC1-12706) ..... 59

# Nomenclature

## Symbols

| | |
|---|---|
| $\bar{T}$ | Average temperature [°C] |
| $Q_c$ | Cooling capacity [W] |
| $A_e$ | cross-sectional area of thermoelement [mm$^2$] |
| $ZT$ | dimensionless figure of merit |
| $x$ | direction along the length of the element (Slab thikness) |
| $I$ | Electric current [A] |
| $W$ | Electrical power [W] |
| $V$ | Electric Voltage [V] |
| $Q_h$ | Heat rejection [W] |
| j | Junction |
| $L_e$ | length of thermoelement [mm] |
| $m$ | mass of the material [kg] |
| $Q_{c_max}$ | Maximum Cooling capacity [W] |
| $\Delta T$ | Maximum temperature difference (℃) |
| $N$ | Number of thermocouples |
| $C$ | specific heat of material |
| $T$ | Temperature [°C] |
| $\Delta T$ | Temperature difference [°C] |
| $t$ | Time [s] |
| $T_c$ | TEC cold side temperature [°C] |
| $T_h$ | TEC hot side temperature [°C] |
| L | total length of thermoelectric air conditioner [mm] |
| $Z$ | the figure of merit $[°C]^{-1} = \alpha^2/\rho k$ |
| $q_x$ | the rate of heat transfer around the differential element |
| $K$ | thermal conductance $[W/°C]$, $K = A_e/L_e$ |
| $k$ | thermal conductivity $[W/m°C]$, $k = k_p + k_n$ |
| $\psi$ | Thermal resistance [°C/W] |
| $R$ | Thermoelectric resistance [Ω] |

## Greek symbols

| | |
|---|---|
| $\sigma$ | electrical conductivity $[\Omega m]^{-1}$ |
| $\rho$ | electrical resistivity [Ωm], $\rho = \rho_p + \rho_n$ |
| $\pi$ | Peltier coefficient [W/A] |
| $\alpha$ | Seebeck coefficient $[V/°C]$, $\alpha = \alpha_p - \alpha_n$ |
| $\gamma$ | TE element geometry metric [m] |
| $\kappa$ | Thermal Conductivity [W/°C $m^2$] |
| $\tau$ | Thomson coefficient [V/°C] |

**PID controller variables and symbols:**

| | |
|---|---|
| $k_d$ | Derivative control gain |
| $k_i$ | Integral control gain |
| $k_p$ | Proportional control gain |
| $u(t)$ | Time domain control signal |
| $e(t)$ | Time domain error signal |
| $y(t)$ | Time domain process signal |
| $r(t)$ | Time domain reference signal |

**Abbreviations**

| | |
|---|---|
| ADC | Analog to Digital Conversion |
| CPU | Central processing unit |
| COP | Coefficient of performance |
| DC | Direct current |
| emf | electromotive force |
| HCS | heat conduction sleeve |
| HVAC | Heating, ventilation, and air conditioning |
| h | hour |
| IC | integrated circuit |
| NN | Neutral Network |
| PV | Photovoltaic System |
| PWM | Pulse Width Modulation |
| DHT22 | Temperature sensor |
| LM35 | Temperature sensor linear output [10 mV/°C] |

| | |
|---|---|
| TE | Thermoelectric |
| TEC | Thermoelectric Cooler |
| TEM | Thermoelectric module |
| TEG | Thermoelectric Generator |
| TER | Thermoelectric refrigerator |

**Subscripts**

| | |
|---|---|
| $c_Actual$ | actual cold side |
| $a$ | Ambient temperature |
| $ambient$ | Ambient temperature |
| $max$ | Based on the maximum of given quantity |
| $cr$ | Ceramic |
| $c$ | Cold |
| $co$ | Cold surface |
| $cond$ | Conduction |
| $fin$ | Finned heat sink |
| $h$ | Hot |
| $ho$ | Hot surface |
| $int$ | Internal space |
| $jc$ | Junction to case |
| $c_max$ | maximum cooling |
| $n$ | n-type element |
| $mp$ | Optimum input current |
| $c_ref$ | reference cold side |
| $sa$ | Sink to Ambient |
| $p$ | p-type element |
| $ha$ | TE hot side to ambient |
| $hs$ | TE hot side to Heat Sink |
| $ext_water_block$ | temperature of external Minichannel block |
| $int_water_block$ | temperature of Internal Minichannel block |
| $water_tank$ | temperature of liquid-cooling tank |
| $TER$ | Thermoelectric Refrigerator |
| $TE$ | Thermo-element |

# Chapter I

# INTRODUCTION AND LITERATURE REVIEW

## I.1. INTRODUCTION

In recent years, energy crunch along with environmental degradation has driven the society in search of novel approach of eco-friendly cooling systems. This can be possible through the evolution of thermoelectric cooling devices and several researches over it have made the above scenario feasible. The cooling system is a crucial process for many applications, ranging from fresh keeping the drink and food to the cooling temperature controllers in electronics, industries and in medical fields such as for surgery works or keeping the medicines in good conditions [6].

A typical thermoelectric cooler works mainly on the Peltier principle [1–3], i.e., a solid-state convertor generating a temperature gradient with application of minimal DC voltage [4, 5]. On application of such low DC voltage, one face of the module becomes colder, while there is a surge in temperature at the other side (Peltier's effect).

Unlike the traditional vapor compression systems, Thermoelectric cooling device have many advantages, and renders certain convenience such as no moving parts, in other words no wear [7] and lesser system weight [8], thus resulting in improved system reliability [9], long lifetime [10], and negligible maintenance [11], works acoustically silent, highly precise temperature control. As a result of smallness and lightweightness, they can be used in every cooling case where conventional cooling system are not applicable.

Thermoelectric are not a new technology and can be implement to any cooling application. Today, thermoelectrics are using in many different fields such as military and space research, to cool medical devices and small electronic components.

Thermoelectric refrigerator systems (TER) are comprised by modules, electrical and thermal insulators, heat sinks, connectors and interface thermal transfer materials [12]. Each of these items puts limits on efficiency of the cooling systems because of temperature [15], structural stress and thermal resistance, tour of thermoelectric legs [13], Seebeck coefficient [14], among the module's faces (hot and cold) [16]. It is to be noted that the same thermodynamic laws govern both the thermoelectric cooler as well as mechanical refrigerants [17]. At this point, basic problems of thermoelectric coolers show up.

However, in case of thermoelectric refrigeration, different roles are played by the direct current and mobile electrons, the former playing the compressor's role [18], while the latter

playing the conventional mechanical refrigerant's role [19]. The working of thermoelectric cooler is based on Peltier effect which states that, based on the current direction in the circuit, the heat is absorbed or rejected [20].

One of the basic problems of thermoelectric cooler is to remove the high dense rejected heat from the hot side of the module [21]. To remove heat from the module surface, fin and fan system are used [22]. However, surface of thermoelectric module is small so, heat accumulate the hot side of thermoelectric and fin which is using to cool hot side of thermoelectric, starts to saturate [23]. When it saturated, in the reverse direction heat transfer starts and cold surface temperature of thermoelectric module starts to increase [24]. Therefore, thermoelectric module efficiency and cooling power decreases and current values, which are applied to thermoelectric module, cannot reach high values [22,24].

To overcome this problem, various modifications are done and liquid cooling systems are developed. In liquid cooling systems, the heat transferred by thermoelectric module is passed to the cooling liquid with the help of heat exchanger [25]. Thus, module performance is tried to increase. However, because of thermal resistance at the contact areas, preventing the Fourier effect was a limited application. So liquid cooling system has become a better solution.

Generally, among the liquid cooling heat exchanger, the most effective one is new generation direct liquid contact heat exchangers [25]. In the scope of this thesis, to prevent the irreversible effects of thermoelectric modules on the cooling performance, two different direct contact liquid heat exchangers are used.

In the outside constructed design, for the hot side of thermoelectric cooler a heat exchanger is used and for the cold side of thermoelectric cooler a pin-fin is used to improve the heat transfer area. According to this assembly, cooling system performance is tested. In the experiment, different cases are observed and besides cold side of the thermoelectric cooler module are also determined with respect to current for both heat exchangers.

In the first case, a thermal analysis was completed for the TEC system to predict their performance. Heat transfer was modeled between three bodies, the thermoelectric modules (TEMs), the environment, and the inside the cooler system. Overall, the system parameters were analyzed using MATLAB simulations to prove that the authenticity formulae used in theory are self-sufficient to be applied in real applications. The system modeling consisted of a model that predicted the performance of the TEMs based on the simulation conditions.

In the second case, a $0.05m^3$ volume without any heat load is cooled by applying a PID control approach for different current values to improve the cooling temperature of thermoelectric cooler system.

In the third case experiment has been done in the TEC cooler at 31°C ambient temperature without any thermal load.

In design model, current-temperature, current-cooling power, current-COP values and cooling power-COP values relations are observed. From the results of experiments, new designed direct liquid contact heat exchangers increased the performance of thermoelectric module, compared to the old heat removal techniques such as fin and fan system and liquid base heat exchangers. New exchangers increased both cooling power and COP values. Besides cold side pin-fin temperatures are decreased as well. One of the basic reasons of this is annihilated contact thermal resistances by help of direct liquid contact heat exchangers. In this way, the pumped heat by the inside thermoelectric modules transferred directly to the cooling liquid and thus irreversible effects are prevented which gives higher cooling power and COP values for the same current.

As a result, to design effective TEC-systems and to extend usage are of thermoelectric cooler systems, new designed direct contact liquid flow heat exchangers are expected to be useful, equipped with a PID controller to quickly achieve cooling performance with low energy consumption.

## I.2. Thesis Motivations

The primary motivation for this thesis is to provide the cooling systems with a repeatable temperature control system without having to find suitable commercial products for every application. The set of design algorithms formulated over the course of this work are of particular value as they should help guide the design of future thermoelectric refrigeration systems with modified requirements.

Applications of specific interest for the developed refrigerator device include maintaining fixed cooling temperature amid a range of ambient temperatures and generating flexible temperature profiles. The practical implementation of a controlled thermoelectric cooler device is useful, and can help provide an added degree of assurance in temperature sensitive systems.

### I.2.1. Approach

The approach adopted to achieve the goal of control and experimental performance investigation performance of thermoelectric cooler composed of TEC devices is as follows:

- A thermal simulation framework is established and validated allows for rapid assessment of TEC and refrigerator system level thermal performance.
- The thermoelectric modules have an optimum current to achieve the maximum COP and the required cooling/heating capacity, by using an appropriate number of thermoelectric modules.
- Through the use of liquid-cooling minichannel heat exchanger, the general trends of TEC performance optimization were also validated. Thus, as long as the thermal resistance could be achieved.
- A PID control approach has been proposed to force the user-desired refrigeration temperature gradient on a thermoelectric refrigerator. The Ziegler-Nichols method has been adopted to set the optimal parameters of the controller.
- The TEC has been used for direct temperature control on the inside of a TE refrigerator and cooling liquid circulates in two minichannel aluminum blocks. The influences of heat sink temperature, flow rate, and current have been analyzed by calculation.

## I.3. Overview of Thermal Management Techniques

### I.3.1. Passive Cooling

Passive cooling is one of the most commonly used thermal management techniques in today's refrigeration technology. This method relies mainly on heat conduction, spreading, and natural convection. Their Advantages include high reliability, low cost and low complexity, while some disadvantages may include low heat removal, bulkiness, and the inability to cool below ambient temperature. Some examples of passive cooling techniques include heat spreaders, natural convection heat sinks.

### I.3.2. Active Cooling

Active cooling is typically more expensive than passive cooling and involves moving parts and/or the input of electrical power. This method actively pumps heat from a heat source to a

heat sink. Some common forms of active cooling involve fan cooled heat sinks, fluid pumped through microchannels, and jet impingement cooling.

Thermoelectric coolers, or TECs, are also a form of active cooling and offer a unique and promising solution to the hot spot problem. Some advantages of TECs include their solid-state design, the absence of moving parts, high reliability, and their capability to selectively target and cool hot spots.

### I.3.3. Basic Thermoelectric Phenomena

The thermoelectric effect can be described as the conversion of energy between electricity and heat. There are three types of thermoelectric effects that occur: the Seebeck effect, the Peltier effect, and the Thomson effect. These effects are found to be thermodynamically reversible [26].

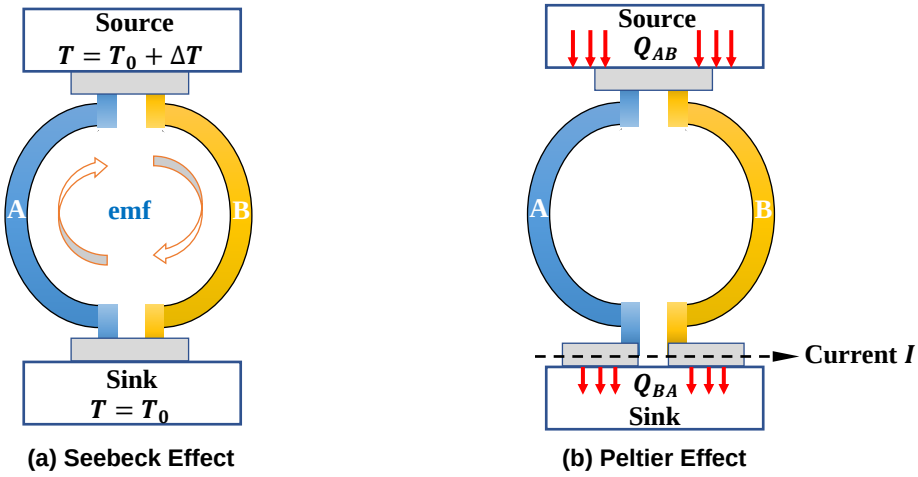



Figure I.1. Conceptual schematic of (a) the Seebeck effect and (b) the Peltier effect

#### I.3.3.1. Seebeck Effect

The Seebeck effect occurs when two dissimilar metals or semiconductors are joined at two points that are maintained at different temperatures [27]. An electromotive force will develop over the closed loop that can be measured. The Seebeck effect for materials A and B, shown in figure I.1(a), is interfacial and arises when charge carriers in a conductor are exposed to a temperature gradient within the conductor. This produces an electric flow of current that lasts as long as there is a temperature difference along the conductor. The heat is

$$V = \alpha_{AB}\Delta T \tag{I.1}$$

where $\Delta T = T_h - T_c$ and $\alpha_{AB} = \alpha_A - \alpha_B$ is called the Seebeck coefficient (also called thermopower) which is usually measured in $\mu V/K$. The sign of $\alpha$ is positive if the electromotive force (emf), tends to drive an electric current through wire A from the hot junction to the cold junction as shown in Figure.1(a). The absolute Seebeck coefficient can be only calculated from the Thomson coefficient. If it is also assumed that there is no voltage drop in the electrodes, the total module voltage is N times the voltage created in one couple. Therefore, equation (I.1) can be changed to:

$$V = N.\alpha_{AB}\Delta T \tag{I.2}$$

### I.3.3.2. Peltier Effect

The Peltier effect is the principal effect concerned with thermoelectric refrigeration or heat pumping. This effect is also interfacial and transports heat between two different conductors, from one junction to another, when an electric current is passed through the closed loop circuit. In Figure I.1(b), heat is absorbed at one junction and carried to the other. The Peltier heat is linear with respect to current, in contrast to the irreversible Joule heat, which is quadratic with respect to current. The rate at which heat is absorbed is proportional to the current and depends on the nature of the two materials comprising the junction. Thus, the Peltier heat absorbed or liberated is

$$Q_{Peltier} = \pi_{AB} I \tag{I.2}$$

where $\pi_{AB}$ is the Peltier coefficient, in units of Watts per Amp (W/A) and the sign of $\pi_{AB}$ is positive if the junction at which the current enters wire *A* is heated and the junction at which the current leaves wire *A* is cooled. This means that heating (or cooling) will produce electricity and electricity will produce heating (or cooling) without a loss of energy.

Like the Seebeck effect, each couple will absorb and reject a certain amount of energy, and thus, N couples will absorb N times the amount of heat of a single couple, assuming they are all at the same temperature. Figure II.2 (in chapter II) shows a module with multiple junctions connected electrically in series, and thermally in parallel. The total heat absorbed or liberated at either the hot side or cold side of the module is given as:

$$Q = N.\pi_{AB} I \tag{I.3}$$

### I.3.3.3. Thomson Effect

Also noteworthy is the Thomson effect, which is a bulk effect that transports heat within a current carrying material at one temperature to the same material at a different temperature (i.e. in a material with a temperature gradient) should absorb or dissipate heat.

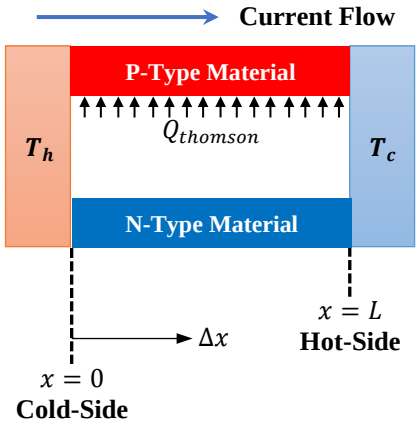



Figure I.2 Thomson heat addition to a thermocouple

The Thomson coefficient is defined as positive if heat must be added to keep the temperature constant. It is dependent on the absolute temperature and the change in the Seebeck coefficient with respect to temperature [26]. Thus, it is dependent on the temperature change and the current along as well as the Thomson coefficient, as given by the sign convention. The sign convention is best described in conjunction with a sketch, such as Figure I.2.

If the current is flowing in the positive *x* direction, as it is in the p-type material, then the Thomson coefficient is negative. If it is the opposite situation, as in the n-type material, the Thomson coefficient is positive. the Thomson heat absorbed or liberated across a wire is

$$Q_{Thomson} = -\tau . I . \nabla T \tag{I.4}$$

where $\tau$ is the Thomson coefficient. The Thomson coefficient is unique among the three thermoelectric coefficients because it is the only thermoelectric coefficient directly measurable for similar semiconductors. Thus, it is proportional to the change in the Seebeck coefficient per change in temperature [26]. The expression is given as,

$$\tau_{AB} = -T . \frac{d\alpha_{AB}}{dT} \tag{I.5}$$

To get a further understanding of the Thomson effect on a material, we need to look at heat rejection/absorption. When current flows through a material with a constant Seebeck coefficient ($\tau_{AB} = 0$), energy is lost solely through Joule heating ($I^2R$). When the Seebeck coefficient is a function of temperature ($\tau_{AB} \neq 0$), the Thomson effect becomes important [26], given as,

$$Q_s = \underbrace{I^2R}_{Joule\ Heating} - \underbrace{\tau_{AB}.I.\Delta T}_{Thomson\ Heating} \quad \text{(I.6)}$$

The subscript, $s$, denotes that this heat is transferred from the sides of the material. The resistance term, $R$, is also be slightly dependent on temperature.

### I.3.3.4. Thermodynamic Relations Between Coefficients (Kelvin Relations)

The relationships between the three thermoelectric effects are important in order to understand the basic phenomena. Thomson [26] studied the relationships thermodynamically and provided two relationships as shown in Equations (I.7) and (8) by applying the first and second laws of thermodynamics with an assumption that the reversible and irreversible processes in thermoelectricity are separable. The Thomson effect is relatively small compared to the Peltier effect, but it plays an important role to deduce the Thomson relationship. The relationships were later completely confirmed by experiments, which are

$$\pi_{AB} = \alpha_{AB}.T \quad \text{(I.7)}$$

$$\tau_{AB} = T\frac{d\alpha_{AB}}{dT} \quad \text{(I.8)}$$

Equation (I.7) leads to the very useful Peltier cooling as

$$\dot{Q}_{Peltier} = \alpha_{AB}.T.I \quad \text{(I.9)}$$

where $T$ is the temperature at a junction between two different materials and the dot above the heat $Q$ indicates the amount of heat transported per unit time.

## I.4. Choosing Materials

A conventional thermoelectric device is typically comprised of an array of P- and N-type semiconductor materials that are oriented in series electrically but in parallel thermally. A high conductivity metal such as copper is typically used to electrically connect the semiconductor

pillars and complete the electric circuit [26]. This circuit is usually sandwiched between two ceramic substrates that are electrically insulated but thermally conductive.

Schematics of a thermoelectric cooler (TEC) and thermoelectric generator (TEG) are shown in Figures I.3(a) and .3(b), respectively. Bismuth telluride ($Bi_2Te_3$) and its alloys are commonly used as the semiconductor materials in many applications because of their high thermoelectric properties, reflected in the commonly-used thermoelectric metric ($Z = \alpha^2/\rho.k$) at near room temperature, which is described later.

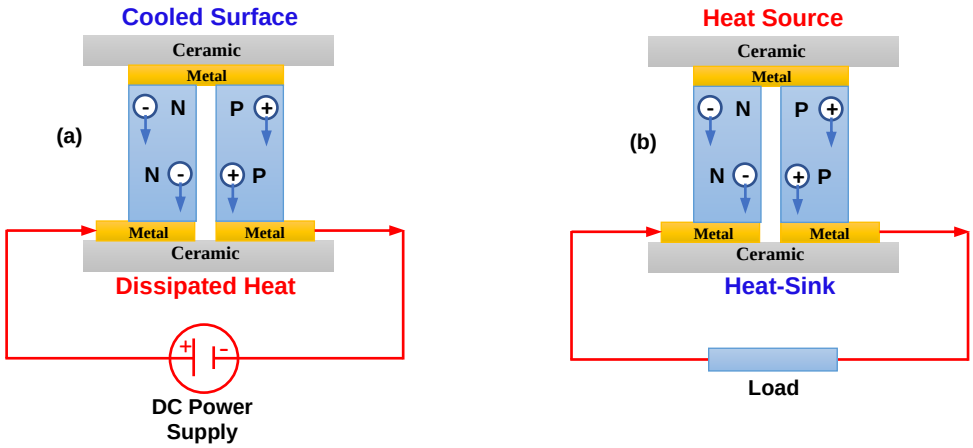



Figure I.3 Functional diagram of (a) thermoelectric cooler (TEC) and (b) thermoelectric generator (TEG)

In particular, $Bi_2Te_3$ shows the best thermoelectric properties at the desired temperature range for thermoelectric refrigerator [28].

## I.5. TEC Advantages

While refrigerators and air-conditioners utilize compressors, condensers and refrigerants to lower temperature; solid state cooling utilizes DC power, heat sinks and semiconductors. [24,29]. This fundamental difference gives solid state thermoelectric coolers the following advantages over conventional devices.

- Environment friendly (as no refrigerants are used). Therefore, leaking problem of refrigerants can also be avoided.
- Can be manufactured in compact sizes using less space.
- Light weight, which can be advantageous where light weight is more important feature than COP. (e.g. in aircrafts).
- Rate of refrigeration and COP can be easily controlled by varying voltage and current.

## I.6. Current Research Works on Thermoelectric Coolers

### I.6.1. Thermoelectric cooler Temperature Control

There exist several approaches for the enhancements of thermoelectric cooling control system performance including (PID) Control [30–33], fuzzy control [34], neural network control, and adaptive control. The concept of thermoelectric self-cooling introduced as a cooling and temperature control of a device using thermoelectric technology without electricity consumption was studied by [29].

From the above concepts, the thermoelectric cooling system performance has been guaranteed by controlling the variation of input current. TEC module of 12706 types which is composed of $Bi_2Te_3$ semiconductor material [35], has been used. Here, the purpose of cooling system control is expected to keep the internal temperature of an object below the ambient temperature of around ±30 °C. Song Shaojing et al. [36] offer to use NN-PID algorithm. It includes three basic values (three-term control P, I and D) parameters. In their work, Song Shaojing et al. adopted their controller model to calculate the control signal and then adjust the current of thermoelectric module. Ning Wang et al. [30], have based on an improved PID algorithm to design an efficient TEC temperature control system. The aim of their research was to determine which energy feedback approach is used to enhance TEC cooling. To improve the energy utilization efficiency of the system, The COP value was increased from 4.2 to 5.08 for changing the duty cycle. In [37], the problem of waste heat accumulation in optical crystals of high-power semiconductor lasers is discussed and an automatic constant temperature control system based on Thermoelectric Cooler is designed for temperature control of the optical crystals in high power semiconductor lasers to ensure its temperature stability. The system mainly includes two parts: human-computer interaction touch screen and TEC control driver module. The system can make the temperature change of optical crystal is less than ± 0.01℃ when Laser diode is working. A classical PID algorithm applied to control and adjust temperature automatically. Jin Wang et al. [38] proposed the use of MATLAB/Simulink environment to develop and simulate control system for thermoelectric cooling. MATLAB itself proved the most popular and reliable software for the purpose of modeling and simulation. Jin Wang et al. were interested in power losses acquired during the cooling process, so their system measured this value and compared it to a fixed threshold. According to that, TEC current was calculated and power was given to drive TEC module. Constant control is achieved with

PI and PWM generator use, which adjusted current and power permanently. The computational model proposed in [39], was conducted to study the influence of the temperature control system on the electric power consumption and coefficient of performance of a thermoelectric refrigerator, in order to make these devices more competitive. This control system supplies the thermoelectric modules with the maximum voltage until the inner temperature reaches the lower limit, and switches them off until the inner temperature reaches the upper limit.

A commercial portable thermoelectric refrigerator was modified to design and develop a new control system to improve the performance of the refrigerator in [40]. The modified refrigerator system can vary the input current of the refrigerator in order achieve an inner temperature of the refrigerator in the desired range. This refrigerator is able to operate using the AC power source from a wall socket or the DC power source from the battery.

All in all, study of those simulation techniques provided several crucial aspects to consider. It is important to note temperature accuracy, and speed of its changes, to design an effective cooling system. Also, different methods of current calculations should be considered to define the best one for precise operation. Moreover, power losses have to be observed because they affect the power applied to the system.

### I.6.2. Performance investigation

Zhu et al. [41] have investigated the impacts of the load current, the geometric size, the ratio of length to cross-sectional area and the substrate's thermal resistance on the cooling performance and response time of the miniature thermoelectric coolers via finite element methods. The results show that reducing TEC's size and ratio of length to cross-sectional area can improve the TEC's performance. Lee et al. [42] have carried out the numerical analysis of the thermoelectric micro-cooler with the three-dimensional model. The temperature difference, the current, the thickness of a thermoelectric element, and the number of thermoelectric pairs on the performance of the cooler have been investigated. Cai et al. [43-44] presented a comprehensive survey of TEC Temperature into effects of cooling load, air temperature and all thermal conductance in heating side on the cooling performance. The authors in [45], conducts numerical performance analysis and optimization of a combined cross-regenerative cross flow thermoelectric assisted indirect evaporative cooling system. A heat and mass transfer model are developed. Performance comparison is conducted under various operating conditions. An experimental performance investigation on thermoelectric cooler box with several positions of

the thermoelectric was performed in [46]. The experiment was conducted for about 18,000 s at the open ambient temperature. The results showed that the COP decreased with the times, and the best position of the thermoelectric placement of the study was on the wall.

### I.6.3. Optimization of TEC

To obtain an optimized performance from thermoelectric cooler various optimization techniques have been used to optimize the operational performance as well as their size. A general approach in evaluating and optimizing thermoelectric cooler (TEC) performance was presented by Hy Zhang in [47]. A multi-objective optimization based on thermoelectric heat exchanger module was presented in [48] for application in CPU cooler. The thermoelectric heat exchanger module coupling multi-parameters is used as a novel method to solve the heat dissipation. Yin, Tao et al [49], have proposed novel general single/multi-parameter optimization model for the thermoelectric cooler (TEC) based on the 1D resistance method, which precisely captures all the thermoelectrical effects and the impacts of temperature-dependent thermoelectric properties. Jeong et al. [50] have investigated one dimensional analytic mode to optimize the TE cooling module. Applying entropy generation analysis method, Wang et al. [51] have studied the optimum configuration of a thermoelectric cooling (TEC) system with a generalized theoretical model. Through operating condition management of the thermoelectric modules (TEM) and design optimization of the heat exchangers linked to the TEM, David et al. [52] have introduced an optimization method for improving thermoelectric heat pump performance. Huang et al. [53] have developed an inverse problem approach which integrates a complete Multiphysics TEC model and a simplified conjugate-gradient method to optimize the geometric structure of TEC. Chen et al. [54] have proposed a model of thermoelectric generator-driven thermoelectric refrigerator with external heat transfer. Zhu et al. [55] have used the theoretical analyze to explore the optimization problems of thermoelectric cooler (TEC) systems applied in electronic cooling which mainly focuses on the optimal heat exchanger configuration of a TEC system. Zhou et al. [56] have proposed a generalized theoretical model for the optimization of a TEC system. The thermal conductance from the cold and hot sides of the system are considered. The results show there are the maximum COP and the maximum cooling capacity of the TEC system, when the finite total thermal conductance is optimally allocated.

### I.6.4. TEC application areas

TEC can be applied in many areas. This overview mainly focuses on two fields. One is the popular electric device. The gradually higher heat fluxes of the microprocessor and the demand for a microprocessor that has a very high computing ability are inevitably contradictions. TEC is an excellent solution. the other is its potential wide used place, the storage of medicine.

With the constant increasing of the microprocessor power dissipation and the size of microprocessor, the heat flux of the microprocessor is gradually higher. Thus, conventional air-cooled cooling systems are no longer adequate to remove these heat fluxes. Gould et al. [57] have investigated the thermoelectric cooling and micro-power generation from waste heat within a standard desktop computer. The thermal cooling enhancement technique of dual processors workstation computer couple thermoelectric air cooler module is studied experimentally in [58]. The temperature distribution inside the computer chassis depends on the density, position of the components inside the computer both active and passive components. Martínez et al. [59] have investigated the simulation of thermoelectric self-cooling applications for both the steady and the transient state of the whole system. The results show the model architecture allows the inclusion of new analytical expressions. TE cooler appears to be especially favorable for automotive applications [60]. Besides the automobile air-conditioning system and automobile mini refrigerators, researchers also utilized TE device to control car seat temperature to either cooling down or heating up [61]. Wiriyasart et al. [62–64] experimentally studied on the thermoelectric air cooler module for thermal cooling enhancement of dual processors work-station computer. The work in [65], aimed at obtaining the optimal cooling performance of a medical non-toxic thermoelectric refrigerator through three groups of experiments.

## I.7. Overview of Thesis

This thesis is organized into chapters; each chapter is focused on an objective to achieve the goal of the research. The aim and end objective of each chapter is summarized below.

- **Chapter I**, presents the motivation behind the research and an outline of the approach adopted to reach the objective. This part is devoted to the general background of the thermoelectric cooling system. The research objectives and thesis structure are also discussed. Brief literature review on the Current Research Works on Thermoelectric Coolers, composed

of the performance investigation, optimized thermoelectric materials for TEC cooling temperature control applications areas, is also presented.

- **Chapter II**, presents a numerical and thermal modeling approach to determine the cooling optimum performance as well as the proposed optimum design to power a small thermoelectric refrigeration system. The model is derived from three energy conservation equations for temperatures at both ends of the thermoelectric materials within a TEM module, as well as the cooling temperature required. The design process focuses on meeting the demand criteria of the application rather than optimizing the system, because no thermal optimization occurs. Modeling approach takes accounts for realistic working conditions to meet the cooling temperature range with simulation results. Current and module optimization were provided to reach minimum temperatures required. One of the objectives of this chapter was to modeling and investigate the optimal design of a thermoelectric cooler applied for a thermoelectric cooler control.

- **In the Chapter III**, a numerical simulation study was conducted to investigate the performance of the TEC cooler system model with PID control strategy. The mathematical model of cooling system created and detailed in chapter I by making energy balance for the TEC cooling system. The simulation of the PID controller was designed by using MATLAB/SIMULINK. To increase the sensevity and stability of the PID system operation, digital filters were used to eliminate the influence of random disturbances of the temperature indicated by the feedback closed-loop. This ensures stable, much faster, and more accurate operation of the controller. The novelty of the presented PID control system is the determination of the TEC temperature based on the solution of the inverse problem of heat conduction formulated for a thermoelectric device.

- **Chapter IV**, presents the experimental design and development of a thermoelectric cooling system. Its mathematical model relating thermal loads and TEC heat capacity is also developed in chapter II. the TEC has been used for direct temperature control on the inside of the refrigerator and cooling liquid circulates in two minichannel heat exchangers block. The influences of the heat exchangers temperature, flow rate, and current have been analyzed. The proposed system is found to have less maintenance and simplicity in design which can easily replace the HVAC system. In the experimental results, the cold side temperature of the thermoelectric cooling unit has decreased quickly. The highest COP has been obtained as 0.73.

▪ **Chapter V**, presents the conclusions, the main contributions reported in this thesis and recommendations for future work are presented.

## I.8. Aims and results obtained in the Thesis

In this thesis, the effects of the proposed PID control on the thermoelectric cooler module. The analytical model was experimentally investigated at high outdoor temperature value without thermal load, and the following main Objectives and results were obtained:

- Design and application of the PID control approach on a thermoelectric refrigeration device.
- Development of a new model of a thermoelectric cooler working with mini-channel heat exchangers takes into consideration the all effects.
- Investigation and realization of the proposed model on a thermoelectric refrigerator.
- Variation of coefficient of performance with cooling power.
- Variation of the lowest achievable temperature values with current.
- The effect of supply current variation on the cooling power of the system.
- Effect of heat exchangers and TEM numbers on the performance of the cooling system.
- Behavior of the cooling system in different PID parameters.

# Chapter II

# MODELLING AND SIMULATION OF THERMOELECTRIC COOLER SYSTEM

## II.1. INTRODUCTION

Most research efforts have focused on enhancing the properties of thermoelectric materials and improving the figures of merit [66–70]. In order to fully utilize enhanced thermoelectric materials, a model of the thermoelectric cooling system (TEC) should be readily available for performance evaluation and system design. Careful engineering of the system should be conducted to meet the performance requirements while staying within the design criteria. Neither Putra and Ahiska [71] nor Guler [72] presented any type of modeling approach of their systems.

Traditional modeling of thermoelectric refrigeration [73,74] has allowed us to reach simple, closed form solutions for the optimum current and minimum temperature possible for thermoelectric refrigeration. However, these approaches make assumptions, which cannot be satisfied in practical applications. Firstly, the traditional model assumes that the current has no effect on the hot/cold side temperatures of the thermoelectric modules. In reality, the temperatures of the hot/cold side of the thermoelectric module changes with current due to the Peltier effect and Joule heating.

Therefore, the traditionally accepted optimum current value $I = \frac{\alpha.T_c}{R}$ does not lead to the minimum temperature in a real system. Secondly, the traditional model assumes that the hot side temperature of the module is known and kept constant at ambient. In practical application, heat should be dissipated to the environment through heat exchangers or heat sinks, which makes the hot side temperature of the module greater than the ambient temperature. An active cooling system with a large amount of energy consumption is necessary to make this temperature difference negligible [75]. Lastly, the traditional model assumes infinite thermal resistance, or perfect insulation, on the surface of the cooling chamber, and does not account for the heat gain of the chamber from the environment. As a result, the minimum temperature occurs when there is no inner heat removal from the refrigerator ($Q_{c_max} = 0$). With finite thermal resistance at the TEC, constant heat removal from the thermoelectric module exists.

Now that we have a basic understanding of how TE devices work, we can look at how these devices can be optimized. The remainder of this chapter will focus on modeling and applying the cooling phenomenon discovered by Jean Peltier. Thus, in particular, will investigate optimum refrigeration conditions for the available TE modules.

## II.2. Description of the main TEC cooler model

### II.2.1. TEC Baseline Model

The schematic diagram in Figure II.1(a) illustrates a basic single-stage TEC design. Multiple thermoelectric (TE) elements are used to construct a thermoelectric cooling device. Electrically, these TE elements are connected in series. Interconnecting p-type and n-type TE elements is achieved with copper tabs. Between two ceramic substrates (thermally conducting), this array arrangement is sandwiched. The exploded view of a practical TEC device is depicted in Figure II.1(b). A thermocouple is the basic physical unit of a thermoelectric cooler's physical model.

A thermocouple is the pair of semiconductor p-type and n-type dissimilar elements. The TE elements pair count can be from few to hundreds, depending on the design. Hence, the performance prediction of the thermoelectric cooling system (with heat sink) is complicated. Furthermore, the thermal resistances in the ceramic substrates, copper conductors, and heat sink contribute to the overall heat flow resistance in the thermoelectric cooling system.

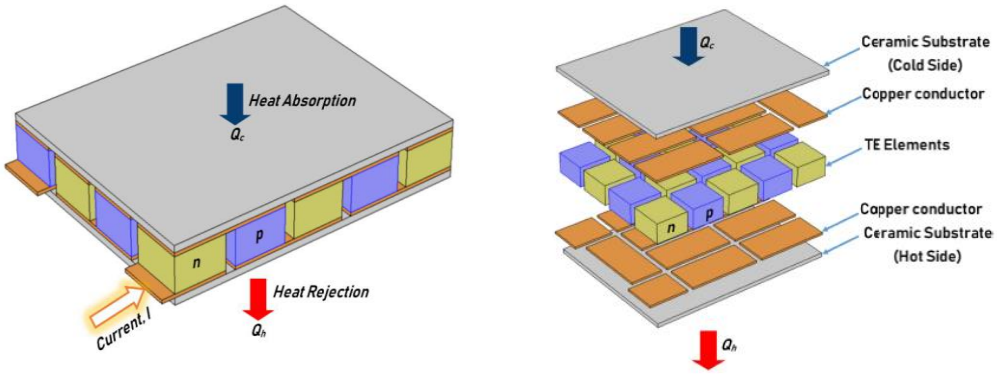



Figure II.1. (a) Single-stage TEC (b) Exploded view of TEC [76]

The performance optimization problem is difficult to solve because of these challenges. The effects of thermal resistance as well as electrical contact resistance are considered in this chapter. The effects of Joule heating and thermal conduction are also taken into account.

A thermal- resistance model has been created for this research study to make the analysis of thermal resistances easier. To develop more realistic thermoelectric cooler model, this model contains thermal resistances of ceramic substrates, copper parts, and hot side heat sink. Figure II.2 illustrates a pair of semiconductor p-type and n-type TE elements.

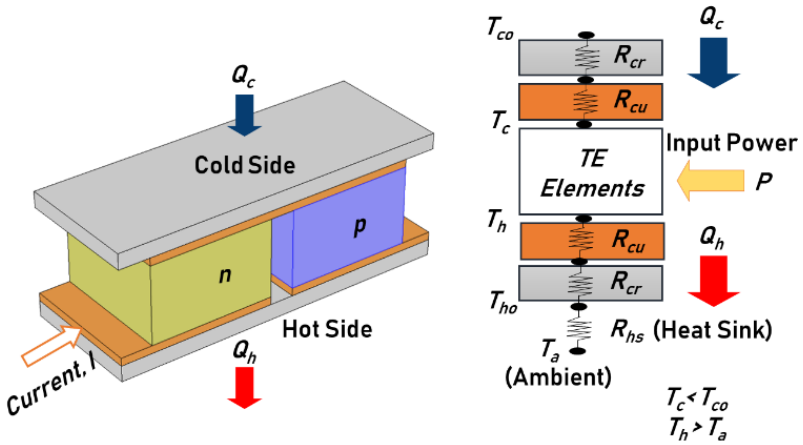



Figure II.2 (a) Thermoelectric couple (b) Thermal resistance model

In this chapter, the thermoelectric refrigeration model is based on the ideal refrigeration cycle. In this way, the calculation of one-dimensional physical model can be simplified. The model is assumed that the structure and material of the semiconductor bridge is completely symmetrical. In order to discuss the intricate issues of TE cooling modeling, we must include the TE module in a refrigeration system. A TE cooling system simply places a TE module in between a heat dissipation device and a liquid-cooled heat sink.

Using heat flow as an electrical analogy to the model of thermal resistance as shown in Figure II.2 (b), the temperatures at the TEC's hot and cold surfaces can be expressed as [77]:

$$T_h = Q_h(R_{hs} + R_{cr} + R_{cu}) + T_a \quad \text{(II.1)}$$

$$T_c = T_{co} - Q_c(R_{cr} + R_{cu}) \quad \text{(II.2)}$$

Where $T_c$ and $T_h$ denote the temperatures on the cold and hot sides of semiconductor elements. $Q_h$ denotes the rate at which heat is rejected from the hot side. $Q_c$ is the rate at which heat is absorbed on the cold side, which is commonly known as the cooling power. $T_{ho}$ and $T_{co}$ denote the temperatures at the thermoelectric cooler's hot and cold surfaces, respectively. $R_{hs}$ denotes the thermal resistance of the hot side heat sink in thermoelectric cooling system, $R_{cr}$ denotes the thermal resistance of the ceramics, and $R_{cu}$ denotes the thermal resistance of the copper parts. $T_a$ denotes the ambient temperature.

The baseline model assumed for our problematic consists of a liquid-cooled heat sink attached directly to the hot-side ceramic of TEC. Depending on which way the electric current flows, a thermoelectric couple provides cooling or heating. Figure II.3 shows this configuration.

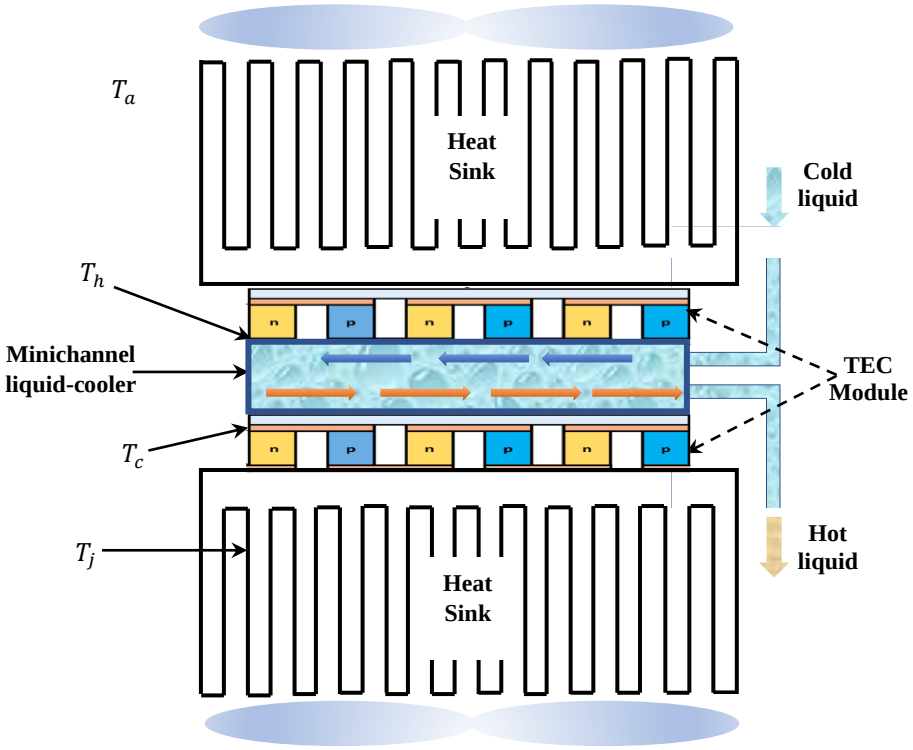



Figure II.3. The baseline model diagram

A thermal resistance network can be generated for the model. Figure II.4 shows the simple one-dimensional resistance network. Note that the heat absorbed flow $Q_c$, is the same through both the interface material and the heat sink.

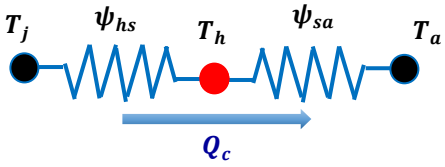



Figure II.4. Baseline model thermal resistance network

The thermal modeling of the TE refrigerated system is aided through the drawing of a resistance network as shown in Figure II.5.

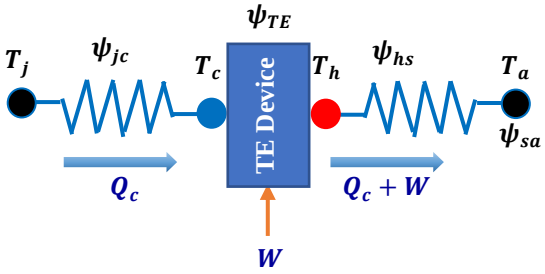



Figure II.5. Thermal Resistance Network for TE Cooler

In Figure II.5, $\psi_{jc}$ and $\psi_{hs}$ are the interface resistances, and $\psi_{sa}$ is the thermal resistance of the heat sink. Analysis of the TE system demands a more rigorous model than the baseline design. As implied by Figure II.5, the operation of the TE module requires external work. That work is needed to drive heat from cold to hot. The input work is converted to heat in the TE module and must be dissipated by the heat sink (as illustrated in Figure II.5 by the additional heat flow term in the heat sink). This additional heat load limits the application of TE refrigeration relative to the baseline configuration, and must be accounted for in the system level modeling [78].

### II.2.2. Assumptions of thermoelectric ideal (standard) equations

The important assumptions of thermoelectric ideal (standard) equations are illustrated Below:

- The Thomson effect is negligible. It has been proven analytically and experimentally that the Thomson effect has a very small effect on the performance of TEC.
- The electrical and thermal resistances between ceramic plates and thermoelectric elements are negligible.
- The convection and radiation losses are negligible.
- The materials properties are assumed to be independent of temperature.

It is of general interest to establish the amount of heat that can be cooled by the TE cooler. This is found through an energy balance on the cold junction of the TE module, and is given by:

$$\begin{cases} Q_c = 2.N.\alpha.I.T_c - \frac{1}{2}I^2.R - \frac{\Delta T}{\psi_{TE}} \\ Q_c = \underbrace{2.N.\alpha.I.T_c}_{\substack{Electron \\ Heat\ Pumping}} - \underbrace{\frac{1}{2}I^2.\frac{2N.\rho}{\gamma}}_{Joule\ Heating} - \underbrace{2N.\gamma.k.\Delta T}_{\substack{Conduction \\ Heat\ Leak}} \end{cases} \quad \text{(II.3)}$$

where:

$$\gamma = \frac{A_e}{L} \quad \text{(II.4)}$$

Note: $\Delta T = T_h - T_c$ and the parameters, $\psi_{TE}$ and $R$, are referred to as the module thermal and electrical resistance, respectively. These are defined as,

$$R = \frac{2N.\rho}{\gamma} \quad \text{(II.5)}$$

$$\psi_{TE} = \frac{1}{2N.k.\gamma} \tag{II.6}$$

The input work, or electric power, used by the TE must overcome the Seebeck voltage as well as the Joule heating.

$$W = \underbrace{2N\alpha.I.\Delta T}_{\substack{Electron\ Heat \\ Pumping}} + \underbrace{I^2.R}_{\substack{Joule \\ Heating}} \tag{II.7}$$

Using these equations along with knowledge of the interface and heat sink thermal resistance, the TEC junction temperature can be found from:

$$T_j = T_a + (Q_c + W)\psi_{ha} - \Delta T + Q_c.\psi_{jc} \tag{II.8}$$

The heat sink thermal resistance has been added to the interface thermal resistance to obtain $\psi_{ha}$.

Since there are a lot of parameters that impact the performance and efficiency of the thermoelectric cooler system, it is useful to look at each individually. Table II.1 gives an indication as to whether each parameter can be optimized and the effect that it has on the performance and efficiency.

| **Parameters** | **Optimization** | **Correlation to $T_j$** | **Correlation to COP** |
|---|---|---|---|
| Heat Input $Q_c$ | No | Positive | Positive |
| Temperature difference $\Delta T$ | No | Negative | Negative |
| Current $I$ | Yes | Indeterminate | Indeterminate |
| Thermal resistance $\psi_{ha}$ | No | Positive | Indirectly Negative |
| Hot-side temperature $T_h$ | No | Depends on $T_c$ and $\Delta T$ | Depends on $T_c$ and $\Delta T$ |
| Cold-side temperature $T_c$ | No | Depends on $T_h$ and $\Delta T$ | Depends on $T_h$ and $\Delta T$ |
| Ambient temperature $T_a$ | No | Positive | Negative |
| Total geometry $N.\gamma$ | Yes | Indeterminate | Indeterminate |
| Seebeck coefficient $\alpha$ | No | Positive | Positive if $T_c > \Delta T$<br>Negative if $T_c < \Delta T$ |
| Electrical resistivity $\rho$ | No | Negative | Negative |
| Thermal conductivity $k$ | No | Negative | Negative |

Table II.1. Optimization potential for the various parameters

Positive correlation means that an increase in the parameter will cause and increase in the given system characteristic, holding everything else constant. Negative correlation means that an increase in the parameter will cause a decrease in the given system characteristic, all other parameters held constant. Indeterminate correlation means that an increase will cause either a positive or a negative response to the characteristic, providing the opportunity for optimization. For instance, if we can decrease the thermal conductivity, holding everything else constant, the heat load would be increased allowing the junction temperature and the COP to rise.

This Table II.1 shows that geometry and current are the only two parameters that can be optimized. It is also interesting to see that there are certain parameters that are positively or negatively correlated for both system characteristics. For example, if the heat input is increased (assuming the work is kept constant) the COP will increase. Similarly, if everything can be kept constant in equation (I.8), an increase in heat load would cause an increase in junction temperature. Therefore, a trade-off is possible between the two characteristics. This situation is what makes it possible to achieve an optimum performance and efficiency at the same time (a happy medium).

A counter situation is also possible. A parameter can be negatively correlated to one characteristic while it is positively correlated to the other characteristic. For example, if the electrical resistivity was to decrease (keeping everything else constant), the junction temperature would decrease and the COP would increase. In both cases, this is due to the fact that parasitic resistive heating would be decreased. If this parameter were independent of the other material properties it would be beneficial to make the electrical resistivity as close to zero as possible (a metal).

## II.3. Modelling and Design of TEC Overview

Figure II.6 demonstrates the relationship between the thermal resistance and heat transfer. Where $Q_h$ is the heat rejected through the external heat sink between the hot side of the module and $T_{ambient}$ the temperature of the environment.

The symbol $\psi_h$ indicates the thermal resistance of the heat sink. $\psi_c$ indicates the thermal resistance for cold side of the module in which $Q_c$ is absorbed by TER space. The thermal resistance of the room and insulation is represented by $\psi_{TER}$ where heat is lost from the internal space to the environment [79].

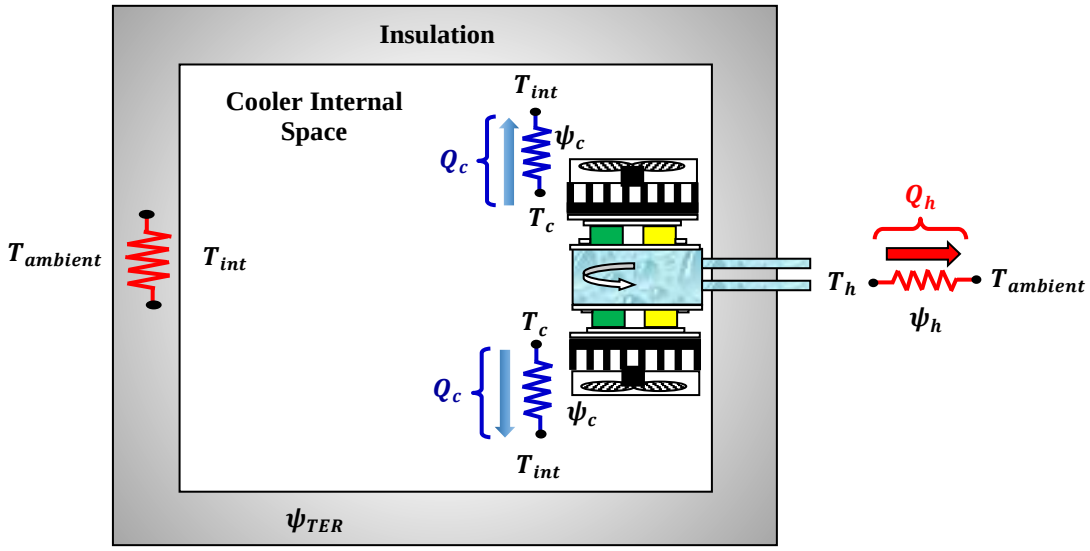



Figure II.6. Modeling schematic of thermoelectric cooling system (TEC).

Heat sinks are passive heat exchangers used to increase the surface area and the amount of heat transfer between the heating side of the thermoelectric modules and the environment. Figure II.6 shows the general locations of the heat sinks inside and outside of the thermoelectric refrigerator [77].

The performance of the fins placed within the room was determined based on the enhancement of heat transfer relative to the case that the interior surface of TER had no heat sinks. Mathematically, fin effectiveness, $\sigma_{fin}$ can be expressed as

$$\sigma_{fin} = \frac{\rho_{fin}}{h.A_e(T_{base} - T_{ambient})} \tag{II.9}$$

Where $\rho_{fin}$ is the conductive heat transfer through the fin, $h$ is the convective heat transfer coefficient across the fins, $A_e$ is the cross-sectional area of the fin base, $T_{base}$ is the base temperature, and $T_{ambient}$ is the ambient temperature of TER.

Shown in Figure II.7 is a comparison of how much the TER inside temperature can be reduced based on the thermal resistance and number of modules. This model assumed that the heat dissipation is split evenly among each of the modules. As seen in the Figure II.6, colder temperatures can be achieved with lower. For each value, however, there exists a single point with the minimum temperature indicating the optimum number of modules to use.

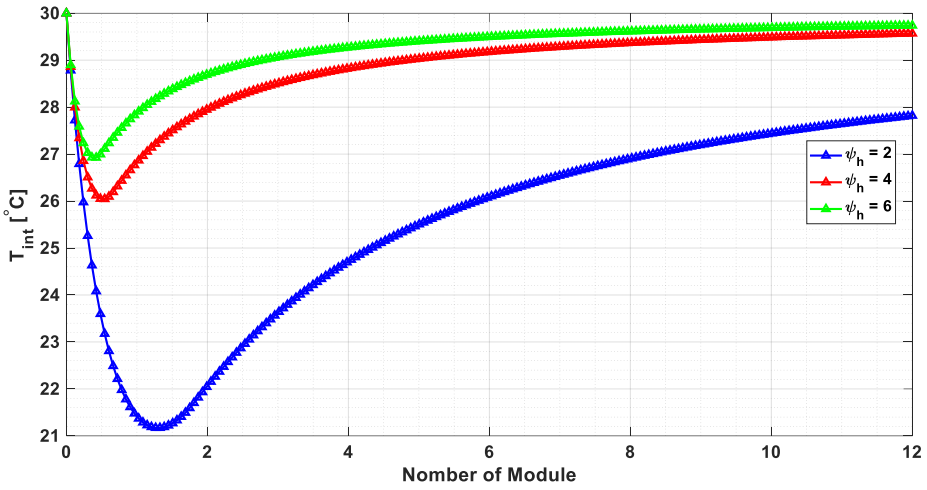



Figure II.7. Cold-side temperature achievable based on number of TEMs and $\psi_h$

The best design iteration tested achieved a lowest temperature of 21°C using three modules. The model suggested decreasing the number of modules while keeping the same. However, for this iteration, each TEM had its own heat sink and fan. This meant that to keep the same for a single module, those three heat sinks would have to be combined to dissipate the heat from that module.

It can also be seen that TEC can be analyzed by Joule heat, which is called heat rejection $Q_h$, from TEC hot side larger than the heat absorption $Q_c$, into TEC cold side.

The input and output heat from two sides of a thermoelectric cooler can be written as follows, [80-88]:

$$Q_c = \alpha . I . T_c - 0.5R . I^2 - \kappa . \Delta T \tag{II.10}$$

$$Q_h = \alpha . I . T_h + 0.5R . I^2 - \kappa . \Delta T \tag{II.11}$$

Where $\alpha, R, \kappa, I, Q_c, Q_h, T_c, T_h$ and $\Delta T$ represent the Seebeck coefficient, electrical resistance, thermal conductance, electrical current, heat rate absorbed from the chamber [$Watts$], heat rate dissipated by the hot side of the TEM [$Watts$], cold surface temperature ($°C$), hot surface temperature ($°C$) and the temperature difference between the cold and hot sides ($°C$) through a TEC, respectively. The temperature difference between the two sides of a TEC can be express as follows:

$$\Delta T = T_h - T_c \tag{II.12}$$

The above two Equations (II.10) and (II.11) are known as the ideal (standard) equations. The first term $\alpha.I.T_c$ is the Peltier/Seebeck effect, which is a reversible process. A higher Peltier/Seebeck effect is needed in order to have a higher cooling or power generation. The second term $0.5R.I^2$ is known as the Joule heating, which is an irreversible process. Finally, the third term $\gamma.(T_h - T_c)$ is the thermal conductance, which is also an irreversible process. The heat flow direction is significant in order to know the type of thermoelectric couple, either a thermoelectric cooler or thermoelectric generator (TEG). By reversing the heat flow direction, the thermoelectric cooler can be represented.

Based on the thermal circuit, $Q_c$ and $Q_h$ can be equated to [89,90]:

$$Q_c = \frac{T_{int} - T_c}{\psi_c} \tag{II.13}$$

$$Q_h = \frac{T_h - T_{ambient}}{\psi_h} \tag{II.14}$$

Where $T_{int}$ is the temperature inside the TEC internal space, $\psi_c$ is the sum of thermal resistances on the TEM cold side in the room, and $\psi_h$ is the sum of thermal resistances on the hot side of the TEM to the environment. Combining equations (II.11) and (II.13) and equations (II.12) and (II.14) [91-92]:

$$\frac{T_{int} - T_c}{\psi_c} = \alpha.I.T_c - 0.5R.I^2 - \kappa.(T_h - T_c) \tag{II.15}$$

$$\frac{T_h - T_{ambient}}{\psi_h} = \alpha.I.T_h + 0.5R.I^2 - \kappa.(T_h - T_c) \tag{II.16}$$

In addition, the heat gain from the environment is given by:

$$m.C.\frac{\partial T_{int}}{\partial t} = \frac{T_{ambient} - T_{int}}{\psi_{TEM}} - \frac{T_{int} - T_c}{\psi_c} \tag{II.17}$$

In the steady state Equation (II.14) becomes:

$$\frac{T_{ambient} - T_{int}}{\psi_{TEM}} = \frac{T_{int} - T_c}{\psi_c} \tag{II.18}$$

Based on equations (II.14), (II.15), and (II.17), by knowing the module properties, the three unknowns $T_{int}$, $T_h$ and $T_c$ can be solved for as a function of current. This was the first model which solved for temperatures of the module solely based on current. Previous attempts to

model thermoelectric refrigeration required knowledge of the temperature difference across the module or the temperature of TER to be able to predict the system's performance. The cooling power of TEMs, the desired temperature difference, the number of TEMs was coupled constraints in modelling. The TEMs have a maximum cooling power because Joule heating counteracts the Peltier effect. In order to increase the cooling power, different approaches were taken. Multiple modules were implemented, or the thermal resistances were lowered to increase the amount of heat absorbed/rejected by the TEM.

The equation (II.13) is given by a steady-state energy conservation of the refrigeration system. This equation matches the heat removed from the TEC internal space with the heat transfer from the environment into the internal TEC area:

$$Q_c = \frac{T_{int} - T_c}{\psi_c} = \frac{T_{ambient} - T_{int}}{\psi_{TER}} \tag{II.19}$$

where $\psi_{TER}$ is the thermal resistance between the TEC internal space and the environment, or the insulation.

With three equations and three unknowns, the temperatures of the TEC internal space $T_{int}$ and the hot $T_h$ and cold side $T_c$ temperatures of the modules can be solved along with the cooling power $Q_c$. The chamber temperature is given by:

$$T_{int} = \left(\frac{1}{\psi_{CT}}\right)\left[\psi_c . T_{ambient} + \psi_{TER}\left(\frac{T_{ambient} + \psi_h I^2 R + \frac{1}{2}\frac{\psi_h \alpha I^2 R + I^2 R}{\kappa} + \left(\frac{\psi_h}{\psi_{CT}} + \frac{\psi_h \alpha I}{\kappa \psi_{CT}} + \frac{1}{\kappa \psi_{CT}}\right) T_{ambient}}{\frac{\psi_h}{\psi_{CT}} + \frac{\psi_h \alpha I + 1}{\kappa \psi_{CT}} + 2\psi_c \alpha I + \frac{\psi_h \alpha^2 I^2}{\kappa} + \frac{\alpha I}{\kappa} + 1}\right)\right] \tag{II.20}$$

where

$$\psi_{CT} = \psi_c - \psi_{TER} \tag{II.21}$$

By applying the first law of thermodynamics, the electric power input in watts required to produce the effect described in equations (II.10) and (Ii.11) can be written as [91]:

$$W = Q_h - Q_c \tag{II.22}$$

which is also equal to:

$$W = \alpha(T_h - T_c).I + R.I^2 \tag{II.23}$$

also,

$$W = V.I \tag{II.24}$$

Hence, voltage becomes

$$V = \alpha(T_h - T_c) + I.R \tag{II.25}$$

The coefficient of performance COP of TER is similar to the thermal efficiency and it is defined as the ratio of the cooling power (or heating power) to the input power [92].

$$COP = \frac{Q_c}{W} = \frac{T_c}{T_h - T_c} \tag{II.26}$$

Substituting Equations (II.10) and (II.11) into (II.23), (II.26) gives [93]

$$COP = \frac{\alpha.I.T_c - 0.5R.I^2 - \kappa.(T_h - T_c)}{\kappa(T_h - T_c).I + R.I^2} \tag{II.27}$$

There are two design patterns including the maximal cooling efficiency design mode and the maximal cooling production mode. The operating mode is changed by changing the voltage. Cooling production $Q_c$ should be correlated with the thermoelectric energy consumption. For maximum cooling power, $Q_{c_max}$ the optimum input current can be found by differentiating Equation (II.10) with respect to current and setting it to zero as follows [93]

$$\frac{\partial Q_c}{\partial I} = \alpha.T_c - R.I = 0 \Longrightarrow I_{mp} = \frac{\alpha.T_c}{R} \tag{II.28}$$

The current in Equation (II.28) can also be represented in terms of $T_c$ [93]:

$$I_{max} = \frac{\alpha(T_c - \Delta T_{max})}{R} \tag{II.29}$$

The maximum temperature difference $\Delta T_{max}$ is the maximum possible difference in temperature which always occurs when the cooling power is at zero and the current is maximum. This is obtained by setting $Q_c = 0$ in Equation (II.10) substituting both $I$ and $T_c$ by $I_{max}$ and $T_h - \Delta T_{max}$, respectively, and solving for $\Delta T_{max}$. The maximum temperature difference is obtained as [93]

$$\Delta T_{max} = \left(T_h + \frac{1}{Z}\right) - \sqrt{\left(T_h + \frac{1}{Z}\right)^2 - T_h^2} \tag{II.30}$$

where the figure of merit $Z$ (unit: $Z^{-1}$) is defined as [93]

$$Z = \frac{\alpha^2}{\rho k} = \frac{\alpha^2}{R\kappa} \tag{II.31}$$

The maximum cooling power $Q_{c_max}$ is the maximum thermal load which occurs at $\Delta T = 0$ and $I = I_{max}$. This can be obtained by substituting both $I$ and $T_c$ by $I_{max}$ and and $T_h - \Delta T_{max}$, respectively, and solving for $Q_{c_max}$. The maximum cooling power for a thermoelectric module with $n$ thermoelectric couples is [93]

$$Q_{c_max} = \frac{n.\alpha^2(T_h - \Delta T_{max})}{2.R} \tag{II.32}$$

The maximum voltage is the DC voltage which delivers the maximum possible temperature difference $\Delta T_{max}$ when $I = I_{max}$. The maximum voltage is obtained from Equation (II.25), which is [93]

$$V_{max} = n.\alpha T_h \tag{II.33}$$

Usually, there are some factors should be taken into account before determining whether adopting maximal cooling production or maximal cooling coefficient design. The primary important factor is the temperature difference between hot side and cold side. Considering the practical operating condition, the theoretical analysis is carried out by setting the temperature of cold side as a constant.

The maximum COP can be obtained by differentiating Equation (II.26) with respect to current and setting it to zero as follows [93,94,95-97]

$$\frac{\partial(COP)}{\partial I} = 0 \Longrightarrow I_{COP} = \frac{\alpha.\Delta T}{R\left[(1+Z\bar{T})^{\frac{1}{2}}-1\right]} \tag{II.34}$$

$$COP_{max} = \frac{T_c}{T_h - T_c}.\frac{\sqrt{(1+Z\bar{T})}+\frac{T_h}{T_c}}{\sqrt{(1+Z\bar{T})}+1} \tag{II.35}$$

where

$$Z\bar{T} = ZT_h\left(1 - \frac{\Delta T}{2T_h}\right) \tag{II.36}$$

A higher value of $Z\bar{T}$ is desirable for both cooling and power generation applications. The difficulty of maximizing $Z\bar{T}$ lies in the fact that the above parameters are generally interdependent [98-99]. Therefore, it is a challenge to develop advanced thermoelectric materials with an optimization of these conflicting properties to increase $Z\bar{T}$. Current thermoelectric devices are considered to be;

- inefficient when ZT is about 1.
- able to recover waste heat when ZT = 2.
- able to match a refrigerator when ZT = 4/5 [100].

For a long time, the best $Z\bar{T}$ has been one for material bismuth telluride $Bi_2Te_3$, which translates to efficiencies of about 5-7% for most applications but falls off rapidly with hot side temperatures of over 230°C [101].

| **Temperature [°C]** | **Type** | **TEM Material** | **ZT Value (Maximum)** |
|---|---|---|---|
| < 150 | p-type | Bismuth Telluride $Bi_2Te_3$ | 0.8 |
| | n-type | Bismuth Telluride $Bi_2Te_3$ | 0.8 |
| 150-500 | p-type | $Zn_4Sb_3$ | - |
| | p:n-type | PbTe | 0.7-0.8 |
| | p-type | TeAgGeSb(TAGS) | 1.2 |
| 500-700 | p-type | $CeFe_4Sb_{12}$ | 1.1 |
| | n-type | $CoSb_3$ | 0.8 |
| 700-900 | p:n-type | SiGe | 0.6-1.0 |
| | p-type | LaTe | 0.4 |

Table II.2 The characteristic of available TEMs materials [102,103]

A dimensionless cooling power $(Q_c/Q_{c_max})$ and COP vs. dimensionless current $(I/I_{max})$can be presented graphically as shown in Figure II.8 assuming $Z\bar{T}_c = 1$. The dimensionless cooling power is obtained from the cooling power found in equation (II.10), where the current is the only variable, and from the maximum cooling power equation (II.32) at given thermoelectric material properties and hot side temperature. This generalized plot shows that the cooling power is inversely proportional to the coefficient of performance especially at smaller temperature difference. Moreover, increasing the temperature difference across the junction will decrease the cooling power and the performance of the TEC [93].

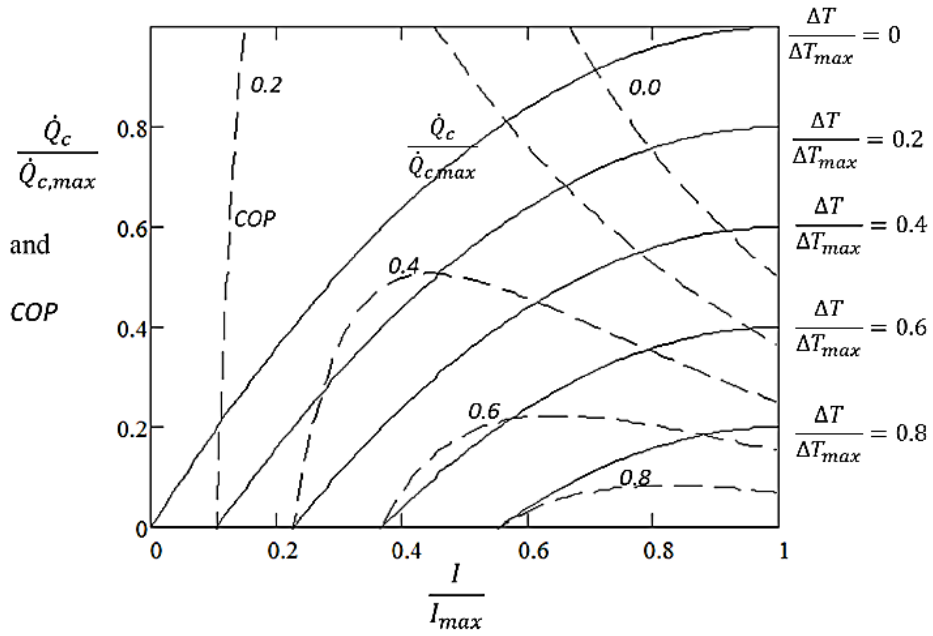



Figure II.8 Generalized charts for TEC where $Z\bar{T} = 1$ [104].

This analysis represents the concepts of only one thermoelectric module where multiple couples are being used in many of the cooling applications. In order to obtain the thermoelectric cooler (TEC) parameters for multiple couples as shown in Figure II.1(a), the unit couple parameters need to be multiplied by the number of couples, $n$, as follows [93]

$$(Q_c)_n = nQ_c \tag{II.37}$$

$$(Q_h)_n = nQ_h \tag{II.38}$$

$$(W)_n = nW \tag{II.39}$$

$$(R)_n = nR \tag{II.40}$$

$$(V)_n = nV \tag{II.41}$$

$$(\kappa)_n = n\kappa \tag{II.42}$$

$$(I)_n = nI \tag{II.43}$$

$$(COP)_n = \frac{(Q_c)_n}{(W)_n} = COP \tag{II.44}$$

The objective of the current chapter can be defined as design and thermal modeling of a thermoelectric cooling system using theoretical and numerical simulation.

## II.4. Results and Discussions

A thermal analysis was completed for the TEC system to predict the performance. Heat transfer was modeled between three bodies, the thermoelectric modules (TEMs), the environment, and the inside the cooler system. Overall, the system parameters were analyzed using MATLAB simulations to prove that the authenticity formulae used in theory are self-sufficient to be applied in real applications. The general system modeling was done in a three-part process: first, the analysis involved multiple models of heat sinks, and material properties subjected to varied working conditions. The second part consisted of a model that predicted the performance of the TEMs based on the simulation conditions.

The assumptions made in this study for modeling were based mostly on the principles surrounding the energy balance equation:

(a) Heat transfer is assumed to take place along the length of TE elements.
(b) The thermoelectric elements have the same cross-section and length.
(c) Thomson effect is not considered.
(d) Steady-state condition is prevailing.
(e) the refrigeration system has a one-dimensional heat flow, constant properties of all materials, and uniform temperature distribution across an infinitesimally small control volume.

Validation of existing thermoelectric module is done to prove the authenticity of the ideal equations using MATLAB functions. A comparison is done between the analytical modeling and MATLAB simulation of the modules under various conditions. Contact resistance is a parameter in studying the behavior of thermoelectric materials that defines the total output of a given module. In the following results, we understand the importance of contact resistance to provide better cooling system performance when contact resistance is included at a constant input current.

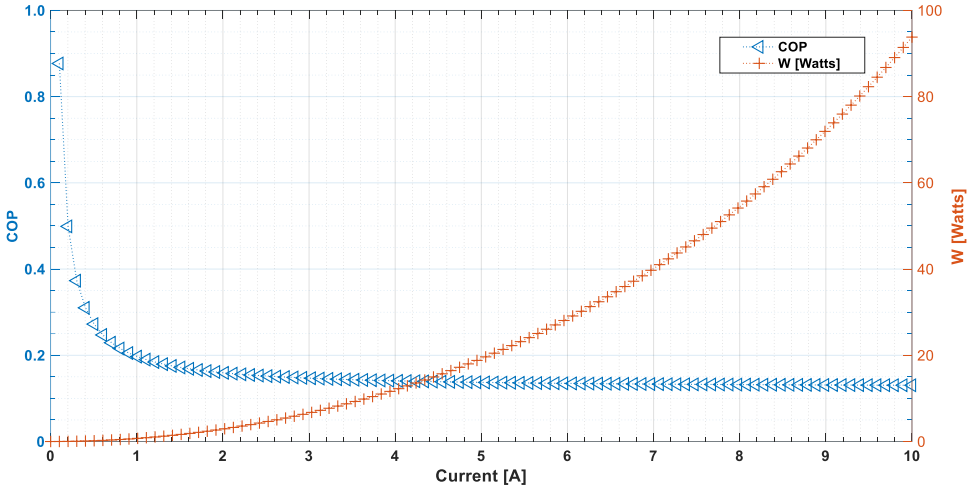
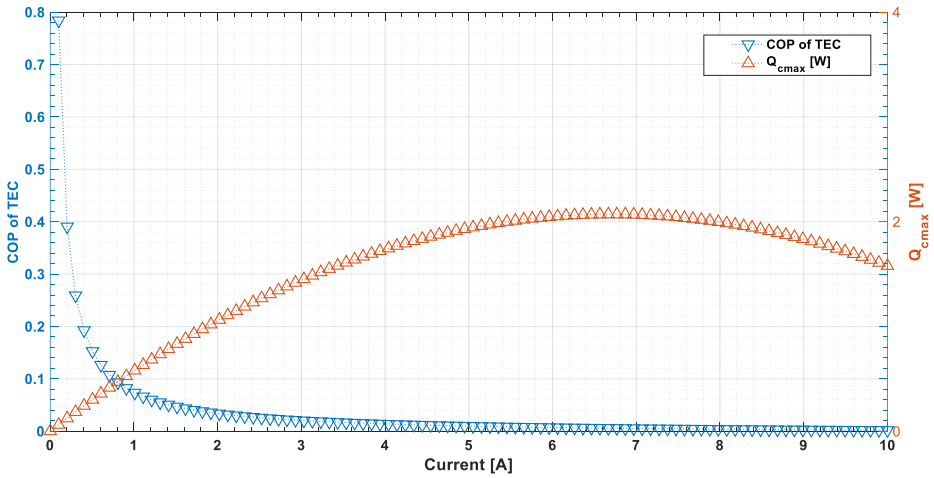
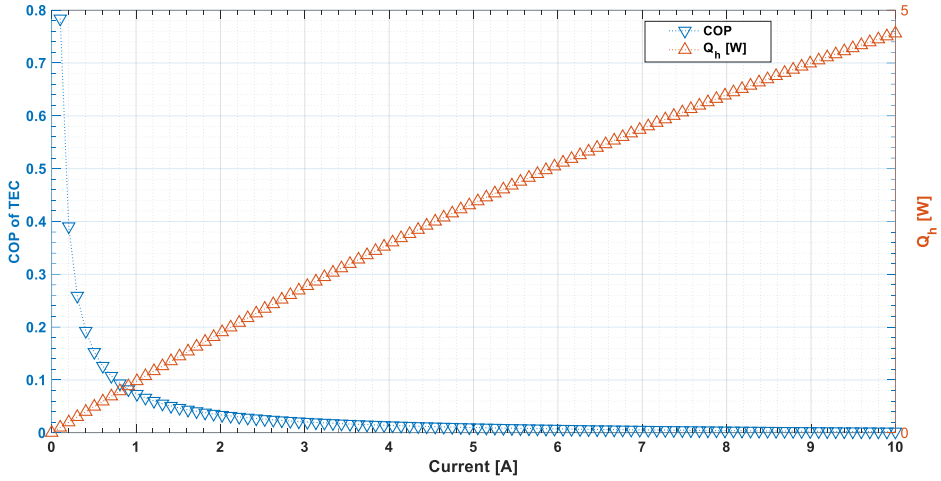



Figure II.9 COP and Power consumption as a function of current.

The COP, power consumption of the TEC system as a function of current are shown in Figure II.9. There is no optimum supply condition for either minimum power consumption or maximum COP. Instead, it was found that more electric supply will lead to more power consumption and a lower COP; however, the system increases in size, and the required cooling power also decreases. Furthermore, for this system, the required cooling power decreases more dramatically than the energy to cool the internal area of TEC system, resulting in a lower COP with increasing of current.




(a)




(b)

Figure II.10 Cooling/Heating power and COP versus input current for given model: (a) Cooling mode and (b) Heating mode.

In Figure II.10(a), the maximum cooling power and COP indicated by red and blue dashed lines, respectively, show fair agreement with data provided in [105]. Similarly, Figure II.10(b) illustrates the heating power and COP versus input current compared against Feher's variable temperature seat VTS heat pump data for the heating mode with good accuracy. The simulation results showed her also acceptable agreement with Feher's experimental data when the flow rate was increased [106].

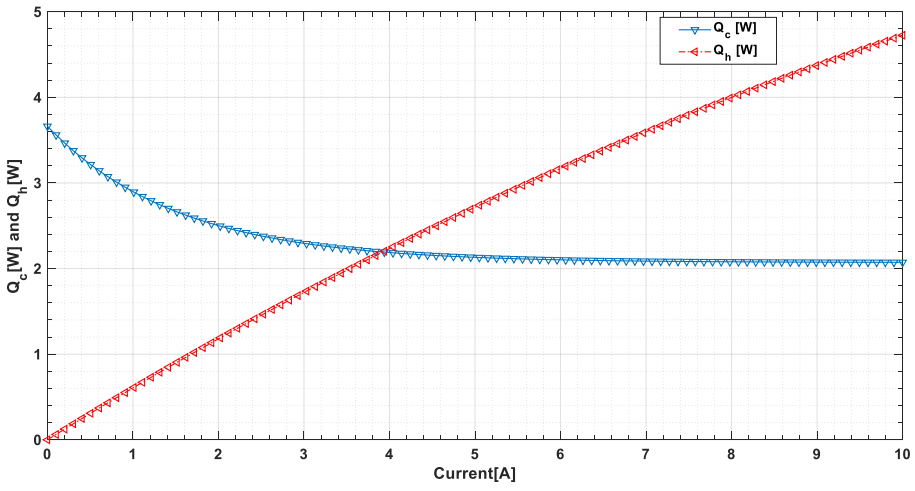



Figure II.11 TEC junctions Cooling/Heating power versus input current.

The simulation results of the heating and cooling power flow are also evaluated at different applied input current values as shown in Figure II.11. These results indicate a good variation although with small errors in the cold and hot junction temperatures. This is usually because

the theoretical junctions' temperature across the thermoelectric device has equal values even at higher input current values.

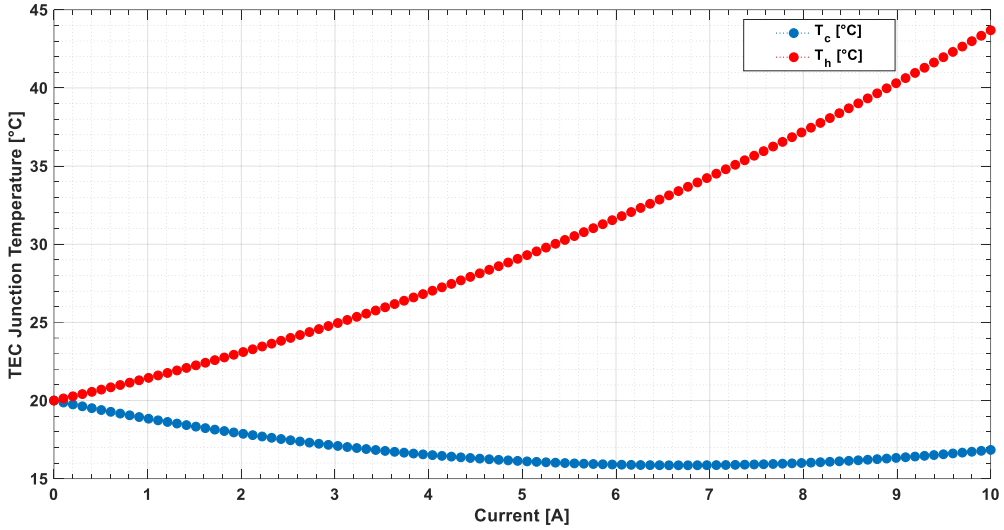



Figure II.12 TEC Hot and cold junction temperatures versus current.

As discussed earlier, one of the thermoelectric devices advantages is that they can provide temperature difference on their two sides, which can be used as a source of cooling and heating depending on the surrounding conditions. The heating mode for the thermoelectric module can be achieved simply by reversing the direction of the applied input current. The analytical cold and hot junction temperatures were simulated with good agreement at variable input current, as shown in Figure II.12.

It can be shown by substituting Equation (II.16) into Equation (II.17) and setting the derivative with respect to current equal to zero ($I = 0$) that the minimum temperature and the maximum cooling power occur at the same current, because the ambient temperature and the insulation thermal resistance do not depend on the current. However, the expression for the optimum current was found to be too complex to present easily.

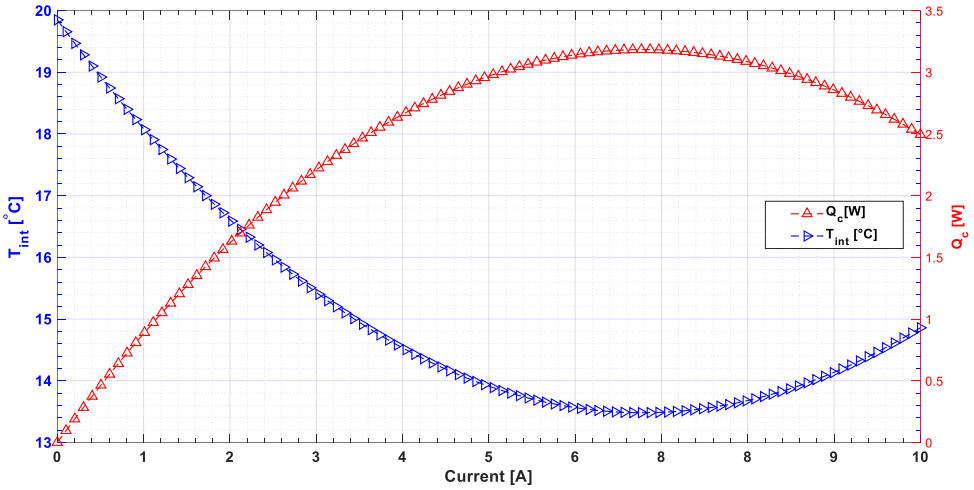



Figure II.13. Refrigeration chamber temperature and cooling power as a function of current.

The minimum temperature and cooling power as a function of current are shown in Figure II.13 for a given system. The maximum cooling power and minimum temperature occur at the same current value, which remains consistent with the ideal model of conventional approaches. The maximum cooling power is not zero, indicating that heat is constantly removed from the system to offset the heat gained from the environment. The optimum current and minimum temperature of the ideal model are depicted in Figure II.13. The optimum current is significantly higher and the minimum temperature is lower than achievable for the system. At the current suggested by the ideal model, the real system would actually heat the system rather than cooling it.

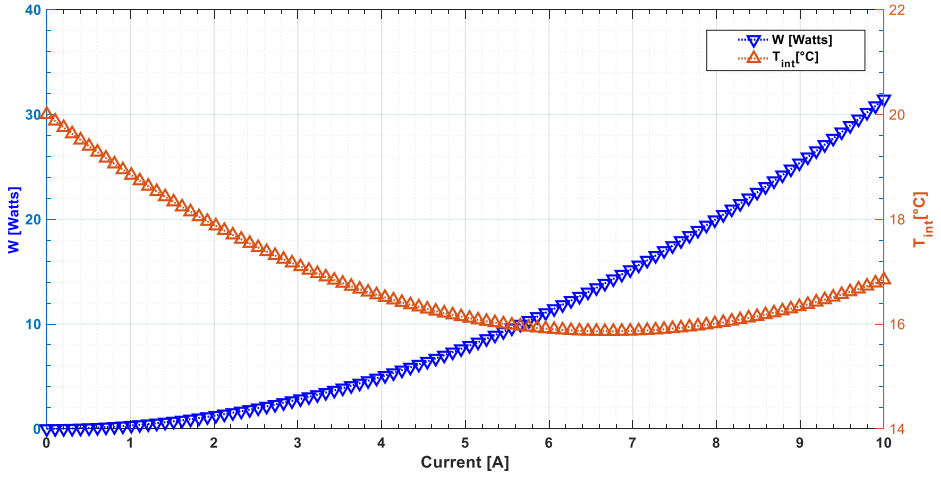



Figure II.14. Power consumption and temperature comparison of the model and the experiment.

Figure II.14 compares by modeling and numerical simulation of the cooling temperature and power consumption of given thermoelectric cooler system (TEC). The steady state temperatures for different current values and power consumption at the minimum cooling temperature are

illustrated. The simulation results fell within 5% of the model predictions. The temperatures were recorded when the system reached steady-state, determined by temperature changes less than 0.1°C in 5 sec. The necessary power given during steady-state operation, and includes 2 W of power needed to run the fan.

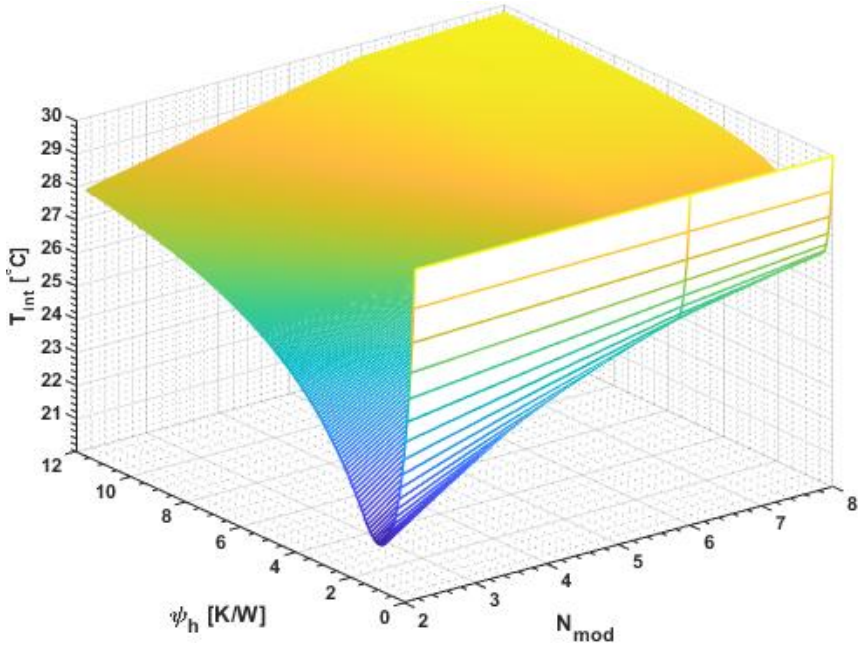



Figure II. 15 Effect of heat sink thermal resistance $\psi_h$ and number of modules $N_{mod}$ on the internal space temperature $T_{int}$ profile.

To achieve thermal impedance matching between the used thermoelectric modules number and the hot/cold side heat sink thermal resistances. The cooling temperature variation of the TEC internal space with variation on TE module number and heat sink hot-side thermal resistance is illustrated in Figure II.15. With increase in the number of modules, the internal cooling temperature increased rapidly. Since the heat input to the refrigerator system increases with increase in the number of TE module, which means that the hot-side temperature of the TE module will increase. The internal space cooling temperature also increases with increase in the heat sink thermal resistance value. Figure II.15 shows that the TE module number and thermal contact resistances variation influence on refrigerator cooling performance.

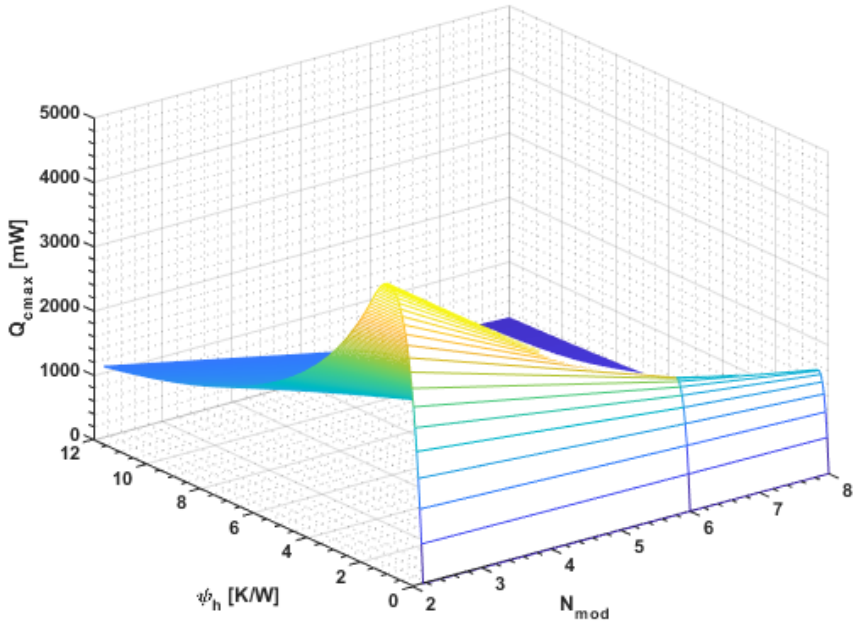



Figure II. 16 Effect of heat sink thermal resistance $\psi_h$ and number of modules $N_{mod}$ on the maximum cooling power $Q_{c_max}$ profile.

The maximum cooling power variation was also studied to achieve matching impedance between the used thermoelectric modules number and the hot-side heat sink thermal resistance is illustrated in Figure II.16. With increase in the number of modules, the TEC maximum cooling power is decreased. The maximum cooling power value also increases rapidly with increase in the heat sink thermal resistance until reaches the value of $\psi_h = 2\ [K/W]$ which corresponds to a maximum value of $Q_{c_max} \approx 4W$ then decreases rapidly. Thus, the TE module number augmentation and thermal contact resistances variation influence on refrigerator maximum cooling power performance.

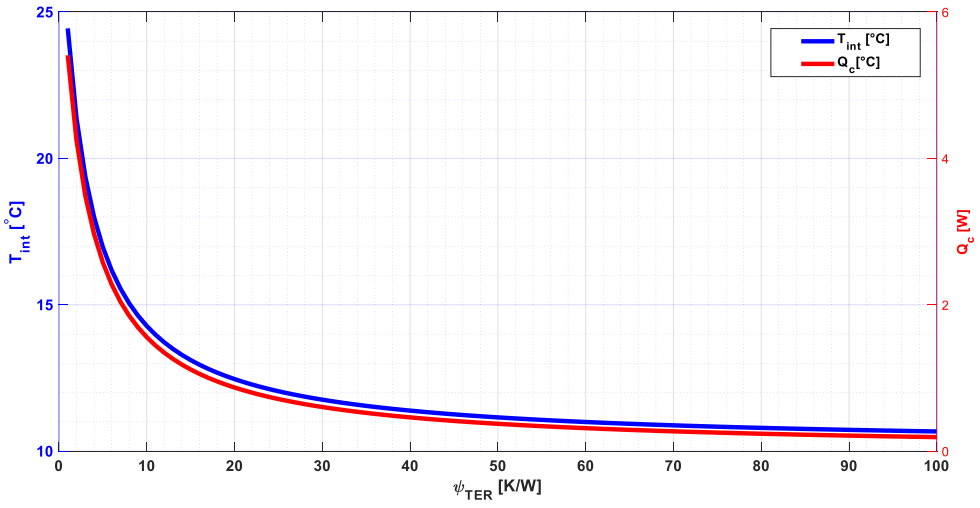



Figure II. 17 Thermoelectric cooling system thermal resistance sensitivity.

The thermal resistance between the cooler internal space, the thermoelectric module, and ambient were considered to improve the performance of the cooler and their effects on the TEC system constraints. Both the TEMs hot and cold side thermal resistances should be lowered to minimize the temperature differences between the hot side of the module and ambient, and between the cold side of the TEM module and the internal space temperature.

Additionally, the cooler internal space resistance should be increased to insulate the system and reduce the heat gain that the module would have to overcome. Figure II.17 shows the change in minimum steady-state thermoelectric cooler temperature and the maximum cooling power rate as one thermal resistance of the cooler system changes while the other two are fixed.

## II.5. Conclusion

This chapter presents a modeling approach to determine the cooling optimum performance as well as the optimum geometry to power a small thermoelectric refrigeration system. The model is derived from three energy conservation equations for temperatures at both ends of the thermoelectric materials within a TEM module, as well as the cooling temperature required.

Modeling approach was provided that accounts for realistic working conditions with simulation results. A further module geometry study was carried to meet the cooling temperature range. With module changes, the temperature goal could be reached, while also reducing the power consumption, and the theoretical size of the cooling system. The design process used in this study focuses on meeting the demand criteria of the application rather than optimizing the system, because no thermal optimization occurs. Current and module optimization were provided to reach minimum temperatures required.

One of the objectives of the present chapter was to investigate the optimal design of a thermoelectric cooler applied for a thermoelectric cooler control. This optimization utilizes a newly developed optimization theory with the dimensional technique to simultaneously obtain the optimum combination of the dimensionless applied current and the dimensionless thermal conductance to determine the optimum cooling/heating power and COPs suitable for a refrigerator temperature controlled. The optimal design of heat pump was analyzed maintaining the same input parameters and overall geometry. The optimized results indicated a decrease in the COP by about 10% in the cooling mode.

# Chapter III

# PID CONTROL DESIGN OF THERMOELECTRIC COOLER

## III.1. INTRODUCTION

Thermoelectric refrigeration has the outstanding advantage of allowing accurate temperature control during heating/cooling has gained increasing attention [107–110,111]. However, on the market there are thermoelectric refrigerators which include on/off temperature control systems, because of their simplicity and low cost. The major problem with this system is that, when the thermoelectric modules are switched off, the heat stored in the heat exchanger at the hot end of the modules goes back into the refrigerator, forming a thermal bridge.

In this chapter, we use a computational model, presented and validated in previous chapter, to study and assess the influence of PID in cooling performance of the TEC system.

A new system model is introduced based on idling currents; that is, once the temperature of the refrigerator reaches the lower limit, the thermoelectric modules are not switched off but supplied with minimum current values. This model simulates the performance of the thermoelectric refrigerator, the heat exchangers, and the thermoelectric modules. Computational results prove that this system reduces the electric power consumption of the refrigerator by at least 40% with respect to that obtained with on/off control systems, and the coefficient of performance increases close to the maximum provided by any other control system.

Some manufacturers provide thermoelectric refrigerators with improved temperature control systems, such as those featuring different levels for the voltage supplied to the modules [112-113] or those including proportional–integral–differential (PID) control systems [114-117, 118]. These two systems improve the performance of the thermoelectric refrigerator and reduce the electric power consumption (EPC) to a great extent. However, their cost is around four times as high as that of a simple on/off control system [119], which explains why there are so many thermoelectric refrigerators on the market including cheap on/off temperature control systems.

Among the types of control used in residential and industrial installations, the PID methods are the most accurated and recommended [111], [114–116], [118]. Due to their simplicity and ability to provide an excellent control performance, they constitute a good solution to the control of large number of current industrial processes, because the implementation of the PID is based on a digital design. Thus, these digital PID include many algorithms to improve their performances, such as autotuning, anti-windup mechanisms, fuzzy fine-tuning, and adaptive.

However, the basic actions remain the same [120]. PID control is based on the mathematical modeling of a problem, represented by a process loop to control.

There exist several approaches for the enhancements of thermoelectric cooling control system performance including Proportional-Integral-Differential (PID) Control which as the most accurated and recommended [114-117,120].

Some methods that combine PID control with fuzzy logic control have been applied in the field of temperature control [121]. From the previous concepts, the thermoelectric cooling system performance has been guaranteed by controlling the variation of input current.

The main objective of this chapter is to provide numerical approach in order to evaluate the TEC performance through its operational parameters. The purpose of cooling system control is expected to keep the internal temperature of an object below the ambient temperature of around 30°C. The refrigerator system was modeled and controlled using the PID based Matlab/Simulink and S-function block to set the error between input current profile and cold-side desired temperature of TEC cooler system.

## III.2. Temperature control approach of TEC

The refrigeration capacity of the TEC refrigerator is affected by the ambient temperature. The lower temperature limits a semiconductor refrigerator can reach is not the same under different ambient temperature conditions. The theoretical expressions developed in [122] are the subject of the control approach proposed in this part.

When designing TEC control, the input electric current must be regulated. The direction of current flow can achieve the conversion between heating and cooling in TEC.

### III.2.1. Structure Design of Control System

Temperature Control systems can be divided into two categories: open-loop control systems and closed-loop control systems. There is no temperature measuring element in the open-loop control system and no feedback signal is used. The system block diagram is shown in Figure III. 1. The advantage of the open loop system is that the system has a simple structure and is easy to debug. However, when the working environment and the performance parameters of the system components change, the controlled quantity of the open loop system will be greatly affected.

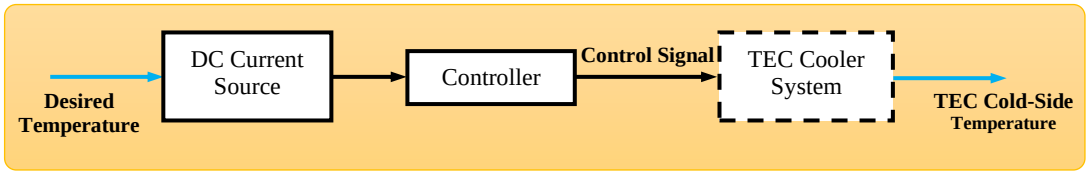



Figure III.1 Open-loop Control system block diagram.

Generally, a high-precision open-loop control system requires that all components have high accuracy and very stable performance. That is, the open-loop control has stricter requirements on the environment and components.

On the other hand, the output signal of the closed-loop control system is not only controlled by the input signal, but also by a feedback signal that is proportional to the output signal. The system block diagram is shown in Figure III.2.

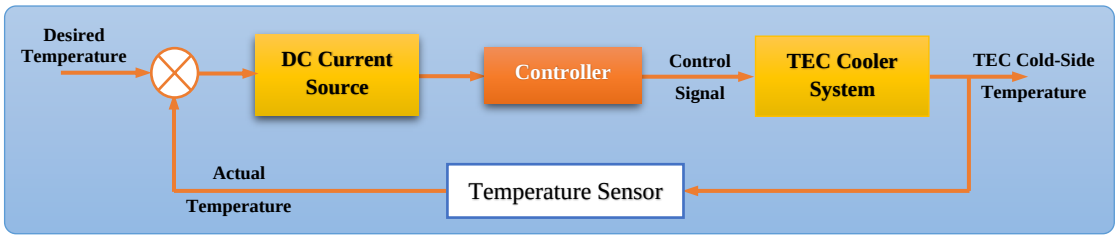



Figure III. 2 Typical temperature feedback control system.

The closed-loop control system itself can detect the difference between the set value of the controlled quantity and the real value. This control structure can significantly reduce the adverse effects of certain component parameters and control object parameters on the controlled quantity, so the requirements for these components are not very strict [120,123].

The closed-loop temperature control system generally consists of three parts: a temperature sensor, a temperature controller, and a temperature regulator.

The temperature sensor collects the temperature of the controlled object, and the temperature controller controls the temperature regulator to heat or cool the controlled object according to the actual temperature compared with desired temperature.

## III.3. PID control algorithm design

This chapter aims to investigate numerically the thermal performance in terms of cooling behavior efficiency of TEC cooler, which was improved and verified with a PID control algorithm.

This type of control works with the difference between the expected value of a process variable and its real value, measured using a sensor. It allows the control with low offset error and good stability, which is the reason why it is widely used in academic projects and industry [123-124].

The proportional action (P mode) adjusts controller output according to the size of the error. It is based on current behavior of the system. The integral action (I mode) is the accumulated effort using the experience information of bygone state to eliminate the steady-state offset and the future trend is anticipated via the derivative action (D mode), which makes use of the predicted future values of the control error and accelerate thus the response time. In order to enjoy the advantages of each of these control modes, these three actions are combined, in such a way that a stable feedback controller is produced, and the control output at desired setpoint is delivered (see Figure III. 3).

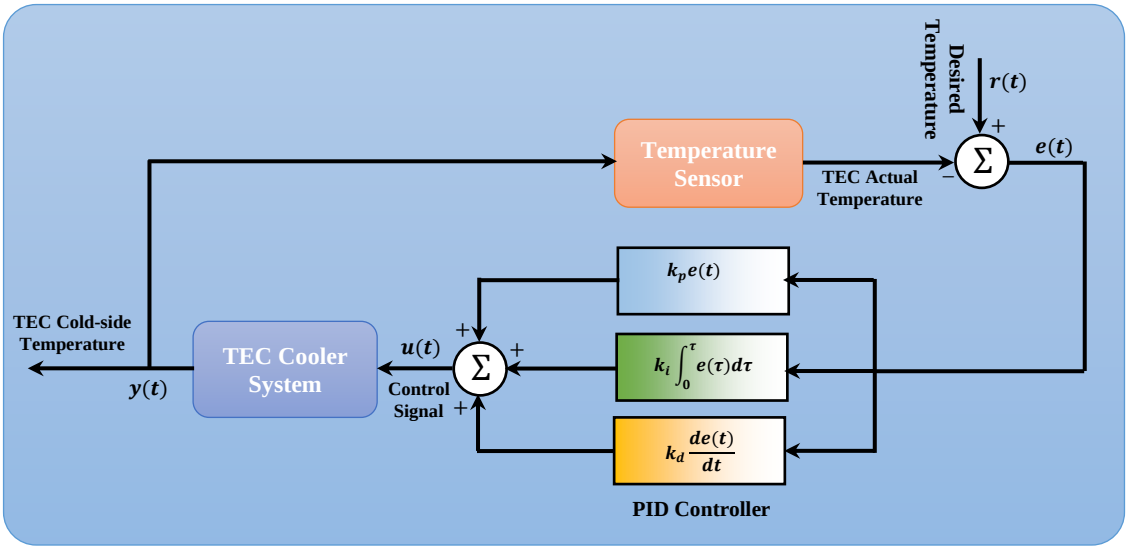



Figure III.3 Functional block diagram of PID controller.

Figure III. 3 shows a closed loop of our thermoelectric cooler control system [125], in which a PID controller operates. A set-point is defined, i.e., a desired value for the controlled variable. The exit of the loop is a sensor that monitors the value of the same variable. The system calculates the difference between the set-point and the measured value and transmits it to the PID controller, which acts to reduce this difference to zero. In the actual system, the Plant is the TEC cooler.

Continuously, a PID controller algorithm calculates an error value $e(t) = r(t) - y(t)$ as the difference between a desired setpoint $r(t)$ and a measured process variable $y(t)$ as the feedback

signal from the process plant and produces a combined response or controlled output signal $u(t)$ which is applied to plant control devices.

Tuning of the PID controller can be performed by understanding the effects each term has on the response. Table III.1 illustrates the behavior of each term as related to the tuning specification. Following these guidelines, the present system has been tuned to shorten settling time when reaching a steady state signal, while also trying to minimize system overshoot.

| | **Transient response** | **Steady-state response** | **Tunning Comments** |
|---|---|---|---|
| **P** term | Increasing $k_p$ generates faster response | Increasing $k_p$ reduces steady-state offset but does not remove it | Increasing $k_p$ increases control signal bandwidth; expect greater signal oscillation with faster control response |
| **I** term | Increasing $k_i$ generates several responses depending on transient signal, may be unstable | Introducing $k_i$ eliminates steady-state offset over time | Increase integration time when fixed input and stable output are required; expect response time to be slower |
| **D** term | Increasing $k_d$ generates several responses and may be unstable, but can be tuned to dampen response | Introducing $k_d$ has no effect on steady-state behavior | Consider transience of input signal; low frequency input can afford longer derivative time for greater damping; expect oscillations for higher frequencies |

Table III.1 Tuning effects of PID controller terms.

The gains or adjustment parameters of the PID can be obtained by different methods. In this work, trial and error method has been adopted; this method makes the adjustment relatively easy. The first step is to set I and D terms to 0. Then, we increase the proportional gain P until we notice an oscillation in the response, which should revolve around the set point. Care should be taken with the stability of the system. From there you can change the full term of the controller. Increasing this term reduces the error between the actual temperature and the desired.

Finally, also modifying the value of the derivative term generates a decrease in overshoot, an increase in gain a maintain of stability, thus providing a system that is very sensitive to noise. The latter parameter is generally used only in systems that require greater precision and control to dealing with sudden and rapid changes in external parameters.

The temporal representation of the actions described above is given below:

$$u(t) = k_p e(t) + k_i \int e(\tau)d\tau + k_d \frac{de(t)}{dt} \quad \text{(III.1)}$$

where $k_p$, $k_i$, and $k_d$ denote respectively, the proportional, integral, and derivative action gain.

The temperature of the thermoelectric cooler system has been set to shorten the stabilization time upon reaching a steady-state signal, while trying to minimize the overshoot of the desired temperature [126,127]. PID regulator is based only on the variation of the temperature measured inside the thermoelectric cooler and not on the knowledge of the underlying system. The response of the controller can be described in terms of the difference made between the desired temperature and the measured temperature [128-129].

$T_p$ is now the sampling period, at a series of sampling points $kT_p$ represents a continuous time $t$. In order to sum data to replace the integral approximately. After the first order, take the difference to replace the integral approximately. To do the following approximate transformation:

$$T_p = kT_p \quad \text{(III.2)}$$

$$\int_0^t e(t) = T_p \sum_{j=0}^{k} e(jT_p) = T_p \sum_{j=0}^{k} e(T_p) \quad \text{(III.3)}$$

$$\frac{de(t)}{dt} = \frac{e(kT) - e[(k-1)T_p]}{T_p} = \frac{e(k) - e(k-1)}{T_p} \quad \text{(III.4)}$$

Among them, $e(k)$ for the system of the deviation of the sampling time of the $k$, $e(k-1)$ for the system of the deviation of the sampling time $(k-1)$, $k$ for sample serial number, $k = 0,1,2,..$ Take the above type in equation (III.3) and (III.4) in the equation (III.1). We can get the discrete PID expression:

$$u(k) = k_p \left( e(k) + \frac{T_p}{T_I} \sum_{j=0}^{k} e(j) + \frac{T_D}{T_p} [e(k) - e(k-1)] \right) \quad \text{(III.5)}$$

Take $\Delta u(k) = u(k) - u(k-1)$, then

$$\Delta u(k) = a_0 e(k) + a_1 e(k-1) + a_2 e(k-2) \quad \text{(III.6)}$$

with: $a_0 = k_p(1 + \frac{T_p}{T_I} + \frac{T_D}{T_p})$, $a_1 = k_p(1 + \frac{2T_D}{T_p})$, $a_2 = k_p(\frac{T_D}{T_p})$.

The equation (III.6) is the incremental PID control algorithm. Its program flow chart is shown in Figure III.4 below.

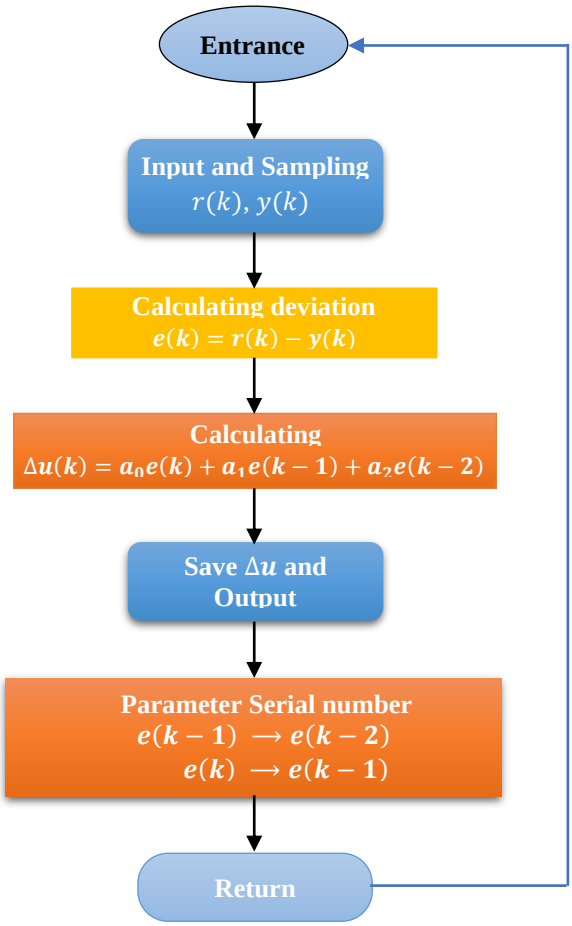



Figure III.4 Incremental PID control algorithm program flow chart.

The feedback control loop designed to regulate the cold flow of the TEC module which decreases the refrigerator actual temperature is based on the minimization of the quantity [124]:

$$e(t) = T_{C_Actual}(t) - T_{C_ref}(t) \tag{III.7}$$

where $T_{C_ref}(t)$ is the user-defined reference cold side temperature of the TEC.

In the closed-loop of the TEC system simulation model, the cold side reference temperature of the TEC model is chosen to be equal to the DC power supply current form as below:

$$T_{C_{ref}}(t) = f(I(t)) \tag{III.8}$$

The TEC model presented in MATLAB/Simulink illustrated in Figure III.6 is developed as a function of time to approximate the evolution of the parameters depending on the temperature

over the length of TEC. S-Function proposed allowing to process a set of programs and interface it with the MATLAB/Simulink model to allow dynamic changes of TEC parameters.

The actual values of $T_h$, $T_c$, and $I$ are respectively used at the input of the thermoelectric refrigeration simulation model. To start the simulation, the initial values shown in Table II. 2 (in chapter II) have been used. The output of this S-function is again used as feedback for the next simulation step.

Some applications require using only one or two terms and setting the other parameters to zero in order to achieve the performance of the appropriate system control. The PID controller is quite more efficient, since the measurement noise of the sensors affects the sensitivity of the derivative action, whereas the absence of an integral action may prevent the closed-loop system from reaching its desired performances [128].

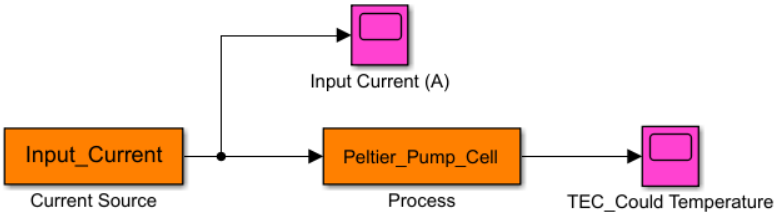



Figure III. 5 Open-loop Simulink block diagram.

Process simulation is necessary to specify effect all variables on the system and then the limiting which variable has a bigger effect during the process [129–130].

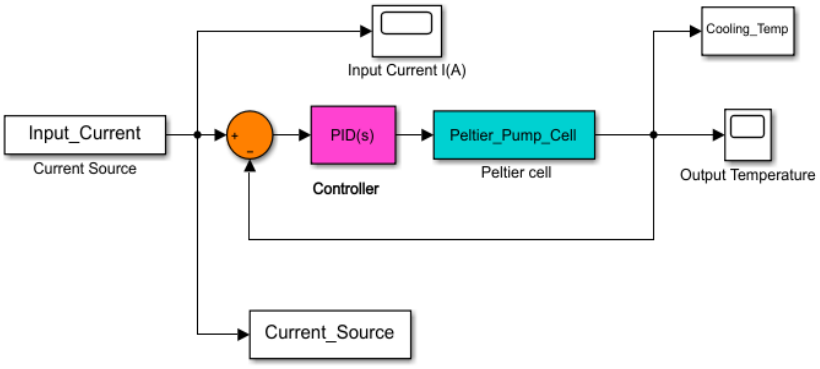



Figure III. 6 Closed-loop Simulink block diagram.

In this study, Simulink/Matlab has been used to the simulation of the TEC cooler model. Simulink of dynamic simulation diagram for open loop system is shown in Figure III. 5, and the Simulink simulation diagram with PID controller is shown in Figure III. 6.

The developed PID controller has been implemented on Matlab/Simulink model in order to impose for simulation the different temperature gradient from the temperature values taken on the cold side of the TEC model. Generation of a certain waveforms of the input DC current is expected to produce specific of TEC cold side temperature response.

However, it is tricky designing a controller adapts to these input and output waveforms of the system. The refrigerator thermal behavior is dynamic and inherently nonlinear. As for the parameters of the PID controller, they will often vary in optimal values under different operating states. Fortunately, in thermoelectric refrigeration systems, the temperature response is slowly occurring over several moments. This allowed us to adjust the PID controller in real-time and by simple modifications of its parameters.

The Zeigler-Nichols closed-loop method is used to manually adjust the PID controller parameters with keeping constant two parameters and varying the remaining ones until the overshoot and settling phase specifications were reached on all ranges of interest [131].

## III.4. Results and discussions

based on the results obtained in the previous chapter, a numerical modeling approach is proposed in order to evaluate the TEC performance through its operational parameters. The refrigerator system was modeled and controlled using the PID based Matlab/Simulink and S-function block to set the error between input current profile and cold-side desired temperature of TEC.

In order to reach the maximum cooling temperature and to ensure the cooling effect of the TEC, the following suppositions and conditions are taken into account:

- The controlled temperature of the Thermoelectric cooler is not lower than the ambient temperature, that is, there is no external heat transfer to the internal space of TEC.
- The cold side of the TEC contact with the heat sink exchanger completely or insulate the untouched parts, that is, there is no heat loss in TEC.
- The temperature rise of the pipe heat conduction sleeve (HCS) can be used to control the cooling capacity of the thermoelectric cooler (TEC) through controlling the electric current using PID algorithm, which is easier to control than air-cooling system [132].

PID Control block receives the values of ($k_p,\ k_i,\ k_d$), and the desired temperature value $T_{c_ref} = 5\ °C$ after computing the difference between this value and the temperature of the cold

side of the TEC Module. The initial value of TEC cold side temperature has been chosen to be equal to the ambient temperature for the different simulation cases, $T_{ambient} = 30\,°C$.

The simulation result of Figure III. 7 shows that the TEC's cold-side can have the lowest temperature of -3.5°C. However, this lowest temperature has lasted only for three seconds and after a period of 20 seconds the value of the temperature of the TEC's cold side reaches is 5 °C and stabilizes at this value when the PID control is applied in both cases. This stable temperature value is used as the reference set value of the PID algorithm. We obviously prove that applying PID into a thermoelectric refrigerator accelerates the cooling rate about three times faster.

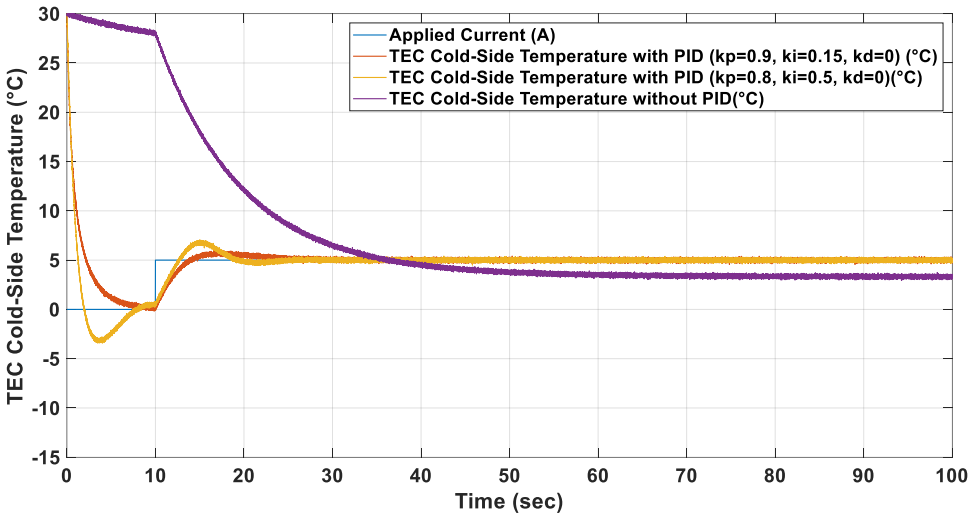



Figure III. 7 Thermoelectric cold-side temperature with PID and Without PID controller.

Based on the closed-loop Ziegler-Nichols tuning method, $k_p$, $k_i$, and $k_d$ were predicted around 0.9, 0.15, and 0 respectively. Varying the $k_p$, $k_i$, and $k_d$ these parameters around the previous values leads us to the conclusion that the best PID parameters fit well with the Ziegler-Nichols prediction.

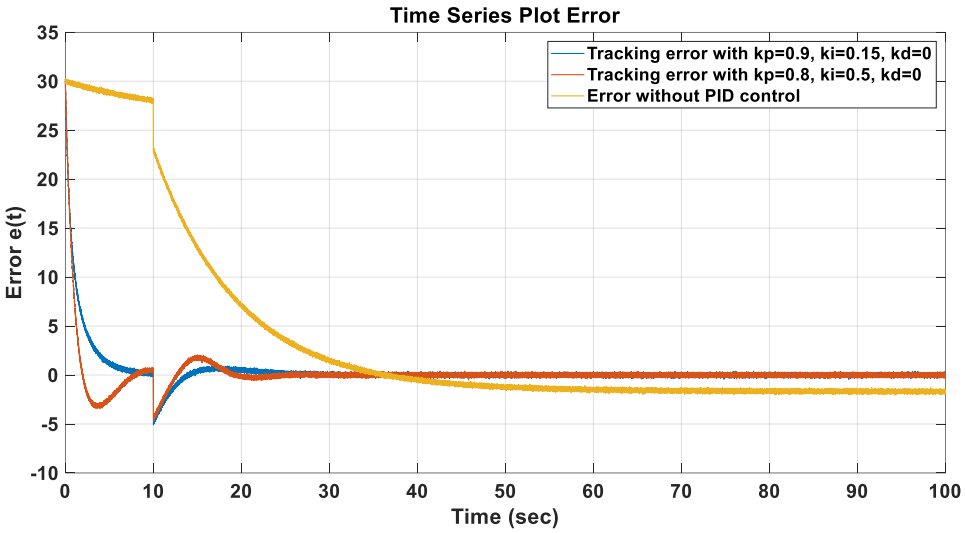



Figure III. 8 Time series error with PID and Without PID controller.

A Comparison of the open-loop error response of the TEC system with respect to the closed-loop error response is illustrated in Figure III. 8. It shows a significant improvement in terms of the desired temperature tracking performances.

## III.5. Conclusion

In this chapter, a numerical simulation study was conducted to investigate the performance of the TEC cooler system model with PID control strategy. The mathematical model of cooling system was created and detailed in chapter I, by making energy balance for the TEC cooling system. The simulation of the PID controller was designed by using MATLAB/SIMULINK.

The TEC cold side temperature is determined using a thermoelectric Peltier model. To increase the sensevity and stability of the PID system operation, digital filters were used to eliminate the influence of random disturbances of the temperature indicated by the feedback closed-loop. This ensures stable, much faster, and more accurate operation of the controller. The controller's parameters were calculated by using Zeigler Nichols closed-loop tuning.

The novelty of the presented PID control system is the determination of the TEC temperature based on the solution of the inverse problem of heat conduction formulated for a thermoelectric device.

PID controller is used to improve the performance of the system by minimizing, the rise time and overshoot. The simulation results have shown that the controller gave better response and performance (reduced steady-state time and eliminate the oscillation in the response 100%) compared without PID controller cases.

# Chapter IV

# EXPERIMENTATION

## IV.1. INTRODUCTION

The experimental conception of TEC cooler required different mechanical subsystems. These subsystems included thermoelectric modules, heat dissipation, refrigeration chamber, and insulation. The thermoelectric modules were the main component of the design that cooled the room. Understanding how the modules worked was crucial for each module performing at its max capabilities. Heat dissipation greatly affected the thermoelectric module's performance. The thermoelectric modules required heat dissipation in order to remove the heat that the module rejected. If the heat dissipation was inadequate, the module could not function as a cooler and, in extreme cases, heated the chamber instead of cooling it. As the TEC temperature cooled lower and became lower than the environment temperature, heat transfer naturally occurs between the environment and the TEC. Insulation needed to be carefully chosen and manufactured to reduce heat transfer.

In this chapter, an experimental and numerical approach is proposed in order to evaluate the TEC cooler performance through its operational parameters. The experimental configuration of refrigerator system was modeled based Matlab/Simulink and S-function block in order to enhance the heat transfer and cooling performance.

## IV.2. The experimental system set-up

The actual setup diagram of the experimental system used in this thesis is shown in Figure IV.1. The whole system was fabricated and constructed locally to be tested under the outdoor condition of the city. The device consists of internal and external heat exchangers. The first one is designed according to the possibility of use in the food industry. As for the second one, it will be used for possible heat dissipation. The heat transfer between these exchangers will be provided by thermoelectric modules with thickness is 3.8 mm., minichannel Heat sink, fans, liquid-cooler storage tank, DC power supply, and coolant circulating pump.

The refrigerator is designed for the experimental study with an inner volume of 0.05 $m^3$. As the device contains a number of these cells in which the consistent selection is the key to the proper functioning of the device, a comparative cell measuring device is designed and constructed. Therefore, it will be possible to determine how a particular cell will behave in the device.

For the proper functioning and use of the properties of Peltier cells, a source using pulse width modulation (PWM) with processor control is designed and constructed. The processor will allow a great variety of the system. It will therefore be possible to find the optimal parameters. The two hot-sides of thermoelectric modules were attached to their inner aluminum minichannel liquid-cooler block illustrated in Figure IV.4(c), whose details are listed in Table IV.1, to absorb the heat flow released in the inside of the TEC. The system was operated without load (water for example).

| Specifications | Value |
|---|---|
| Dimensions (LxWxH) [mm] | 40x40x12 |
| Internal fin thickness [mm] | 0.5 |
| Spacing [mm] | 1 |

Table IV.1 Specifications of the minichannel liquid-cooler block.

To eliminate the thermal contact resistance effect in each surface of the TEC, a paste with high thermal conductivity has been used. The experimental set-up has been designed so that the heat sink is in the internal part of the refrigerator. However, the TEC is in the middle and vertical to the wall (refer to Figure IV.1).

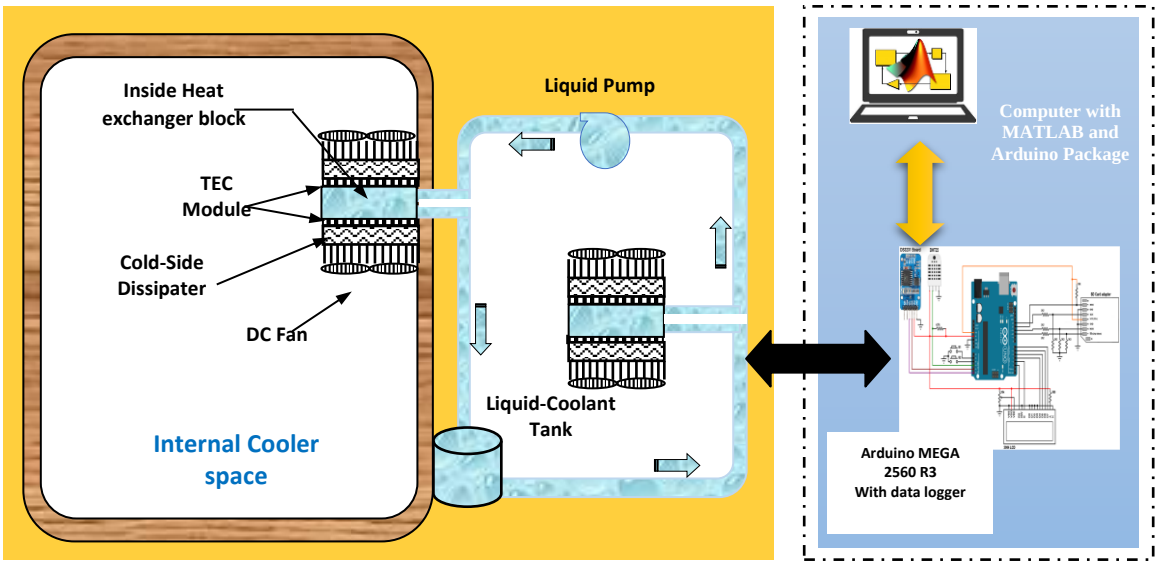



Figure IV.1 Schematic diagram of the experiment set-up

## IV.3. Experimental Method

The Peltier thermoelectric module constituted of two symmetrical internal heat sinks, two TEC cells placed symmetrically with respect to the liquid-cooler block of the internal exchanger, and two external heat sinks located in the upper part of the inner case. One of the heat sinks has been installed to increase the cooling of the refrigerator internal space and the other to improve the heat rejection effect.

A cold-water circulation system was used to cool the surfaces of the modules inside the refrigerator. In order to keep the liquid-cooler at the same temperature (always between 13°C and 15°C) during the measurements, a PID-controlled water distributor with LM35 temperature sensor input, is used. Here, it is important to highlight that the reference temperature can be adjusted. The volume of liquid in the cooled-circuit has been chosen to be 0.3 L. To detect the thermal values of the hot ($T_h$) and cold ($T_c$) surfaces, two DHT22 types thermocouples have been used to find the temperature difference ($\Delta T$) between surfaces of TEMs.

A data acquisition system, At Mega Arduino 2560 and MATLAB/Simulink, allows the periodical acquisition on the related measures in real-time. The water flow has been regulated by the power supply voltage of the pump. The water leaving the system has been passed through another heat exchanger block which is located outside the refrigerator for water cooling by the TEC cold sides and the hot sides of outer TECs are provided by fans (12V-3A) in order to evacuate the heat released in the minichannel cooler block and to reduce water temperature. DC power supply has been used to provide the power required in cooling fans.

The Arduino platform has been chosen to control the cooling flow. Arduino which is based on a simple board and an IDE environment, is one of the most popular open-source platforms today.

The main goal is to improve the performances of the designed refrigerator using a PID algorithm. The refrigerator COP and its Inner temperature have been adopted as two different performance indices. To enhance the refrigeration performance, the temperature of the circulating water must be maintained. The COP expression is the ratio between the cooling production and electrical power consumption of the refrigerator which it indicated in the equation (I.26) (in chapter I) [133,134].

## IV.4. Hardware construction

Figure IV.2 shows the hardware architecture details of the cooling system, with thermoelectric modules (TEM), fans and heat sinks. Thermal paste and screws have been used to merge each of them. The displays of the full assembly of the thermoelectric refrigerator installation have been powered with a DC source (voltage = 12.0 V, current = 5.0 A).

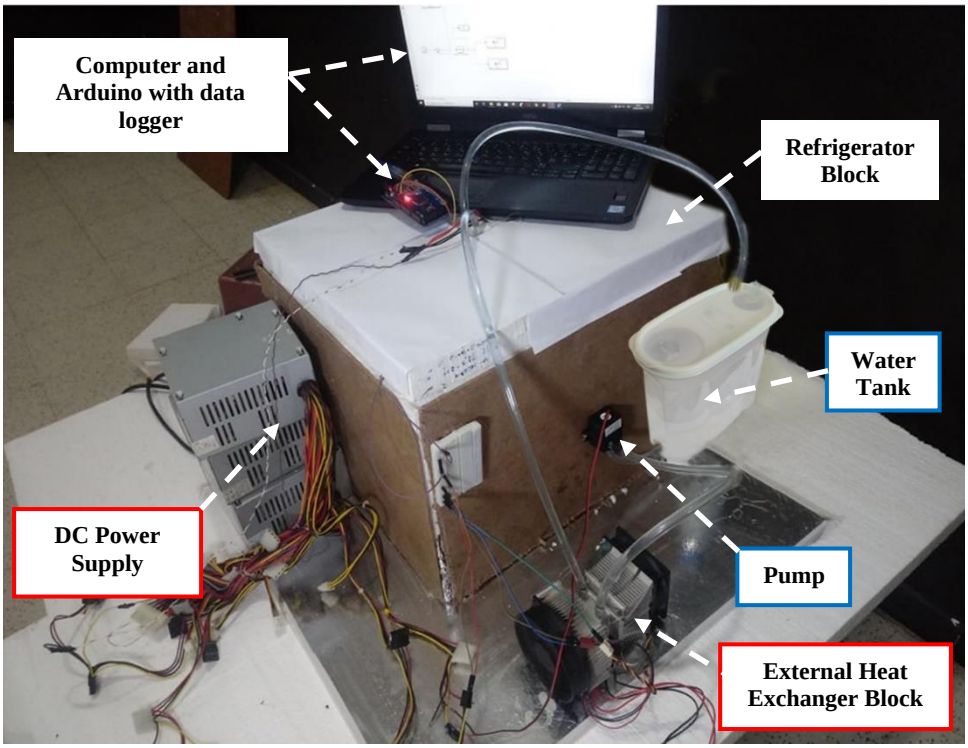



Figure IV.2 A complete assembled to the thermoelectric refrigerator.

To obtain a stable decrease of temperature in the internal of the refrigerator box, the experiment has been lasted two hours and a half long. During this experience, the TEC Peltier device surface temperatures ($T_c$ and $T_h$), the temperature of internal space Tint have been measured using temperature sensors then logged.

The temperature of the ambient ($T_{ambient}$) has been measured and recorded every 60 seconds because the experiment has been conducted in an open environment.

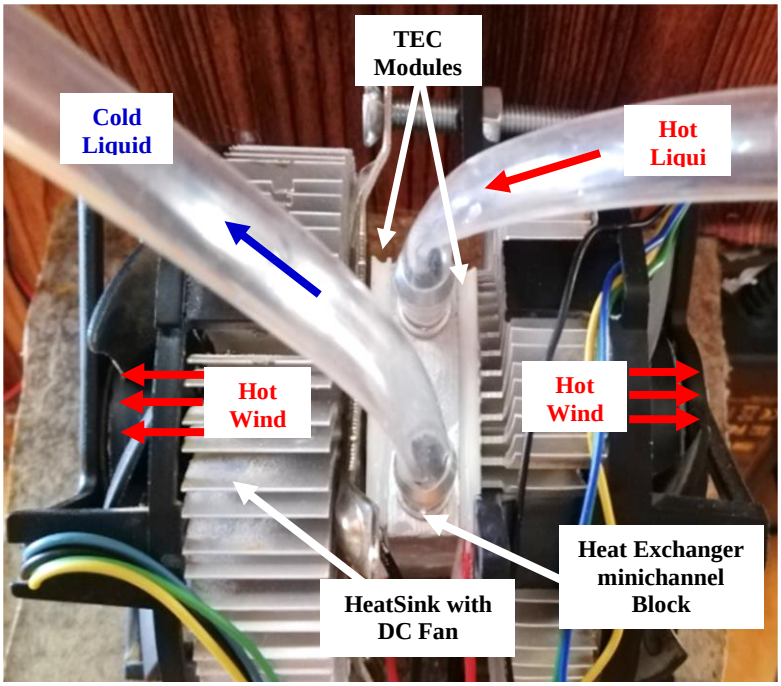



Figure IV.3 External configuration of the minichannel cooler Block.

Figure IV.3 shows the details of the external set-up of the heat exchanger block made for cooling liquid, with TEC modules, heat sinks and fans. Thermal paste and screws were used to join each of them.

## IV.5. Effective Material Properties

### IV.5.1. Heat Sink design

For a more effective transfer and dissipation of the heat generated at the hot and cold side of the module, a heatsink and a DC fan (12V-3A) is used in order to dump the heat gained in the heat sink and maintain a constant temperature tank.

When designing a thermoelectric cooler, it is particularly important to choose and use suitable thermal grease and a heat sink of a proper size and design.

The heat sink in the TEC cold side is made of aluminum alloy. The heat sink and cooling fan dimensions are 40mm×40mm with 11 fins witch as shown in Figure IV.5(a) and IV.5(b) respectively, which is the same size as that of the TEC. The dimensions of the heat sinks are as follows:

| Sr. Nº. | Dimensions | Hot side Heat sink (Plate Fin) | Col side Heat sink (Pin Fin) |
|---|---|---|---|
| 1 | Fins | 17 | 11 |
| 2 | Height (H)[mm] | 30 | 30 |
| 3 | Length (L)[mm] | 90 | 40 |
| 4 | Width (W)[mm] | 70 | 40 |
| 5 | Base Thickness (b)[mm] | 3.5 | 3 |
| 6 | Fin Thickness (t)[mm] | 1 | 1 |
| 7 | Fin Spacing (s)[mm] | 4 | 3 |
| 8 | Thermal Conductivity (W/m°C) | 170 | 170 |

Table IV.2 Heatsink Dimensions.

A tool that functions to help transfer heat by conduction, there are 2 parts of the heatsink, namely the heat absorbing section and the cooling section, the heat absorption section is usually made of aluminum. This cooling technology was invented by Daniel L. Thomas in 1982 [135].

In the process of heat transfer by conduction there is a fast heat is delivered through the hot side of TEM. A conceptual illustration of the heat flow is modeled in Figure IV.4. There are quantities that affect the rate of heat conductivity, namely the surface area of the object, the length or thickness of the object and is also influenced by a quantity $\kappa$ called thermal conductivity. The rate of heat transfer that occurs in conduction heat transfer is proportional to the following equation which is called Fourier's law and is the basic conduction equation [136], [77]. The basic equation for conduction:

$$Q_{cond} = \kappa . A \frac{\Delta T}{\Delta x} \quad \text{(IV.1)}$$

$\kappa: Thermal\ conductivity$
$A: cross - sectional\ area$
$\Delta x: thickness\ of\ the\ heatsink$
$\Delta T: Change\ in\ temperature$

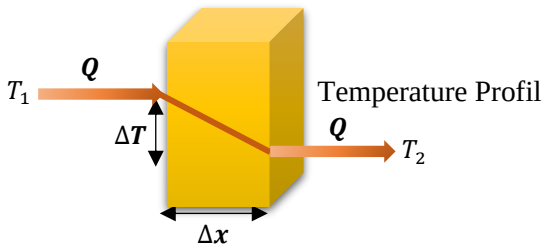



Figure IV.4 Heat flow by conduction through a uniform slab [137]

### IV.5.2. DC Fan design

Cooling Fan is used to carry the heat from one side to another. It cools the particular area by pulling the hot air away from that particular area. In the set-up thermoelectric refrigeration process, there are four fan cooling used on both sides of the module which as shown in Figure IV.5(a). Cooling fan takes away the heat from the one side and discharges it to the surrounding atmosphere. Figure IV.5 shows the design with two heat sinks and two DC fan. This design was used for the internal and external heat rejected configuration.

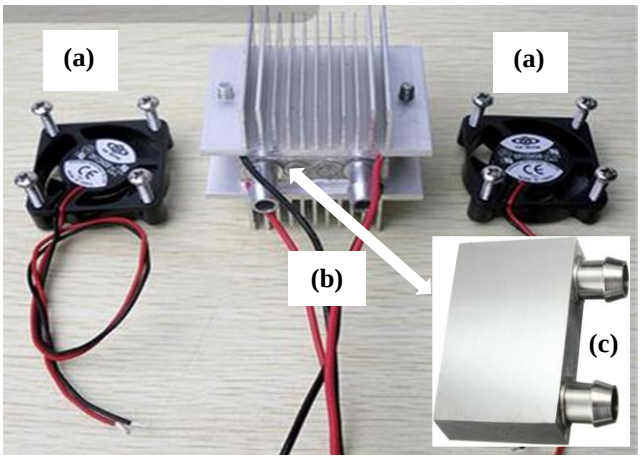



Figure. III.5 (a) DC Fan used in the TEC System
(b) The design with two Heat Sink (c) minichannel cooler block

Basically, the fans used are similar to ones that are found in CPU of computer.

### IV.5.3. Temperature Sensors

There are several methods to measure temperature. One of these methods is using integrated circuit (IC) temperature sensors. The output signal of such sensors can be voltage-based or current-based. LM35 is an IC temperature sensor which has voltage-based output signal (refer to Figure IV.6(b)) [138].

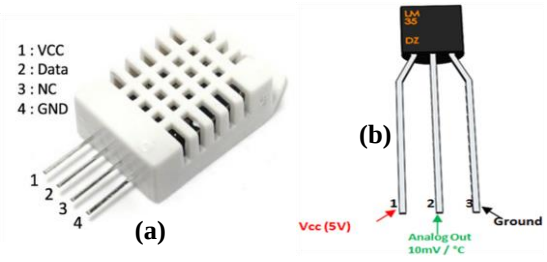



Figure.IV.6 Temperature sensors: (a) DHT22 sensor (b) LM35 sensor.

LM35 temperature sensor has linear output (10 mV/°C). Regarding the abovementioned advantages, LM35 is chosen for temperature measuring in our experimentation. The output signal of LM35 informs the Arduino about the environment temperature.

The DHT22 sensors measurement are easy and quick, are great for data logging. DHT sensors are made of two parts as shown in Figure IV.6 (a), a capacitive humidity sensor and a thermistor. There is also an inside chip that does some ADC conversion and spits out a digital signal with the temperature and humidity. The digital signal is fairly easy to read using any microcontroller.

### IV.5.4. TEC Device Selection

To increase the maximum cooling capacity ($Q_{c_max}$), two thermoelectric coolers (TEC) type TEC1–12706 ($Bi_2Te_3$) which is having 127 couples (see Figure IV.7), were used in this experimental configuration. Their catalog data are presented in Table IV.3. The TEC module dimensions are 40mm×40mm.

| **Parameter** | **Specification** |
|---|---|
| Hot-side temperature[°C] | 30 |
| Maximum Temperature difference $\Delta T_{max}$[°C] | 67 |
| Maximum Absorbed heat Power $Q_{max}$ [W] | 63 |
| Number of the thermocouples, *n* | 127 |
| Material | Aluminum Oxide |
| Thickness [mm] | 3.8 |
| Length [mm] | 40 |
| Width [mm] | 40 |
| Geometric factor, Ge [mm] | 1.2 |
| Length of element, Le [mm] | 2 |
| Maximum Electric current $I_{max}$ [A] | 6.4 |
| Maximum Voltage $V_{max}$ [V] | 15.4 |
| Measured Resistance R[Ω] | 25 |
| Seebeck coefficient ($\alpha$) [V/°C] | $2.2x10^{-4}$ |
| Electrical resistivity ($\rho$) [Ω.cm] | $1.2x10^{-2}$ |
| Thermal conductivity ($\kappa$) [W/cm.°C] | $1.62x10^{-2}$ |

Table IV.3 Performance specifications of Thermoelectric Module (TEC1-12706).

The modules were connected electrically in parallel. The cascade stacking of the TEC modules both shortens the time necessary to reach negative temperatures and served as thermal

boundary after switching off the power supply. A creative solution was applied to control the water flows through the minichannel cooler block at the hot side of the TEMs.

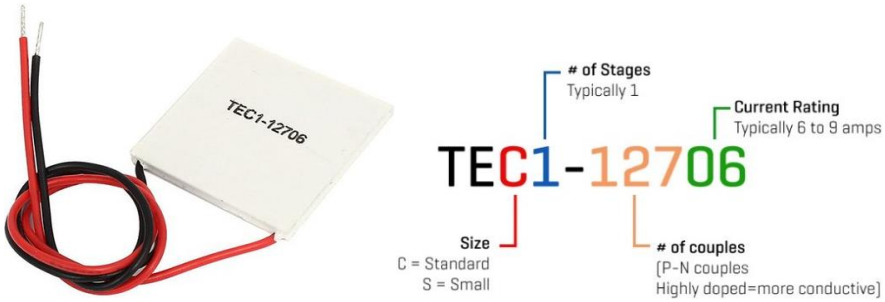



Figure IV.7 Thermoelectric module TEC1-12706

## IV.6. Experimental Results and analysis

When designing the experimental TEC system, the input electric current must be regulated as detailed in the previous chapter. The direction of current flow can achieve the conversion between heating and cooling in TEC [139-141].

The ambient temperature can be influenced the cooling efficiency of the refrigerator. However, the cooling temperature that the TEC device can reach is not the same under different values of ambient temperature.

Joule effect and thermal conductivity reduce the cooling performance of the TEC. The use of a fan is necessary for heat dissipation under the cooling condition of TEC, which allowed to reduce the influence of the refrigeration effect due to thermal conductivity and Joule effect.

Practically, when powering TEC with DC source and controllable input current, the temperature values of the cold and hot sides can be obtained with two DHT22 sensors (accuracy of up to 0.1°C).

The TEC input current varied from 0A to 6A with a step of 1A was adjusted and simulated the variation of the temperature after waiting 10 seconds to reach the steady-state in the TEC system.

The electric power supply used in each TEC is equal to 60 W. The liquid cooler in the internal minichannel cooler block used to reject the released heat from the hot side of the TEC was absorbed by the pump to cool it by the external liquid-cooler block.

The cooling of the sides of the thermoelectric cascade is realized in the internal space of refrigerator by minichannel cooler block with forced convection provided by an external pump.

Aiming to accelerate the cooling, the inner minichannel is made of aluminum with coefficient of heat conductivity 80 (W/m°C). A heat sink with DC cooling Fan contacts with the cooling side of the Peltier modules through thermal paste with coefficient of heat conductivity 6 (W/m°C).

During 150 min of the experimental studies, the following initial conditions were selected:

- Ambient temperature (environment) has been varied between 30°C and 31°C
- Inlet liquid cooling temperature in aluminum minichannels block is 30.25ºC
- The refrigeration system is powered by direct current stabilized power supply for 2.5 h;
- the refrigeration system is then powered off without opening the compartment aiming to monitor the dynamic of the change of the temperature and humidity over the subsequent 1 h.

Figure IV.8 shows that the inner temperature values and time were measured for finding the temperature increases rate and the ambient temperature of refrigerator. During the interval of time between 0 and 20 minutes, the inside temperature of refrigerator box has been decreased rate of 1.5 °C/min. The minimum temperature has reached -10.1 °C.

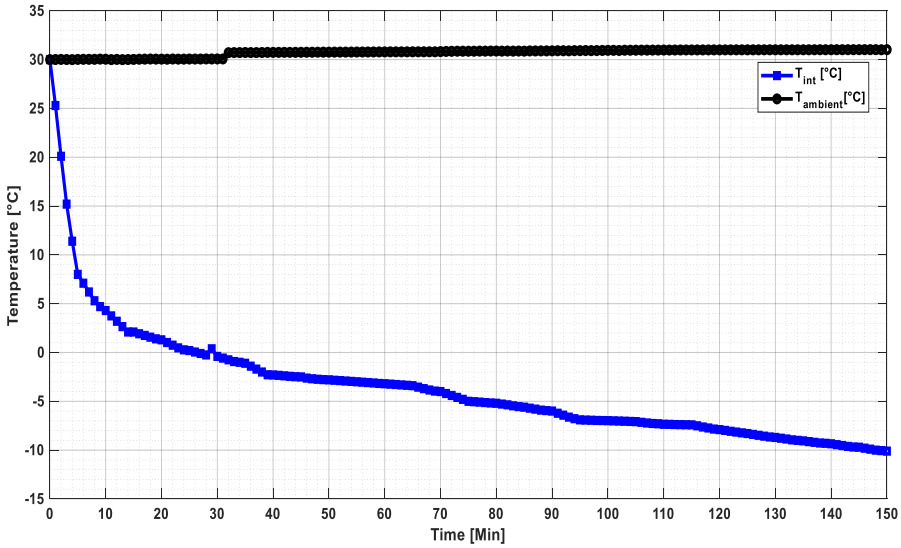



Figure IV.8 Inner temperature, ambient temperature of TE refrigerator profiles versus time.

The TEC's lower-cooling behavior at temperature differences between the inside and outside surfaces of the Peltier Module (or fins), has driven to a gradually decreases in the associated coefficient of performance (COP) as shown in Figure IV.9. The COP value changes from 0.73 to 0.1 during the experiment. We have found that COP value of refrigerator are notably low.

Moreover, it was seen that the COP value of the whole system are better to the similar studies in the literature.

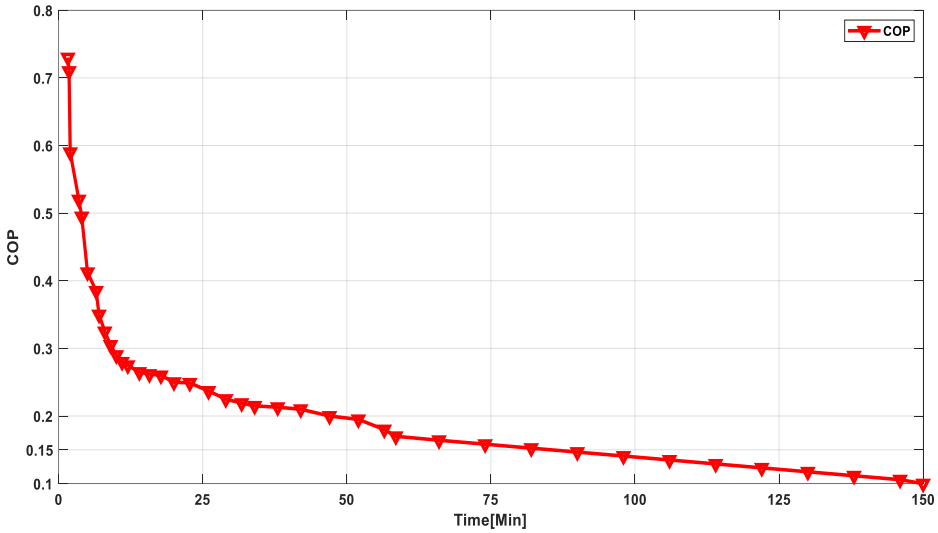



Figure III.9 COP variations during test time.

In Figure IV.10 we illustrate the variations of cold side temperature and hot side temperature of inside thermoelectric modules, as well as the ambient temperature versus time for 1 L/min flow rate. From Figure IV.10, we can see that the cold side temperature of the thermoelectric cooling unit decreases quickly during the first 30 min then it stays steadily below −5.0 °C after two hours.

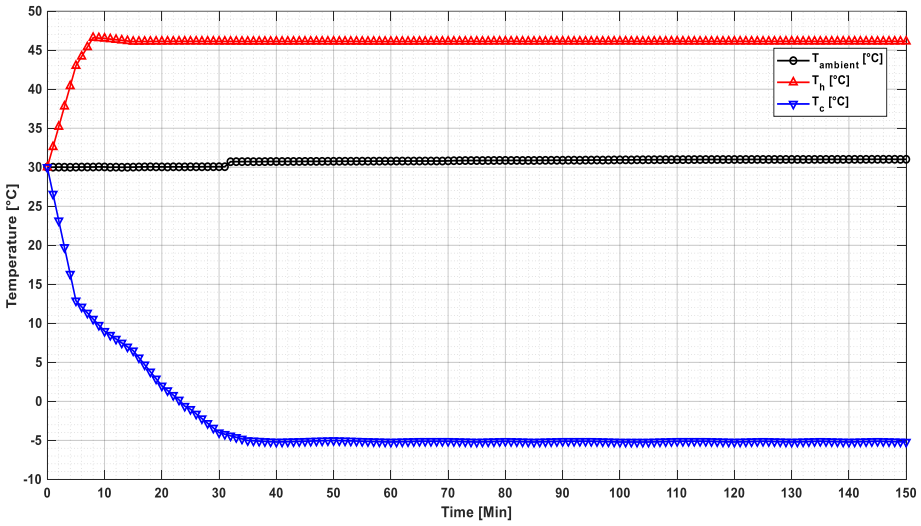



Figure III.10 Experimental relationship of time and temperatures.

After 10 min, hot temperature $T_h$ has approached to 46.01°C. After 14 minutes have elapsed, it was rather constant. As for $T_c$, it has got closer to −5.0°C after 30 min (refer to Figure IV.10).

The ambient temperature has been varied between 30°C and 31°C during the experiment. The temperature span between the two sides of the TEC has reached 51.01°C after only 30 minutes.

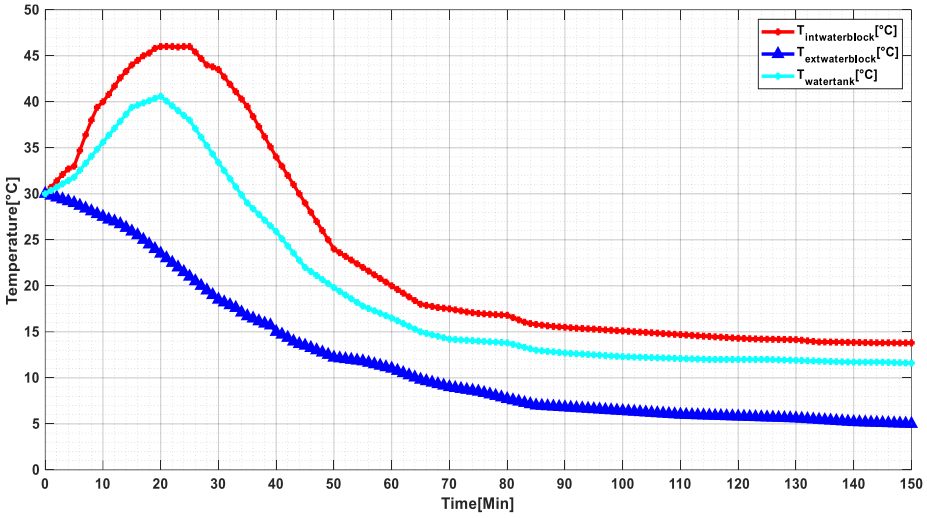



Figure IV.11 Experimental relationship of time and temperatures of internal minichannel block $T_{int_water_block}$, external minichannel block temperature $T_{ext_water_block}$, and cooling storage tank temperature $T_{water_tank}$.

As it can be seen in Figure IV.11, the water temperature in the internal minichannel block increases to 46.01 °C after 20 min then it drops to 15 °C after 90 min. After 120 min, the water temperature in the external cooling minichannel block reaches about 5.0 °C. As for the volume of cooling liquid in the tank, it is constant during the experiment. We can see that the temperature of the liquid in the storage tank increases from 30 °C to 40 °C in 20 min and then drops to around 12 °C after 90 min.

## IV.7. Conclusion

The experimental design and development of a thermoelectric based cooling system is presented in this chapter. Its mathematical model relating thermal loads and TEC heat capacity is also developed in chapter II. the TEC has been used for direct temperature control on the inside of a TE refrigerator and cooling water circulates in two water aluminum blocks. The influences of heat sink temperature, flow rate, and current have been analyzed by calculation.

The proposed system is found to have less maintenance and simplicity in design which can easily replace the HVAC system.

In the experimental results, the cold side temperature of the thermoelectric cooling unit has decreased quickly in the first 30 min then it remained steady below −5 °C after two hours.

The highest COP has been obtained as 0.73. The COP value has decreased over time during the cooling period and to get closer to zero, which means that these systems work in time-dependent conditions.

Some concluding remarks are as follows:

1) The proposed system shows improvement in cooling performance due to liquid cooling circulation by spraying it through the hot side compartment.

2) Since, current through TECs is in series, the cooling performance of both TECs are quite same.

3) The number of TEC modules required for the desired cooling system can be estimated by considering the effective area of heat sink at the cold side of TECs obtained by heat load analysis.

4) To improve the cooling performance of the proposed system, a heat sink with more cooling effective area can be chosen.

# Chapter V

# CONCLUSIONS AND FUTURE WORK

# V.1. CONCLUSIONS

### V.1.1. Broad-Based Findings

Several things can be concluded about the modeling, control and experiment investigation of Thermoelectric refrigerator from this thesis. It is evident that the approaches were taken in place in this thesis could provide solutions in terms of modeling, control and, design of thermoelectric refrigerators.

First a thermal simulation framework is established and validated allows for rapid assessment of TEC and refrigerator system level thermal performance.

For an application with fixed working temperatures $T_h$ and $T_c$, the thermoelectric modules have an optimum current to achieve the maximum COP and the required cooling/heating capacity $Q_c/Q_h$, by using an appropriate number of thermoelectric modules. Geometry factor and working temperatures $T_h$ and $T_c$, they have no relationship with the cooling capacity. The required number of the thermoelectric modules for optimum current and COP decreases with the increase of the hot side temperature and increases with the increase of the cold side temperature.

Through the use of liquid-cooling minichannel heat exchanger, the general trends of TEC performance optimization were also validated. Thus, as long as the thermal resistance could be achieved.

The notion of stability under operating constraints is a delicate step for thorough an appropriate behavior of the TE refrigerator. In this thesis, a PID control technique has been proposed to force the user-desired refrigeration temperature gradient on a TE refrigerator. The Ziegler-Nichols method has been adopted to set the parameters of the controller. The component derived from the controller has not been used, so the controller functions have been utilized as PI controller. Even in this case, the transient characteristic has a relatively small overshoot and a short stabilization time, especially with a large decrease in the recipient temperature.

The results of simulations in the case of using PID controller have shown its performance in terms of stability. The response time for the various tests is for the variations of PID controller parameters on one hand, and on the other hand, the change the power supply profile of the TEC. Through the different simulation results with PID controller, for $k_p = 0.9$, $k_i = 0.15$, $k_d = 0$,

the proposed controller has reached an error of 0.1°C with minimal overshoot less than 20 seconds. In the experimental results, the cold side temperature of the thermoelectric cooling unit has decreased quickly in the first 30 min then it remained steady below −5 °C after two hours.

In the worst case, the controller effect exhibits a cooling temperature slight overshoot of 5 °C. Generally, the temperature fluctuates only by a value corresponding to the resolution bit of the analog-digital converter. The PID method is useful for remedying transient heat transfer issues, where response time is as important as heat transfer.

In this study, the TEC has been used for direct temperature control on the inside of a TE refrigerator and cooling water circulates in two water aluminum blocks. The influences of heat sink temperature, flow rate, and current have been analyzed by calculation. The highest COP has been obtained as 0.73. This value has decreased over time and to get closer to zero, which means that these systems work in time-dependent conditions. This study shown that it is possible to achieve high COP values for TE refrigerator when the suitable heat sink is used.

The proposed control system has been validated by the Matlab/Simulink model which has proved its ability to keep the operating temperature profile constant following the modification of the supply DC current. This increases the overall energy efficiency of the cooler and verifies the TEC control methods. The cold side reference temperature chosen as equal to direct current form, where $T_{c_ref} = 5$°C.

To summarize, the targets stated at the beginning of thesis were achieved.

### V.1.2. Contributions

❖ The main contribution from this work is the use of the PID based Matlab/Simulink and S-function block to set the error between input current profile and cold-side desired temperature of TEC cooler system. This contribution aims to provide numerical approach in order to evaluate the TEC performance through its operational parameters. The purpose of cooling system control is expected to keep the internal temperature of an object below the ambient temperature of around 30°C.

❖ Furthermore, a new mathematical and thermal modeling of thermoelectric refrigerator based on the physics of the thermoelectric effect has been proposed. This model can be used to very exactly predict the transient and steady-state behaviour of a complete thermoelectric

system including heat sinks and liquid-cooler minichannels, given the material properties are known.

## V.2. Suggestions for Future Work

Although substantial work has been carried out during this research, there are still quite a few opportunities to develop this thermoelectric refrigerator in order to improve the system's performance further. These may be indicated as follows:

### V.2.1. Thermoelectric Refrigerator Control

❖ There are ample opportunities to improve a thermoelectric cooler control systems with the migration to new control approaches and that currently available solutions can be optimized for better using and functioning in reality.

### V.2.2. Thermoelectric Refrigerator Design

❖ Due to the larger temperature difference between the hot and cold side of thermoelectric modules in the thermoelectric refrigerator, the COP of the system is much lower. The hot side heat sink system could be improved to reduce the hot side temperature and therefore improve the COP. This improvement could be achieved by developing a heat pipe heat sink system.

❖ Further investigations of the combining the PV into the thermoelectric refrigeration system could be carried out in order to have autonomous design. The further investigations should include the optimum design of the PV system for a specific thermoelectric refrigeration system application.

# REFERENCES

# REFERENCES


[1] J.H. Meng, X.D. Wang, X.X. Zhang, Transient modeling and dynamic characteristics of thermoelectric cooler. Appl. Energy 108, 340–348 (2013)

[2] T. Gong, L. Gao, Y. Wu, H. Tan, F. Qin, T. Ming, J. Li, Transient thermal stress analysis of a thermoelectric cooler under pulsed thermal loading. Appl. Therm. Eng. 162, 114240 (2019)

[3] J. Wang, P. Cao, X. Li, X. Song, C. Zhao, L. Zhu, Experimental study on the influence of Peltier effect on the output performance of thermoelectric generator and deviation of maximum power point. Energy Convers. Manag. 200, 112074 (2019)

[4] D. Enescu, E.O. Virjoghe, A review on thermoelectric cooling parameters and performance. Renew. Sustain. Energy Rev. 38, 903–916 (2014)

[5] D. Zhao, G. Tan, A review of thermoelectric cooling: materials, modeling and applications. Appl. Therm. Eng. 66, 15–24 (2014)

[6] L.G.L. Ponce, F. Chejne, L.M.R. Aristeguieta, C.A. Gómez, A.F.M. Cano, Predicting a thermal stimulator's heating/cooling rate for medical applications. Appl. Therm. Eng. 163, 114376 (2019)

[7] G. Chen, Y. Tang, Z. Wan, G. Zhong, H. Tang, J. Zeng, Heat transfer characteristic of an ultrathin flat plate heat pipe with surface-functional wicks for cooling electronics. Int. Commun. Heat Mass Transf. 100, 12–19 (2019)

[8] P. MohanKumar, V. Jagadeesh Babu, A. Subramanian, A. Bandla, N. Thakor, S. Ramakrishna, H. Wei, Thermoelectric materials—strategies for improving device performance and its medical applications. Sci 1, 37 (2019)

[9] L. Chen, F. Meng, Y. Ge, F. Sun, Optimum variables selection of thermoelectric generator-driven thermoelectric refrigerator at different source temperature. Int. J. Ambient Energy 33, 108–117 (2012)

[10] A. Şişman, H. Yavuz, The effect of Joule losses on the total efficiency of a thermoelectric power cycle. Energy 20, 573–576 (1995)

[11] S.A. Omer, D.G. Infield, Design optimization of thermoelectric devices for solar power generation. Sol. Energy Mater. Sol. Cells 53, 67–82 (1998)

[12] X. Lin, S. Mo, L. Jia, Z. Yang, Y. Chen, Z. Cheng, Experimental study and Taguchi analysis on LED cooling by thermoelectric cooler integrated with microchannel heat sink. Appl. Energy 242, 232–238 (2019)

[13] J. Mao, H. Zhu, Z. Ding, Z. Liu, G.A. Gamage, G. Chen, Z. Ren, High thermoelectric cooling performance of n-type Mg3Bi2- based materials. Science 365, 495–498 (2019)

[14] E. Kanimba, Z. Tian, A new dimensionless number for thermoelectric generator performance. Appl. Therm. Eng. 152, 858–864 (2019)

[15] P. Naphon, S. Wiriyasart, C. Hommalee, Experimental and numerical study on thermoelectric liquid cooling module performance with different heat sink configurations. Heat Mass Transf. 55, 1–10 (2019)

[16] A. Fabián-Mijangos, G. Min, J. Alvarez-Quintana, Enhanced performance thermoelectric module having asymmetrical legs. Energy Convers. Manag. 148, 1372–1381 (2017)

[17] S.M. Pourkiaei, M.H. Ahmadi, M. Sadeghzadeh, S. Moosavi, F. Pourfayaz, L. Chen, M.A. Yazdi, R. Kumar, Thermoelectric cooler and thermoelectric generator devices: a review of present and potential applications, modeling and materials. Energy (2019).

[18] J. Batra, V. Dabra, P. Sharma, V. Saini, Performance evaluation of thermoelectric refrigerator based on natural and forced mode of cooling processes, Advances in Fluid and Thermal Engineering (Springer, Singapore, 2019), pp. 317–324

[19] Y. Wang, Y. Shi, D. Liu, Performance analysis and experimental study on thermoelectric cooling system coupling with heat pipe. Procedia Eng. 205, 871–878 (2017)

[20] W. He, G. Zhang, X. Zhang, J. Ji, G. Li, X. Zhao, Recent development and application of thermoelectric generator and cooler. Appl. Energy 143, 1–25 (2015)

[21] R. Bhuiya, N. Shah, D. Arora, N-V.Krishna, S. Manikandan, C. Selvam, R. Lamba. Thermal management of phase change material integrated thermoelectric cooler with different heat sink geometries. Journal of Energy Storage 51, (2022) 104304.

[22] Sang J.Park, K-M. Bang, B. Kim, P. Ziolkowski, J-R. Jeong, H. Jin. Adaptive Thermoelectric Cooling System for Energy-Efficient Local and Transient Heat Management. Applied Thermal Engineering. (2022) 119060

[23] S. Wiriyasart, C. Hommalee, P. Naphon. Thermal cooling enhancement of dual processors computer with thermoelectric air cooler module. Case Studies in Thermal Engineering 14 (2019) 100445.

[24] F. Afshari , M-A. Ceviz, E. Mandev, F. Yıldız. Effect of heat exchanger base thickness and cooling fan on cooling performance of Air-To-Air thermoelectric refrigerator; experimental and numerical study. Sustainable Energy Technologies and Assessments 52 (2022) 102178.

[25] M. Gökçek, F. Şahin. Experimental performance investigation of minichannel water cooled-thermoelectric refrigerator. Case Studies in Thermal Engineering 10 (2017) 54–62.

[26] K. Yazawa, J-H. Bahk, A. Shakouri. Thermoelectric Energy Conversion devices and Systems. World Scientific Publishing. Vol. 7, 2021.

[27] M. Naghmegou, F. Torabi, H. Borgheipour. Investigation of conjugate heat transfer in environmental-friendly device thermoelectric beverage cooler design. International Journal of Environmental Science and Technology (2022) 19:3655–3668.

[28] H. Ruan, H. Xie, J. Wang, J. Liao, L. Sun, M. Gao, C. Li. Numerical investigation and comparative analysis of nanofluid cooling enhancement for TEG and TEC systems. Case Studies in Thermal Engineering 27 (2021) 101331.

[29] A. Martínez, D. Astrain and A. Rodríguez. Experimental and analytical study on thermoelectric self-cooling of devices. Energy, 2011, vol. 36, issue 8, 5250-5260

[30] W. Ning, L. Zhouxiao, D. Can, Z. Jiannan, S. Guorong, J. Hongzhi, G. Xiumin, High efficiency thermoelectric temperature control system with improved proportional integral differential (PID) algorithm using energy feedback technique, IEEE Trans. Ind. Electron. (2022).

[31] G. Engelmann, M. Laumen, J. Gottschlich, K. Oberdieck, R.W. De Doncker, Temperature-controlled power semiconductor characterization using thermoelectric coolers, IEEE Trans. Ind. Appl. 54 (3) (2018) 2598–2605.

[32] D. F. Sinulingga Sundayani, F.M. Prasetyawati, M. Palebangan, F.A. Suhendi, T.A. Ajiwiguna, I.W. Fathonah, PID temperature controlling of thermoelectric based cool box, in: 2017 International Conference on Control, Electronics, Renewable Energy and Communications (ICCREC), 2017.

[33] H. Huang, S. Fu, P. Zhang, L. Sun, Design of a Small Temperature Control System Based on TEC. 2016 9th International Symposium on Computational Intelligence and Design (ISCID), 2016.

[34] T.H. Kwan, X. Wu, Q. Yao, Complete implementation of the combined TEG-TEC temperature control and energy harvesting system, Control Eng. Pract. 95 (2020), 104224.

[35] Ctirad Uher, Materials Aspect of Thermoelectricity, CRC Press, Tay & Franc Group, 2017.

[36] S. Shaojing, Q. Qin, Temperature Control of Thermoelectric Cooler Based on Adaptive NN-PID, 2010 International Conference on Electrical and Control Engineering, 25-27 June 2010, pp. 2245–2248. Wuhan, China.

[37] Jiaqiang Li , Xiaoming Xu , Jinyu Zhang ,Xuemei Wang , Jian Cao. High Power Laser Constant Temperature Control System.Proceeding of 2017 IEEE Int Conf on Machtronics & Autom, August 6-9, Japan.

[38] Jin Wang et al. Research on Intelligent Temperature Control Technology for Spacecraft with Instantaneous High Power Load. 2021 J. Phys.: Conf. Ser. 1871 012052.

[39] D. ASTRAIN, A. MARTI´NEZ, J. GORRAIZ, A. RODRIGUEZ, AND G. PEREZ. Computational Study on Temperature Control Systems for Thermoelectric Refrigerators. Journal of ELECTRONIC MATERIALS, Vol. 41, No. 6, 2012.

[40] M Saifizi et al. Development and investigation of thermoelectric cooling performance based on space scales. IOP Conf. Ser.: Mater. Sci. Eng. 429 (2018) 012083

[41] Zhu Wei, Deng Yuan, et al. Finite element analysis of miniature thermoelectric coolers with high cooling performance and short response time. Microelectron J 2013;44:860–8.

[42] Lee Kong Hoon, Kim Ook Joong. Analysis on the cooling performance of the thermoelectric micro-cooler. Int J Heat Mass Transf 2007;50:1982–92.

[43] Y. Cai, W.W. Wang, W.T. Ding, G.B. Yang, D. Liu, F.Y. Zhao, Entropy generation minimization of thermoelectric systems applied for electronic cooling: parametric investigations and operation optimization, Energy Convers. Manag. 186 (2019) 401–414.

[44] Y. Cai, Y. Wang, D. Liu, F.Y. Zhao, Thermoelectric cooling technology applied in the field of electronic devices: updated review on the parametric investigations and model developments, Appl. Therm. Eng. 148 (2019) 238–255.

[45] Y. ZHOU, T. ZHANG, F. WANG, Y. YU. Numerical Study and Optimization of a Combined Thermoelectric Assisted Indirect Evaporative Cooling System. Journal of Thermal Science Vol.29, No.5 (2020) 1345-1354.

[46] M. Mirmanto, S. Syahrul, Y. Wirdan. Experimental performances of a thermoelectric cooler box with thermoelectric position variations. Engineering Science and Technology, an International Journal 22 (2019) 177–184

[47] Hy Zhang. A general approach in evaluating and optimizing thermoelectric coolers. International Journal of Refrigeration 33(6):1187-1196, 2010.

[48] Cai Yang, Di Liu, Jing-Jing Yang, Yu Wang. Optimization of Thermoelectric Cooling System for Application in CPU Cooler. Energy Procedia 105:1644-1650, 2017.

[49] Yin, Tao & He, Zhi-Zhu, 2021. "Analytical model-based optimization of the thermoelectric cooler with temperature-dependent materials under different operating conditions," Applied Energy, Elsevier, vol. 299(C).

[50] Jeong Eun Soo. A new approach to optimize thermoelectric cooling modules. Cryogenics 2014;59:38–43.

[51] Wang Xiao, Yu Jianlin, et al. Optimization of heat sink configuration for thermoelectric cooling system based on entropy generation analysis. Int J Heat Mass Tra 2013;63:361–5.

[52] David Benjamin, Ramousse Julien, et al. Optimization of thermoelectric heat pumps by operating condition management and heat exchanger design. Energy Convers Manage 2012;60:125–33.

[53] Huang Yu-Xian, Wang Xiao-Dong, et al. Geometry optimization of thermoelectric coolers using simplified conjugate-gradient method. Energy 2013;59:689–97.

[54] Chen Lingen, Meng Fankai, et al. Effect of heat transfer on the performance of thermoelectric generator-driven thermoelectric refrigerator system. Cryogenics 2012;52:58–65.

[55] Zhu Lin, Tan Hongbo, et al. Analysis on optimal heat exchanger size of thermoelectric cooler for electronic cooling applications. Energy Convers Manage 2013;76:685–90.

[56] Zhou Yuanyuan, Yu Jianlin. Design optimization of thermoelectric cooling systems for applications in electronic devices. Int J Refrig 2012;35:139–1144.

[57] Gould CA, Shammas NYA, et al. Thermoelectric cooling of microelectronic circuits and waste heat electrical power generation in a desktop personal computer. Mater Sci Eng B 2011;176:316–25.

[58] S. Wiriyasart, C. Hommalee, P. Naphon. Thermal cooling enhancement of dual processors computer with thermoelectric air cooler module. Case Studies in Thermal Engineering 14 (2019). 100445.

[59] Martínez A, Astrain D, et al. Dynamic model for simulation of thermoelectric self-cooling applications. Energy 2013;55:1114–26.

[60] Yang J, Stabler F. Automotive applications of thermoelectric materials. Journal of Electronic Materials. 2009;38:1245-1251

[61] Choi H, Yun S, Whang K. Development of a temperature-controlled car-seat system utilizing thermoelectric device. Applied Thermal Engineering. 2007;27:2841-2849

[62] S. Wiriyasart, C. Hommalee, P. Naphon, Thermal cooling enhancement of dual processors computer with thermoelectric air cooler module, Case Stud. Therm. Eng. 14 (2019), 100445.

[63] S. Wiriyasart, P. Naphon, C. Hommalee, Sensible air cool-warm fan with thermoelectric module systems development, Case Stud. Therm. Eng. 13 (2019), 100369.

[64] C. Hommalee, S. Wiriyasart, P. Naphon, Cold-hot water dispenser with thermoelectric module systems, heat transfer, Asian Research (2019) 1–9.

[65] Rong-Rong He, Huai-Yu Zhong, Yang Cai, Di Liu, Fu-Yun Zhao. Theoretical and Experimental Investigations of Thermoelectric Refrigeration Box Used for Medical Service. Procedia Engineering 205 (2017) 1215–1222.

[66] K. Sakai, M. Karppinen, J.M. Chen, R.S. Liu, S. Sugihara, and H. Yamauchi, Appl. Phys. Lett. 88, 232102 (2006).

[67] H.C. Hsu, W.L. Lee, K.K. Wu, Y.K. Kuo, B.H. Chen, and F.C. Chou, J. Appl. Phys. 111, 103709 (2012).

[68] S. Wang, S. Chen, G. Yan, F. Liu, S. Dai, J. Wang, et al., Thin Solid Films 534, 168 (2013).

[69] L.H. Yin, R. Ang, B.C. Zhao, Y.N. Huang, Y. Liu, S.G. Tan, et al., Solid State Commun. 158, 16–19 (2013).

[70] N. Sun, S.T. Dong, B.B. Zhang, Y.B. Chen, J. Zhou, S.T. Zhang, et al., J. Appl. Phys. 114, 043705 (2013).

[71] N. Putra, J. Med. Eng. Technol. 33, 232 (2009).

[72] J.Luo, Optimumal location of heat transfer surface area for cooling load and COP optimization of a thermoelectric refrigerator 2003.

[73] S.W. Angrist, Direct Energy Conversion (Boston: Allyn and Bacon, 1965).

[74] D.M. Rowe, CRC Handbook of Thermoelectrics (Boca Raton: CRC Press, Inc., 1995).

[75] Ohara, B., Wagner, M., Kunkle, C. et al. Residential Solar Combined Heat and Power Generation using Solar Thermoelectric Generation. J. Electron. Mater. 44, 2132–2141 (2015).

[76] J. M. Giri and P. K. S. Nain, "Performance Optimization of Thermoelectric Cooler Using Genetic Algorithm," Mathematical Modelling of Engineering Problems, vol. 7, no. 3, pp. 427–435, 2020.

[77] K. Yazawa, J-H. Bahk, A. Shakouri. Thermoelectric Energy Conversion devices and Systems. World Scientific Publishing. Vol. 7, 2021.

[78] Xing Lua, Dongliang Zhaob, Ting Maa, Qiuwang Wanga and al. Thermal resistance matching for thermoelectric cooling systems. Energy Conversion and Management 169 (2018) 186–193.

[79] Kyle Pietrzyk, Joseph Soares, Brandon Ohara, Hohyun Lee. Power generation modeling for a wearable thermoelectric energy harvester with practical limitations. Applied Energy 183 (2016) 218–228.

[80] B.V.K. Reddy, Matthew Barry, John Li, Minking K. Chyu, Mathematical modeling and numerical characterization of composite thermoelectric devices, Int. J. Therm. Sci. 67 (2013) 53-63.

[81] Reiyu Chein, Guanming Huang, Thermoelectric cooler application in electronic cooling, Appl. Therm. Eng. 24 (2004) 2207e2217.

[82] Yuanyuan Zhou, Jianlin Yu, Design optimization of thermoelectric cooling systems for applications in electronic devices, Int. J. Refrig. 35 (2012) 1139- 1144.

[83] Limei Shen, Fu Xiao, Huanxin Chen, Shengwei Wang, Investigation of a novel thermoelectric radiant air-conditioning system, Energy Build. 59 (2013) 123-132.

[84] Matthieu Cosnier, Gilles Fraisse, Lingai Luo, An experimental and numerical study of a thermoelectric air-cooling and air-heating system, Int. J. Refrig. 31 (2008) 1051-1062.

[85] Reiyu Chein, Yehong Chen, Performance of thermoelectric cooler integrated with microchannel heat sinks, Int. J. Refrig. 28 (2005) 828-839.

[86] Chen, W.-H., Liao, C.-Y., Wang, C.-C. & Hung, C.-I. Evaluation of power generation from thermoelectric cooler at normal and low temperature cooling conditions. Energy for Sustainable Development 25, 8–16 (2015).

[87] Chen, M. & Snyder, G. J. Analytical and numerical parameter extraction for compact modeling of thermoelectric coolers. International Journal of Heat and Mass Transfer 60, 689–699 (2013).

[88] Enescu, D. & Virjoghe, E. O. A review on thermoelectric cooling parameters and performance. Renewable and Sustainable Energy Reviews 38, 903–916 (2014).

[89] Siahmargoi, M., Rahbar, N., Kargarsharifabad, H. et al. An Experimental Study on the Performance Evaluation and Thermodynamic Modeling of a Thermoelectric Cooler Combined with Two Heatsinks. Sci Rep 9, 20336 (2019). https://doi.org/10.1038/s41598-019-56672-9

[90] Berbman, T. L. & Incorpora, F. P. Fundamentals of heat and mass transfer. (Willey, 2011).

[91] H. Lee, "The Thomson Effect and the ideal equation on Thermoelectric Coolers," Energy, vol. 56, pp. 61-69, 2013.

[92] H. Lee, Thermal Design: Heat Sinks, Thermoelectrics, Heat Pipes, Compact Heat Exchangers, and Solar Cells, Hoboken: John Wiley & Sons, Inc., 2010.

[93] H. Lee, A. Attar and S. Weera, "Performance Prediction of Commercial Thermoelectric Cooler Modules using the Effective Material Properties," Journal of Electronic Materials, vol. 44, no. 6, pp. 2157-2165, 2015.

[94] Dongliang Zhao, Gang Tan. A review of thermoelectric cooling: Materials, modeling and applications. Applied Thermal Engineering 66 (2014) 15-24.

[95] W.D. Liu , L. Yang , Z.G. Chen , Nano Today 35 (2020) 100938 .

[96] W.D. Liu , L. Yang , Z.G. Chen , J. Zou , Adv. Mater. 32 (2020) e1905703 .

[97] W.D. Liu , D.Z. Wang , Q. Liu , W. Zhou , Z. Shao , Z.G. Chen , Adv. Energy Mater. 10 (2020) 20 0 0367 .

[98] Tritt, T.M. Thermoelectric phenomena, materials, and applications. Annu. Rev. Mater. Res. 2011, 41, 433–448.

[99] H. Lee, A. Atta and S. Weera, "Performance prediction of commercial thermoelectric cooler modules using the effective material properties," Journal of Electronic Materials, vol. 44, no. 6, pp. 2157-2165, 2015.

[100] Bell LE. Cooling, heating, generating power, and recovering waste heat with thermoelectric systems. Science 2008;321(5895):1457–61.

[101] Fairbanks J. Thermoelectric applications in vehicles status 2008. US Dep. Energy 2008.

[102] Hamid Elsheikh, M. et al., 2014. A review on thermoelectric renewable energy: Principle parameters that affect their performance. Renewable and Sustainable Energy Reviews, 30, pp.337–355.

[103] Ssennoga Twaha, Jie Zhu, Yuying Yan, Bo Li. A comprehensive review of thermoelectric technology: Materials, applications, modelling ansd performance improvement. Renewable and Sustainable Energy Reviews 65 (2016) 698–726.

[104] Lee, H. (2010). Thermal Design: Heat Sinks, Thermoelectrics, Heat Pipes, Compact Heat Exchangers, and Solar Cells. Hobooken: John Wiley & Sons, Inc.

[105] G. S. Nolas, J. Sharp and H. J. Goldsmid, "Thermoelectrics," Springe, Heidelberg, Germany, 2001.

[106] M. H. Makhmalbaf, "Experimental study on convective heat transfer coefficient around a vertical hexagonal rod bundle," Heat and Mass Transfer, vol. 48, no. 6, pp. 1023-1029, 2012.

[107] M. Aghbashlo, M. Tabatabaei, M.H. Nadian, V. Davoodnia, S. Soltanian, Prognostication of lignocellulosic biomass pyrolysis behavior using ANFIS model tuned by PSO algorithm, Fuel 253 (2019) 189.

[108] N. Lerkkasemsan, Fuzzy logic-based predictive model for biomass pyrolysis, Appl. Energy 185 (2017) 1019.

[109] Y. Kondratenko, O. Kozlov, O. Korobko, Development of Intelligent Controllers for Pyrolysis Reactors Control Systems Based on Their Mathematical Models, Collection of Scientific Publications NUS, 2015.

[110] A. Inayat, A.M. Nassef, H. Rezk, E.T. Sayed, M.A. Abdelkareem, A.G. Olabi, Fuzzy modeling and parameters optimization for the enhancement of biodiesel production from waste frying oil over montmorillonite clay K-30, Sci. Total Environ. 666 (2019) 821.

[111] Qahtan A. Mahmood, Amer T. Nawaf. Performance analysis of continuous stirred tank heater by using PID -cascade controller. Materials Today: Proceedings 42 (2021) 2545–2552

[112] L.E. Bell, Science 321, 1457 (2008).

[113] http://www.waeco.com/en/products/3111.php Accessed July 2022.

[114] W. Ning, L. Zhouxiao, D. Can, Z. Jiannan, S. Guorong, J. Hongzhi, G. Xiumin, High efficiency thermoelectric temperature control system with improved proportional integral differential (PID) algorithm using energy feedback technique, IEEE Trans. Ind. Electron. (2022).

[115] G. Engelmann, M. Laumen, J. Gottschlich, K. Oberdieck, R.W. De Doncker, Temperature-controlled power semiconductor characterization using thermoelectric coolers, IEEE Trans. Ind. Appl. 54 (3) (2018) 2598–2605.

[116] D. F. Sinulingga Sundayani, F.M. Prasetyawati, M. Palebangan, F.A. Suhendi, T.A. Ajiwiguna, I.W. Fathonah, PID temperature controlling of thermoelectric based cool box, in: 2017 International Conference on Control, Electronics, Renewable Energy and Communications (ICCREC), 2017.

[117] H. Huang, S. Fu, P. Zhang, L. Sun, Design of a Small Temperature Control System Based on TEC. 2016 9th International Symposium on Computational Intelligence and Design (ISCID), 2016.

[118] Jia-liang Song, Wen-long Cheng, Zhi-ming Xu, Shuai Yuan, Ming-hou Liu. Study on PID temperature control performance of a novel PTC material with room temperature Curie point. International Journal of Heat and Mass Transfer 95 (2016) 1038–1046

[119] Astrain, D., Martínez, A., Gorraiz, J., Rodríguez, A., & Pérez, G. (2012). Computational Study on Temperature Control Systems for Thermoelectric Refrigerators. Journal of Electronic Materials, 41(6), 1081–1090.

[120] Yong-Duan Song, Control of Nonlinear Systems via PI, PD and PID Stability and Performance, CRC Press Taylor & Francis Group, 2018.

[121] T.H. Kwan, X. Wu, Q. Yao, Complete implementation of the combined TEG-TEC temperature control and energy harvesting system, Control Eng. Pract. 95 (2020), 104224.

[122] A. Kherkhar, Y. Chiba, A. Tlemçani, H. Mamur. Thermal investigation of a thermoelectric cooler based on Arduino and PID control approach. Case Studies in Thermal Engineering 36 (2022) 102249.

[123] K.J. Astrom, T. Hagglund, Advenced PID Control, ISA Instrumentation, Systems and Automation Society, 2006.

[124] A. Boubaris, N. Vagiannis, G. Chatziaggelou, N. Chatzipapas, N. Papanikolaou, Implementation of current and ventilation control for enhanced TEC performance, in: 2019 Panhellenic Conference on Electronics & Telecommunications (PACET), 2019.

[125] W. Shibin, W. Kun, X. Peng, H. Yajin, Numerical and experimental verification of the single neural adaptive PID real-time inverse method for solving inverse heat conduction problems, Int. J. Heat Mass Tran. (2022), 122657.

[126] D. Astrain, A. Martínez, A. Rodríguez, Improvement of a thermoelectric and vapour compression hybrid refrigerator, Appl. Therm. Eng. 39 (2012) 140–150.

[127] D. Enescu, C. Diaz, A. Ciocia, A. Mazza, A. Russo, Experimental Assessment of the Temperature Control System for a Thermoelectric Refrigeration Unit. 2018 53rd International Universities Power Engineering Conference (UPEC), 2018.

[128] D.W. Wardhana, A. Wahyudi, H. Nurhadi, Design of a PID control system for controlling azimuth turret axis on a 20mm eebec turret gun, ITS Engineering Journal 5 (2) (2016) 512–516.

[129] E. Marlin, Process Control: Designing Processes and Control Systems for Dynamic Performance, McGraw-Hill, 2000.

[130] R. Brian, B. Ben, Process Dynamics and Control, Modelling for Control and Prediction, John Wiley and Sons Ltd., Netherlands, 2006.

[131] J.C. Basilio, S.R. Matos, Design of PI and PID controllers with transient performance specification, IEEE Trans. Educ. 45 (4) (2002) 364–370.

[132] Kaiguo Fan, Jianying Xiao, Ruoda Wang, Rui Gao. Thermoelectric-based cooling system for high-speed motorized spindle I: design and control mechanism. The International Journal of Advanced Manufacturing Technology (2022) 121:3787–3800.

[133] H. Sadighi Dizaji, S. Jafarmadar, S. Khalilarya, A. Moosavi, An exhaustive experimental study of a novel air-water based thermoelectric cooling unit, Appl. Energy 181 (2016) 357–366.

[134] D. Enescu, E.O. Virjoghe, A review on thermoelectric cooling parameters and performance, Renew. Sustain. Energy Rev. 38 (2014) 903–916.

[135] A. Dan, T. Pada, and K. Tec. Technical and economic analysis of the use of aluminum and copper heatsink in TEC Altis-2 components. No. August 2016, 2019.

[136] Rokhimi. Learning aid conduction heat conduction rate. Vol.6, pp. 270-274, 2015.

[137] P. Studi, T. Mesin, F. Engineering, U. Muhammadiyah, and S. Utara, Final project of convection heat transfer analysis on electronic component coolers. 2019.

[138] C. Liu, W. Ren, B. Zhang, and C. Lv, "The application of soil temperature measurement by LM35 temperature sensors," 2011 International Conference on Electronic & Mechanical Engineering and Information Technology, Harbin, China, pp. 1825-1828, 12-14 Aug. 2011.

[139] L. Fanming, Z. Yafeng, A new design of precision temperature controller based on TEC, Journal of Chinese Inertial Technology 12 (6) (2004) 61–64.

[140] Z. Ye, Z. Qingming, M. Congxiao, L. Sen, A practical semiconductor cooling temperature control circuit, J. Nat. Sci. Hunan Normal Univ. 13 (4) (1997) 50–53.

[141] Y. Huang, H. Chen, Y. Ruan, C.Z. Chen, Research on semiconductor laser reinforcement under wide temperature environment, Journal of Hua zhong University of Science and Technology 25 (4) (1997) 5–6.

# APPENDIX

# Specification of Thermoelectric Module

## TEC1-12706

## Description

The 127 couples, 40 mm × 40 mm size single stage module is made of selected high performance ingot to achieve superior cooling performance and greater delta T up to 70 °C, designed for superior cooling and heating up to 100 ℃ requirement. If higher operation or processing temperature is required, please specify, we can design and manufacture the custom made module according to your special requirements.

## Features

- High effective cooling and efficiency.
- No moving parts, no noise, and solid-state
- Compact structure, small in size, light in weight
- Environmental friendly, RoHS compliant
- Precise temperature control
- Exceptionally reliable in quality, high performance

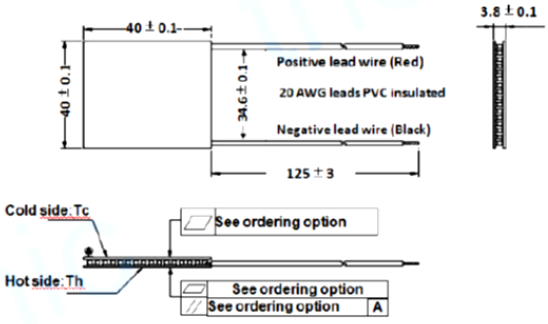
## Application

- Food and beverage service refrigerator
- Portable cooler box for cars
- Liquid cooling
- Temperature stabilizer
- Photonic and medical systems

## Peformance Specification Sheet

| | | | |
|---|---|---|---|
| Th(℃) | 27 | 50 | Hot side temperature at environment: dry air, $N_2$ |
| $DT_{max}$(℃) | 70 | 79 | Temperature Difference between cold and hot side of the module when cooling capacity is zero at cold side |
| $U_{max}$(Voltage) | 16.0 | 17.2 | Voltage applied to the module at $DT_{max}$ |
| $I_{max}$(amps) | 6.1 | 6.1 | DC current through the modules at $DT_{max}$ |
| $Q_{Cmax}$(Watts) | 61.4 | 66.7 | Cooling capacity at cold side of the module under DT=0 ℃ |
| AC resistance(ohms) | 2.0 | 2.2 | The module resistance is tested under AC |
| Tolerance (%) | ± 10 | | For thermal and electricity parameters |

## Geometric Characteristics Dimensions in millimeters




## Sealing Option

**A. Solder:**

1. T100: BiSn (Tmelt = 138 °C)

**B. Sealant:**

1. NS: No sealing (Standard)
2. SS: Silicone sealant
3. EPS: Epoxy sealant
4. Customer specify sealing other than above

**C. Ceramics:**

1. Alumina ($Al_2O_3$, white 96%)
2. Aluminum Nitride (AlN)

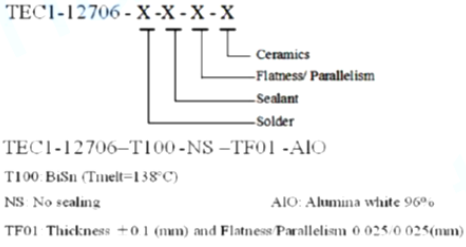
**D. Ceramics Surface Options:**

1. Blank ceramics (not metallized)
2. Metallized (Au plating)

## Ordering Option

| Suffix | Thickness (mm) | Flatness/ Parallelism (mm) | Lead wire length(mm) Standard/Optional length |
|---|---|---|---|
| TF | 0:3.8±0.1 | 0:0.035/0.035 | 125±3/Specify |
| TF | 1:3.8±0.05 | 1:0.025/0.025 | 125±3/Specify |
| TF | 2:3.8±0.025 | 2:0.015/0.015 | 125±3/Specify |
| Eg. TF01: Thickness 3.8 ± 0.1 (mm) and Flatness 0.025 / 0.025 (mm) | | | |

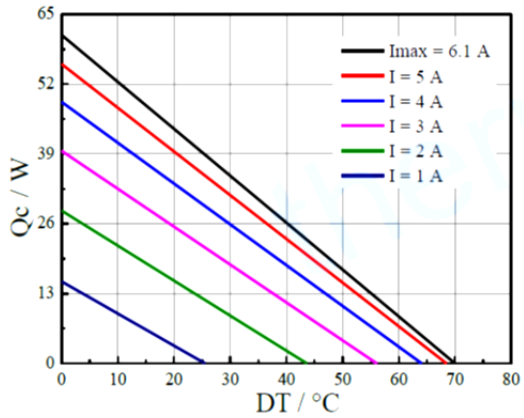
## Naming for the Module



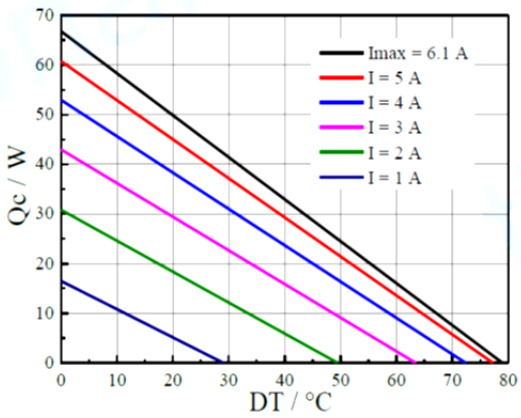
# Specification of Thermoelectric Module

## TEC1-12706

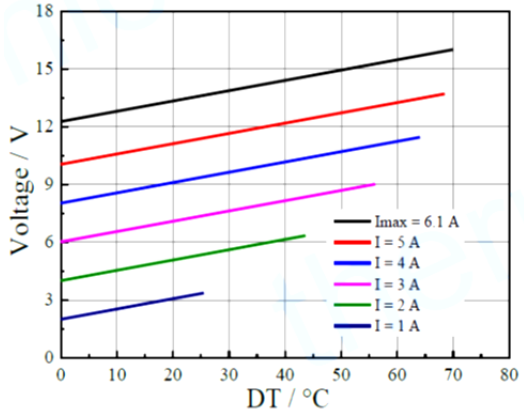
### Performance Curves at Th=27 ºC

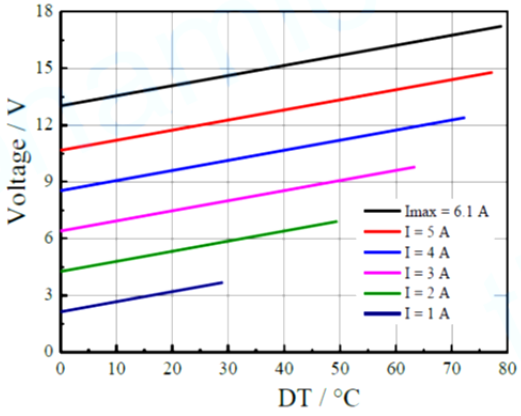



### Performance Curves at Th=50 ºC

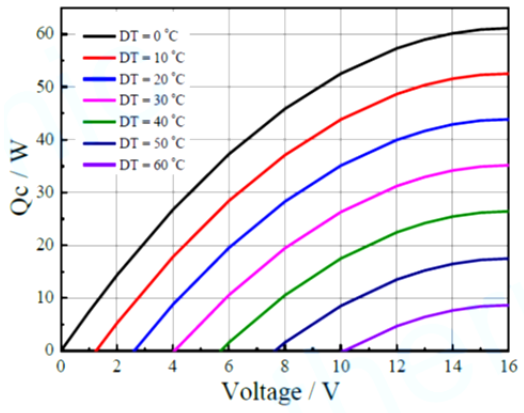


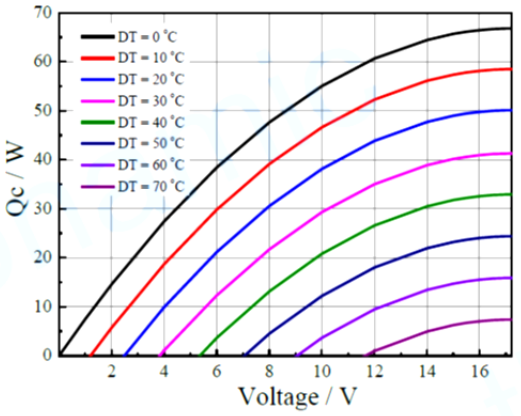

Standard Performance Graph Qc= f(DT)




Standard Performance Graph V= f(ΔT)



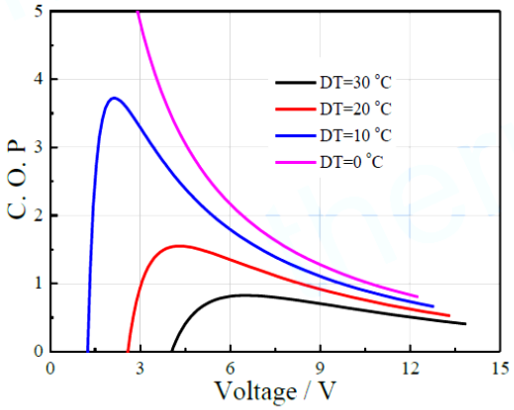




Standard Performance Graph Qc= f(V)

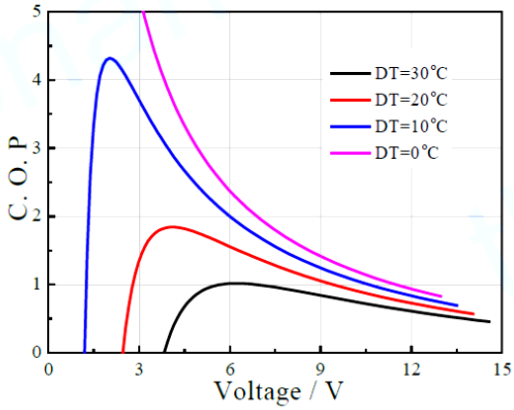
# Specification of Thermoelectric Module

## TEC1-12706

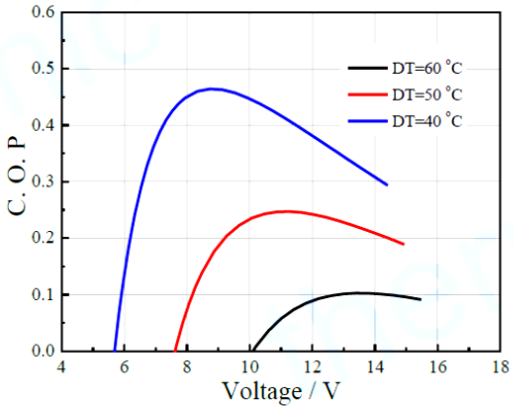
### Performance Curves at Th=27 ºC

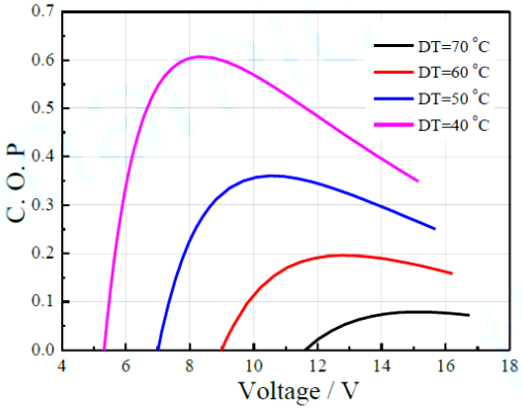



### Performance Curves at Th=50 ºC




Standard Performance Graph COP = f(V) of ΔT ranged from 0 to 30 ˚C




Standard Performance Graph COP = f(V) of ΔT ranged from 40 to 60/70 ˚C

Remark: The coefficient of performance (COP) is the cooling power Qc/Input power (V × I).

## Operation Cautions

- Cold side of the module sticked on the object being cooled
- Hot side of the module mounted on a heat radiator
- Storage module below 100 ºC
- Operation below $I_{max}$ or $V_{max}$
- Work under DC

## List of Publications:

1- **A. Kherkhar**, Y. Chiba, A. Tlemçani, H. Mamur. Thermal investigation of a thermoelectric cooler based on Arduino and PID control approach. *Case Studies in Thermal Engineering* 36 (2022) 102249.

## List of International and national conferences:

1- **A. Kherkhar**, Y. Chiba, A. Tlemçani. Investigation of Cooling Performance for Thermoelectric Refrigerators with Cooled Water Effects Design. *Algerian Symposium on Renewable Energy and Materials ASREM2022,* March 16-17, 2022, Medea- Algeria.